Paul-Ehrlich-Institut

TECHNISCHE UNIVERSITÄT DARMSTADT

Impaired Nrf1-dependent gene expression in cells replicating HCV results in elevated cholesterol levels and impacts the size of lipid droplets

Vom Fachbereich Biologie

der Technischen Universität Darmstadt

Zur Erlangung des Grades

Doctor rerum naturalium

(Dr. rer. nat.)

Dissertation

von Patrycja Schorsch

Erstgutachterin: Prof. Dr. Beatrix Süß

Zweitgutachter: Prof. Dr. Eberhard Hildt

Darmstadt 2024

Schorsch, Patrycja: Impaired Nrf1-dependent gene expression in cells replicating HCV results in elevated cholesterol levels and impacts the size of lipid droplets

Darmstadt, Technische Universität Darmstadt

Jahr der Veröffentlichung der Dissertation auf TUprints: 2024

Tag der mündlichen Prüfung: 21.03.2024

Ehrenwörtliche Erklärung:

Ich erkläre hiermit, dass ich die vorliegende Arbeit ohne unzulässige Hilfe Dritter angefertigt habe. Sämtliche aus fremden Quellen direkt oder indirekt übernommenen Gedanken sowie sämtliche von Anderen direkt oder indirekt übernommenen Daten, Techniken und Materialien sind als solche kenntlich gemacht.

Ferner erkläre ich, dass ich bei der Verfassung der Dissertation die "Grundsätze zur Sicherung guter wissenschaftlicher Praxis an der Technischen Universität Darmstadt" und die "Leitlinien zum Umgang mit digitalen Forschungsdaten an der TU Darmstadt" in den jeweils aktuellen Versionen beachtet habe. Die Arbeit wurde bisher bei keiner anderen Hochschule zu Prüfungszwecken eingereicht.

Darmstadt, den 24.06.2024

.....

List of tables 8
List of figures 8
List of abbreviations 9
1 Introduction 13
1.1 Hepatitis C virus 13
1.1.1 Epidemiology and disease 13
1.1.2 Treatment and therapy 13
1.1.3 History and classification of hepatitis C virus 14
1.1.4 Genome organization 14
1.1.5 HCV virion structure 16
1.1.6 HCV viral proteins 16
1.1.6.1 Core 16
1.1.6.2 E1 and E2 17
1.1.6.3 p7 17
1.1.6.4 NS2 17
1.1.6.5 NS3 18
1.1.6.6 NS4A 18
1.1.6.7 NS4B 18
1.1.6.8 NS5A 18
1.1.6.9 NS5B 19
1.1.7 Life cycle of HCV 19
1.1.7.1 Entry and uncoating HCV 19
1.1.7.2 RNA translation and replication 21
1.1.7.3 Assembly and release 22
1.1.8 Model systems 23
1.2 Lipids as key factors in cellular membranes, energy storage and signaling pathways 25
1.2.1 Cellular cholesterol homeostasis 26
1.2.1.1 Cholesterol Uptake 26
1.2.1.2 Cholesterol Biosynthesis and Uptake 26
1.2.1.3 The LDLR and Cholesterol Uptake 27
1.2.1.4 Cholesterol modulating drugs 28
1.2.2 HCV exploits lipids for its life cycle 29
1.2.3 HCV and oxidative stress 32
1.2.3.1 Implications for Insulin Signaling and Metabolism 32
1.2.3.2 Intracellular membrane rearrangement, mitochondrial dysfunction and ER stress 33

1.2.3.3 Keap1-Nrf2-ARE signaling pathway in HCV infection 34
1.3 Nuclear factor erythroid 2-related factor 1 (Nrf1) 36
1.3.1 Nrf1 processing 36
1.3.2 Nrf1 is a cholesterol sensor 39
2 Aim of this study 41
3 Materials 42
3.1 Cells 42
3.1.1 Prokaryotic cells 42
3.1.2 Eukaryotic cells 42
3.2 Plasmids 42
3.3 Oligonucleotides 42
3.3.1 RT-qPCR-Primer 42
3.3.2 Cloning primers 43
3.3.3 Sequencing primers 43
3.3.4 siRNA 43
3.4 Antibodies 43
3.4.1 Primary antibodies 43
3.4.2 Secondary antibodies 44
3.5 Fluorescent dye 44
3.6 Molecular weight markers 44
3.6.1 DNA markers 44
3.6.2 Protein markers 44
3.7 Enzymes 44
3.8 Inhibitors 45
3.9 Reagents for cell culture 45
3.10 Chemicals 45
3.11 Kits 46
3.12 Buffers and solutions 47
3.13 Devices 48
3.13.1 Electrophoresis 48
3.13.2 Microscopy 48
3.13.3 Imaging 48
3.13.4 PCR-Cycler 48
3.13.5 Centrifuges 48
3.13.6 Other devices 49
3.14 Relevant materials 49
3.15 Software 49

4 Methods 50
4.1. Cell biology 50
4.1.1. Prokaryotic cell culture 50
4.1.2. Eucaryotic cell culture 50
4.1.3. Electroporation of Huh7.5 cells 50
4.1.4. Transfection of Huh7.5 cells 50
4.1.5. Silencing of gene expression 51
4.1.6. Cell harvest and lysis 51
4.1.7. Treatments 51
4.2 Molecular biology 51
4.2.1. Agarose gel electrophoresis 51
4.2.2. Determination of nucleic acid concentration 52
4.2.3. Isolation of plasmid DNA 52
4.2.4. Generation of competent bacteria 52
4.2.5. Transformation of competent bacteria 52
4.2.6. Phenol/chloroform extraction of nucleic acids 52
4.2.7. *In vitro* T7 transcription 53
4.2.8. RNA isolation 53
4.2.9. cDNA synthesis 53
4.2.10. Real-Time qPCR 53
4.2. Protein biochemistry 55
4.2.1. Protein quantification by Bradford assay 55
4.2.2. SDS-PAGE 55
4.2.3. Western blot 55
4.2.4. Half-life determination 56
4.2.5. Luciferase reporter assay 56
4.2.6. End point dilution assays (TCID50) 56
4.2.7. Indirect immunofluorescence microscopy 56
4.5.1.1 Standard indirect immunofluorescence staining 56
4.5.1.2 Filipin staining 57
4.5.2 Immunohistochemistry 57
4.4 Microscopy 57
4.4.1 Confocal laser scanning microscopy 57
4.5.1 Statistical analysis 58
5 Results 59
5.1 Decreased amount of Nrf1 in HCV replicating cells 59
5.2 Silencing of Nrf1 favours HCV life cycle 62
5.3 Overexpression of Nrf1 fragments restricts HCV replication, assembly and release 65

5.4 Extranuclear sMaf proteins have the capacity to withdraw Nrf1 from the nucleus.....69
5.5 Impaired activation of Nrf1/ARE-dependent gene expression by extranuclear sMaf-variant.....73
5.6 Impaired activation of LXR promoter in HCV positive cells.....74
5.7 Impaired Nrf1-LXR-axis contributes to elevated cholesterol levels in HCV replicating cells 76
5.8 Inhibition of Nrf1 modulates the host-kinome related to inflammation, innate immunity and lipid metabolism 77
5.9 Modulation of Nrf1 activity directly affects LD size and number.....79
6 Discussion.....82
7 Summary.....86
8 Zusamenfassung.....87
9 References.....89
10 Acknowledgments 107

List of tables

Table 1. Summary of in vitro and in vivo models for hepatitis C virus (Wang 2013).....24
Table 2. Major Nrf1 structural domains (Zhang and Xiang 2016). 37
Table 3. Master mix for cDNA synthesis 53
Table 4. RT-qPCR sample composition. 53
Table 5. RT-qPCR program for intracellular RNA aplification. 54
Table 6. RT-qPCR program for extracellular RNA aplification. 55

List of figures

Figure 1. Hepatitis C virus genome organization and the membrane topology of cleaved viral proteins (Bartenschlager et al. 2013).. 15
Figure 2. HCV lipoviroparticle structure (Morozov and Lagaye 2018). 16
Figure 3. The HCV Entry Process (Wong-Staal et al. 2010). 20
Figure 4. Replication machinery of HCV (Tabata et al. 2020). 22
Figure 5. Overview of HCV constructs (Elgner 2016, modified). 24
Figure 6. Intracellular cholesterol trafficking (Merscher et al. 2014). 28
Figure 7. HCV causes changes in lipid metabolism and steatosis (Elgretli et al. 2023).....29
Figure 8. Models for the formation of membrane curvature and viral replication complexes (Zhang et al. 2019). 31
Figure 9. Various interactions between HCV and the hepatocyte insulin signaling pathway (Gastaldi et al. 2017). 33
Figure 10. The cytoprotective defense system regulated by Nrf2 (Tonelli et al. 2018).....35
Figure 11. Schematic picture of Nrf2 under constitutive, oxidative stress conditions and HCV infection (Hammad et al. 2023, modified). 36
Figure 12. The model of the molecular mechanisms that regulate Nrf1 (Zhang et al. 2014)..39
Figure 13. Nrf1 is an ER cholesterol sensor (Widenmaier et al. 2017). 40
Figure 14. HCV has no effect on Nrf1 half-life. 61
Figure 15. HCV infection regulates Nrf1. 63
Figure 16. Nrf1 knockdown in single cells. 64
Figure 17. Overexpression of Nrf1 restricts HCV. 68
Figure 18. sMaf affects localization of Nrf1 fragments. 72
Figure 19. Impaired activation of Nrf1/ARE-dependent gene expression by coexpression of an extranuclear sMaf-variant HCV-positive or negative cells were cotransfected with a reporter construct expressing the luc reporter gene under the control of the NQO1 promoter and expression vectors encoding for the sMaf fusion proteins sMaf-NES or sMaf-NLS. 74
Figure 20. Nrf1 fragments modulate cellular cholesterol. 76
Figure 21. Inhibitory fragments of Nrf1 modulate the host-kinome related to inflammation, innate immunity and lipid metabolism 78
Figure 22. LDs analysis upon Nrf1 overexpression. 80

List of abbreviations

Abbreviation	Meaning
%	percent
(-)-strand	negative sense strand
(+)-strand	positive sense strand
°C	degrees Celsius
25CHC	25-hydroxycholesterol
3'	three prime
5'	five prime
aa	amino acid
ABCA1	ABC-transporter A1
ABCG1	ABC-transporter G1
ABCG5 ABCG8	ATP-binding cassette transporters sub-family G members 5 and 8
ABC-transporter	ATP-binding cassette transporter
ACAT	Acyl-CoA-Cholesterol-Acyltransferase
ACAT2	acyl-cholesterol acyl transferase
ALT	Alanine aminotransferase
AP-1	Activating protein-1
apoA-I	apolipoprotein A-I
ApoB100	apolipoprotein B100
ApoB-100	Apolipoprotein B
ApoCI	Apolipoprotein C-I
ApoCII	Apolipoprotein C-II
ApoCIII	Apolipoprotein C-III
ApoE	apolipoprotein E
ARE	Antioxidant response element
ARFP	Alternative reading frame protein
ATF4	Activating transcription factor-4
ATP	Adenosine triphosphate
bp	base pairs
BSA	Bovine serum albumin
bZIP	basic leucine zipper
CAT	Chloramphenicol acetyltransferase
CBP	CREB-binding protein
CD81	Cluster of Differentiation 81
CDC	Centers for Disease Control and Prevention
cDNA	Complementary DNA
CH25H	cholesterol 25-hydroxylase
CIDEB	cell death-inducing DFFA-like effector b
CLDN1	tight junction proteins claudin-1
CLDN-1	Claudin-1
CLDN6	tight junction proteins claudin-6
CLDN9	tight junction proteins claudin-9
CLSM	confocal laser scanning microscopy
CMV	Cytomegalovirus
CNC	Cap N´Collar
CRE	cis-responsive element
CREB	c-AMP response elementbinding protein
CTCF	corrected total cell fluorescence
C-terminal	carboxyterminal
DENV	Dengue virus
DMEM	Dulbecco’s Modified Eagle Medium
DMSO	Dimethyl sulfoxide

Abbreviation	Meaning
dsRNA	double stranded RNA
DTT	1,4-Dithiothreitol
ECL	Enhanced chemiluminescence
EGFR	receptor tyrosine kinases epidermal growth factor receptor
EMCV	Encephalomyocarditis virus
EphA2	ephrin receptor A2
EpRE	Electrophile response element
ER	Endoplasmic reticulum
g	gravitational constant
GAGs	glycosaminoglycans
GPx1	Glutathione peroxidase-1
Grb2	Growth factor receptor binding Protein-2
GSH	Glutathione
GST	Glutathione-S-Transferase
h	hours
H2O2	hydrogen peroxide
HBV	Hepatitis B virus
HCC	Hepatocellular carcinoma
HCV	Hepatitis C virus
HCVcc	cell culture derived HCV
HCVpp	HCV pseudoparticles
HDL	high-density lipoprotein
HIV	Human Immunodeficiency Virus
HMGCR	HMG-CoA reductase
HMGCS	HMG-CoA synthase
HO•	hydroxyl radicals
HRP	Horseradish peroxidase
HSPGs	proteoglycans
Huh 7.5	Human hepatoma cell line
hVAP-A	Human vesicle associated membrane protein A
IFN	Interferon
IMM	inner mitochondrial membrane
IRES	Internal ribosomal entry site
IRF-3	Interferon regulatory factor-3
JFH1	Japanise fulminate hepatitis
Keap1	Kelch-like ECH-associated protein
LD	Lipid droplets
LDH	lactate dehydrogenase
LDL	Low density lipoprotein
LDLR	LDL-receptor
L-SIGN	C-type lectins liver/lymph node-specific intercellular adhesion molecule-3-grabbing integrin
Luc	luciferase
LXR	liver X receptor
M	molar
MAPK	Mitogen-activated protein kinases
MARE	Maf recognition element
MAVS	mitochondrial antiviral signalling protein
MDA5	melanoma differentiation-associated 5
min	minutes
mL	millilitres
mM	millimolar

Abbreviation	Meaning
MVB	multivesicular bodies
MVK	methyl vinyl ketone
NANBH	Non-A/Non-B hepatitis
NCR	Non-coding region
Neh	Nrf2-ECH-homology
NES	Nuclear export signal
NF-E2	Nuclear factor erythroid-2
NFE2L1	nuclear factor erythroid-2-like 1
NFkB	Nuclear factor kappa B
NLS	Nuclear localisation signal
nM	nanomolar
nm	nanometres
NO	nitric oxide
NO2	nitrogen dioxide
NO3	nitrate
NPC1L1	cholesterol transporter Niemann-Pick C1-like 1
NQO1	NAD(P)H-quinone oxidoreductase 1
Nrf1	Nuclear factor erythroid 2-related factor 1
Nrf1	NF-E2 related factor-1
Nrf2	NF-E2 related factor-2
NS	Non-structural
NTD	nucleotide-binding domain
N-terminal	aminoterminal
$O_2^{\bullet-}$	superoxide anions
OMM	outer mitochondrial membrane
ORF	Open reading frame
ORF	open reading frame
OS	Oxidative stress
OSBPL1A	oxysterol-binding protein-related protein 1A
OSBPL1B	oxysterol-binding protein-related protein 1B
PBMCs	peripheral blood mononuclear lymphocytes
PBS	Phosphate-buffered saline
PCR	Polymerase chain reaction
PEG	polyethylene glycol
PERK	PKR-like endoplasmic resident kinase
PI3K	Phosphatidylinositol 3-kinase
PI3P	phosphatidylinositol 3-phosphate
PKC	Protein kinase C
PKR	Protein kinase R
PM	plasma-membrane
POI	protein of interest
poly-A	polyadenylation
pORF	protein encoded by ORF
PPAR	peroxisome proliferation-activated receptor
PRR	pathogen-recognition receptors
PSAP	proline-alanine-serine-proline
PSMB5	Proteasome subunit beta type-5
qPCR	quantitative polymerase chain reaction
R2	coefficient of determination
Rab	ras-related protein
Rabex-5	rabaptin-5-associated exchange factor for Rab5
RC	replicon complex

Abbreviation	Meaning
RdRp	RNA-dependent RNApolymerase
RIG-I	Retinoic acid-inducible gene-I
RNP	Ribonucleoprotein
RNS	reactive nitrogen species
ROIs	Reactive oxygen intermediates
ROS	Reactive oxygen species
RT	Reverse transcription
s	seconds
SCARB1	scavenger receptor class B member 1
SERCA	sarcoplasmic/endoplasmic reticulum calcium ATPase
siRNA	short interfering RNA
sMafs	Small Maf proteins
SNARE	Soluble N-ethylmaleimide-sensitive-factor attachment receptor
SR-BI	Scavenger-receptor class B type-I
SRE	sterol-regulatory element
SREBF1	sterol regulatory element binding transcription factor 1
SREBP	sterol regulatory element-binding protein
ssRNA	single stranded RNA
STARD3	protein-related lipid transfer domain protein 3
STAT	signal transducer and activator of transcription
SVR	sustained virological response
TCID50	half maximal tissue culture infection dose
TF	transcription factor
TfR1	transferring receptor 1
TG	triglycerides
TGN	trans-Golgi network
TMD	transmembrane domain
VLDL	very low-density lipoprotein
VLP	virus-like particle
VRC	viral replicon complex
WHO	World Health Organization
WNV	West Nile Virus
ZIKV	Zika virus
µg/mL	micrograms per millilitre
µg/µL	micrograms per microliter
µM	micromolar

1 Introduction

1.1 Hepatitis C virus

1.1.1 Epidemiology and disease

Hepatitis C is a viral infection caused by the hepatitis C virus (HCV) and affecting the liver. The World Health Organization (WHO) estimated that in 2019, globally, 57,8 million (0,8%) people were living with chronic HCV infection (Cui et al. 2023). Accurate determination of global incidence of HCV is heavily limited due to the limited epidemiological data. HCV is mainly transmitted through contact with infected blood. The commonly observed primary modes of infection include the transmission through contaminated blood products or unsterilized equipment and less commonly vertical transmission (Terrault et al. 2020; Petruzziello et al. 2016). The occurrence of hepatitis C virus infection displays regional variations across countries, making it a substantial global public health concern. Furthermore, the mode of HCV transmission exhibits diversity depending on the specific geographic regions (Polaris Observatory HCV Collaborators 2017). Non-sterile traditional practices or medical and dental procedures are responsible for a significant number of infections in developing regions, whereas intravenous drug users have the highest prevalence of HCV in developed countries (Centers for Disease Control and Prevention (CDC) 2011).

The incubation period of HCV infection may vary, ranging from a few weeks to several months (Westerhoff and Ahn 2018; Loomba et al. 2011). During this time, disease may not cause any clear symptoms that can be mistaken for other illnesses. Development of acute infection often goes unnoticed, as during this time the symptoms may not be severe enough to raise concern, or there might be an absence of symptoms altogether (Lee et al., 2021). Approximately15% of individuals infected with HCV can experience spontaneous clearance of the virus, meaning without the need for medical intervention. Contrarily, the remaining 85% of infected will develop chronic hepatitis, which means the virus persists in their body for an extended period (Alter 1997; Nawaz et al. 2015). Many factors contributing to the spontaneous elimination of HCV have been identified. They can be categorized into virus-related and host-related factors. Virus-related factors include the virus's genotype and its ability to rapid mutation and host-related factors include for example gender and age (Sullivan et al. 2007). Approximately 20-25% of people with chronic infection will develop cirrhosis over a 25–30-year period The progression of chronic hepatitis C differs from person to person. (Lingala and Ghany 2015). However, certain factors can accelerate the progression of liver disease in certain patient groups. Known factors include: co-infection with HBV or HIV, older age or continuous exposure to alcohol (Graham et al. 2001; Wiley et al. 1998; Poynard et al. 1997). Additionally, cirrhosis patients have a 2-5% risk of developing hepatocellular carcinoma (HCC) (Yang et al. 2019). Due to the severity of chronic hepatitis C and its potential complications, liver failure resulting from this condition is one of the primary reasons for liver transplants (Rungta 2021).

1.1.2 Treatment and therapy

The initial treatment for chronic Hepatitis C involved monotherapy with IFN-α. Its success was limited, resulting in response rates of only 6 to 20% in cases (Chen et al. 2010). Later on, ribavirin was combined with IFN-α treatment. Afterwards, another important development emerged with the creation of pegylated interferon, which involved attaching poly (ethylene glycol) (PEG) to recombinant IFN-α, resulting in a more controlled release over time and improved virological response rates. Despite this, the therapy's prominent side effects persisted, highlighting the necessity for a better alternative (Alexopoulou and Karayiannis 2015).

Nowadays, directly acting antivirals are used for the treatment of HCV infection. DAAs act directly on viral proteins, inhibiting their replication and assembly. The main classes of DAAs include protease inhibitors, polymerase inhibitors and NS5A inhibitors (Bhattacharjee et al. 2021). Numerous clinical trials have demonstrated the remarkable efficacy of DAAs in treating HCV infection. These trials have shown that DAAs can achieve high sustained virological response (SVR) rates, indicating viral clearance, even in patients with previously limited treatment options, such as those with cirrhosis or liver transplant recipients (Bourlière 2017; Piecha 2020; Verna 2020). The shorter treatment duration and reduced side effects associated with DAAs have significantly improved patient adherence and overall treatment outcomes (Marshall et al. 2018; Schlabe and Rockstroh 2018). Inhibitors targeting the NS3/4A protease play a role in inhibiting the replication of the HCV. By disrupting the NS3/4A protease enzyme, these drugs are primarily used against genotype 1 of the virus. However, compared to other direct-acting antiviral classes, NS3/4As have longer treatment regimens, more side effects and a higher susceptibility to the virus developing resistance. Approved NS3/4A protease inhibitors include Grazoprevir, Paritaprevir, Voxileprevir and Glecaprevir. NS5B inhibitors exhibit efficacy across all genotypes and are generally well-tolerated. They show the least susceptibility to viral resistance. Current NS5B inhibitors for hepatitis C treatment include Sofosbuvir and Dasabuvir. NS5A inhibitors block virus's ability to assemble new virions, proving effective against all virus genotypes. Nevertheless, they may be poorly tolerated and are prone to resistance. Combining NS5A inhibitors with alpha pegylated interferon or ribavirin enhances their efficacy. Examples include Elbasivr, Ledipasvir, Ombitasvir, Velpatasvir and Pibrentasvir (Oancea et al. 2020; McLaughlin and Esterly, 2015)

Despite these significant advancements, challenges remain in the fight against HCV. The high cost of the drugs and the emergence of HCV resistance to DAAs still limit the therapy's accessibility and effectiveness (Pawlotsky et al., 2015). This highlights the urgent requirement for progress in HCV treatments and vaccines.

1.1.3 History and classification of hepatitis C virus

Hepatitis C virus (HCV) is an RNA virus in the *Flaviviridae* family that belongs to the *Hepacivirius* genus. HCV strains are categorized into eight distinct genotypes, labeled from one to eight, with dissimilarities observed at 31–33% of nucleotide sites. Within each genotype, multiple subtypes exist, exhibiting variations at less than 15% of nucleotide sites, resulting in a current count of 86 identified subtypes (Roudot-Thoraval 2020).

During the 1970s, viral hepatitis was primarily attributed to two pathogens: hepatitis A virus (HAV) and hepatitis B virus (HBV). However, in 1975, a novel form of viral hepatitis was discovered in post-transfusion patients and termed NANBH (non-A-non-B hepatitis) (Feinstone et al. 1975). Larger clinical studies became possible in 1989 as a result of the discovery of the hepatitis C virus and the development of sensitive technologies for identifying HCV RNA in patient serum.

1.1.4 Genome organization

Hepatitis C virus (HCV) has single-stranded, positive-sense RNA genome with a size of 9.6 kB. HCV genome lacks a protective cap and contains a single open reading frame (ORF) flanked by 5' and 3' untranslated regions (UTR) (Lohmann et al., 1999; Wang 2013) (Figure 1. A). The 5' UTR is highly conserved and contains a type III IRES (internal ribosome entry site), enabling the initiation of genome translation in a cap-independent manner. Contrarily, the 3'-UTR consists of a short variable region, a poly(U/UC) region of 80 nucleotides and the conserved X-tail of 98 nucleotides. These elements are essential for the virus's replication

process (78). The ORF encodes a polyprotein of approximately 3,000 amino acids. This polyprotein undergoes co- and post-translational cleavage by both viral and host proteases, resulting in the formation of ten viral proteins (Figure 1. B).

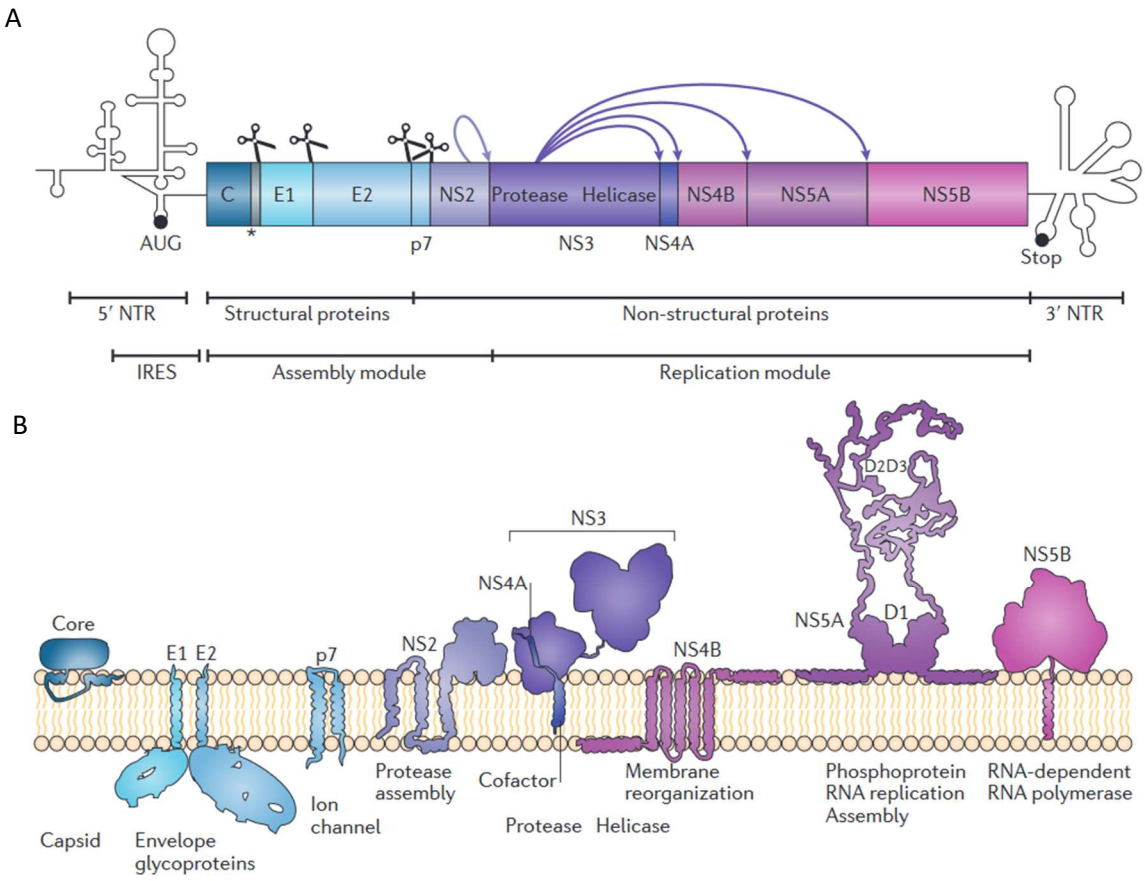

Figure 1. Hepatitis C virus genome organization and the membrane topology of cleaved viral proteins (Bartenschlager et al. 2013). (A) The hepatitis C virus (HCV) has a single long open reading frame (ORF) encoding a polyprotein, flanked by 5′ and 3′ non-translated regions (NTRs) with predicted secondary structures. Start and stop codons of the ORF are marked. The 5′ NTR contains an internal ribosome entry site (IRES). The viral assembly module requires the core (C) protein, envelope glycoproteins (E1 and E2), p7 and NS2, essential for virus formation. The replication module includes other non-structural proteins crucial for RNA replication. Polyprotein cleavage, mediated by cellular signal peptidases, occurs at specific ORF positions. A marked asterisk indicates cleavage removing the carboxy-terminal region of the core protein, carried out by cellular signal peptide peptidase. Viral proteases are responsible for other cleavages, shown by scissors. (B) Membrane topologies and functions of the HCV polyprotein cleavage products: Each protein attaches to intracellular membranes via transmembrane segments or amphipathic α-helices (core protein and NS5A). NS3 binds to membranes through a small α-helix and the cofactor NS4A, intercalating into NS3's amino-terminal protease domain. While only NS5A is shown as a dimer here, it's important to note that most, if not all, HCV proteins form homo- or heterodimers (e.g., core protein and E1-E2) or oligomeric complexes (e.g., p7).

The proteins Core, E1 and E2, form the structural proteins of HCV and form the viral particles and are encoded at the N-terminus. The non-structural proteins NS3, NS4A, NS4B, NS5A and NS5B form the replication complex, which is critical for viral replication (Bartenschlager et al. 2013) Additionally, there are two other proteins: the ion channel p7 and the non-structural protein NS2, which are not integral components of the particles, but support the formation of viral particles (Bartenschlager et al. 2010).

1.1.5 HCV virion structure

The Hepatitis C Virus is an enveloped virus, surrounded by a lipid bilayer derived from the host's cells. Two viral glycoproteins, E1 and E2, are embedded into the lipid bilayer. They facilitate the virus's entry into host cells. Nucleocapsid, localized at the core, consist of homooligomerized core proteins, which encapsulate the viral single-stranded RNA (ssRNA) genome. The nucleocapsid is localized within the lipid envelope and the envelope and nucleocapsid forms the HCV viral particle (Figure 2). The HCV viral particles show pleomorphism, meaning they come in various shapes and sizes, displaying a diameter ranging from approximately 40 (naked capsids) to 75 (enveloped virus) nanometers (nm) (Gastaminza et al. 2010). Additionally, the HCV virions are heavily associated with lipoproteins and apolipoproteins, leading to the formation of lipoviroparticles (LVPs). Some of the apolipoproteins involved in the formation of LVPs include: ApoE, ApoB-100, ApoCI, ApoCII and ApoCIII. These LVPs exhibit different densities depending on their composition, ranging from 1,05 to 1,19 grams per milliliter (g/ml). Lower density lipoviroparticles tend to be more infectious (Budkowska 2017). Furthermore, the apolipoproteins are important in HCV entry into host cells. Roughly half of the total HCV lipids are found in very-low-density lipoproteins (VLDL) and low-density lipoproteins (LDL) with cholesteryl esters (Dubuisson and Cosset 2014). These lipoprotein complexes facilitate the virus's attachment and fusion with the host cell membrane and as a result initiating the infection process.

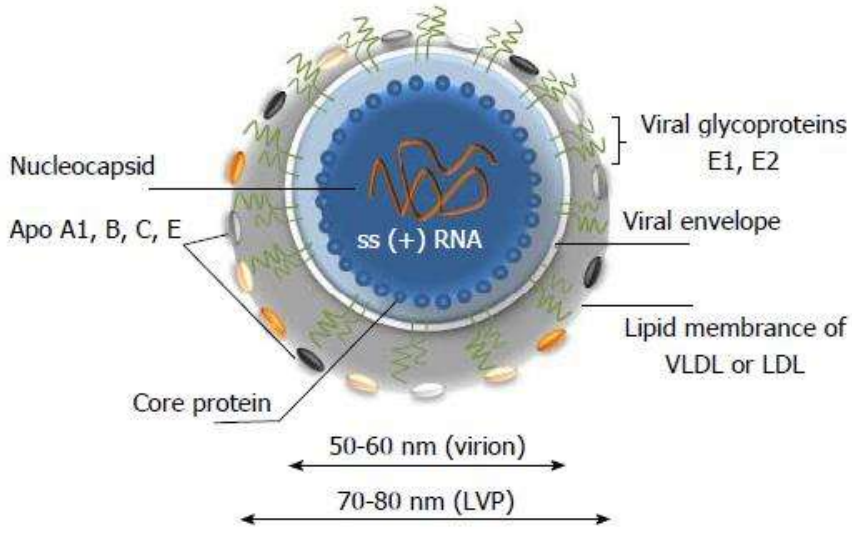

Figure 2. HCV lipoviroparticle structure (Morozov and Lagaye 2018). The virion's surface is surrounded by a lipid membrane composed of low-density lipoproteins (LDL) and very low-density lipoproteins (VLDL) (grey) and covers the core of the virus (blue) and the viral RNA (orange). The lipid bilayer partially embeds heterodimers of glycoproteins E1 and E2, forming spikes or projections on the virion's surface. This association with LDL and VLDL contributes to a non-icosahedral morphology of the virion. Depending on the viral source, the shape and size of the particles may vary.

1.1.6 HCV viral proteins

1.1.6.1 Core

The RNA-binding protein core is a highly conserved viral component with a size of 21 kDa, responsible for forming the viral capsid (McLauchlan 2000). It consists of three distinct domains, each serving essential functions. Domain 1 is a hydrophilic RNA-binding domain involved in oligomerization. Domain 2, a hydrophobic membrane-binding region, anchors the mature core to the ER and the surface of LDs, where the assembly of virions occurs (Hope et al. 2002; Boulant et al. 2006). Domain 3, also hydrophobic, acts as a signal peptide, facilitating the translocation of E1 into the ER lumen. Afterwards, the cellular signal peptide peptidase

cleaves the signal peptide, leading to the maturation of the core protein (McLauchlan 2000). The core protein plays a crucial role in recruiting nonstructural proteins to the LDs (Miyanari et al. 2007). Moreover, it possesses diverse regulatory functions and is involved in HCV pathogenesis by affecting various host cell processes (Khaliq et al. 2011). Notably, Core participates in the deregulation of cell signaling pathways, contributing to the development of hepatocellular carcinoma (HCC) (Pascut et al. 2021). Furthermore, Core's impact on miRNAs allows for the inhibition of the interferon response, promoting viral replication and altering hepatic lipid metabolism (Pascut et al. 2021).

1.1.6.2 E1 and E2

The envelope proteins, E1 and E2, possess 4-6 and 11 N-glycosylation sites, respectively and form non-covalent heterodimers. Upon expression in the host cell, E1 and E2, form non-covalent heterodimers. This enhances the stability and functionality of both proteins. The molecular weights of E1 and E2 vary depending on the extent of glycosylation. E1 has a molecular weight of approximately 33 kDa, while E2 has a higher molecular weight of about 70 kDa (Deleersnyder et al. 1997). The formation of E1E2 complexes is facilitated by their C-terminal transmembrane domains (TMDs). Additionally, these transmembrane domains contribute to the retention of E1 and E2 within the ER, which is an important step in the viral life cycle (Moradpour et al. 2007). Glycosylation of the proteins takes place within the ER lumen. Once the viral particles are matured and assembled, the E1E2 complexes are incorporated into the envelope membrane surrounding the virus. E2 is responsible for receptor binding, allowing the virus to recognize and attach to hepatocytes and this binding initiates the process of infection, as the virus gains entry into the host cell. E1 is known to possess fusogenic properties. After the virus is endocytosed into the host cell, E1 aids in the fusion of the viral envelope with the membrane of the endosome. This fusion enables the release of the viral nucleocapsid into the cytoplasm of the infected cell. Moreover, E2 contains two hypervariable regions (HVR1 and HVR2), which are constantly under selective pressure from mutations. This adaptive evolution is a survival strategy of the virus to evade the host's immune response. These regions are preferentially targeted by the host's immune system, which produces neutralizing antibodies to combat the virus. By continuously mutating these regions, the virus can escape detection and neutralization, allowing it to persist and spread within the host (Ashfaq et al. 2011).

1.1.6.3 p7

The small membrane protein p7 has a molecular weight of 7 kDa and is primarily situated in the ER, where it forms oligomers, creating a cation channel. p7 protein consists of two transmembrane domains and takes part in virus assembly and HCV infectivity (Griffin et al. 2003; Steinmann et al. 2007). Apart from its ion channel activity, p7 also fulfills other functions like: involvement in the subcellular localization of NS2, facilitation of membrane-to-membrane adhesion at lipid rafts and contribution to membrane permeabilization (Tedbury et al. 2011; Lee et al. 2020).

1.1.6.4 NS2

NS2 is a protein with a molecular weight of 21-23 kDa and consist of four transmembrane domains (TMDs). NS2is not essential for viral replication, but plays a crucial role in the formation of mature virions (Ashfaq et al. 2011; Isken et al.2015). In the cytoplasm, the C-terminal region of NS2 interacts with NS3 to build the metalloprotease NS2-3 (Grakoui et al. 1993). Afterwards, NS2-3 cleaves itself, resulting in the release of NS3 (Lorenz et al. 2006).

1.1.6.5 NS3

The NS3 protein, has a molecular weight of 67 kDa, plays a crucial role in various aspects of the viral life cycle. Positioned at the C-terminus, it contains an NTPase/helicase domain, which holds a great significance for the replication process (Dimitrova et al. 2003). This domain is considered to be the initiator of replication, as it facilitates the release of double-stranded RNA, unwinds secondary RNA structures and aids in the dissociation of bound proteins from the RNA template. Additionally, it actively promotes the efficient dissociation of replicated RNA, ensuring the successful progression of the replication process (Serebrov and Pyle 2004; Dubuisson 2007). Notably, the N-terminal region of NS3, encompassing the first 185 amino acids, serves as a serine protease, which is responsible for precisely processing the viral polyprotein. This protease activity is crucial for generating functional viral proteins required for the HCV life cycle (Gallinari et al. 1998). Beyond its direct role in viral replication and polyprotein processing, NS3 exhibits capabilities in modulating the innate immune response within the infected cell. It achieves this by disrupting the RIG-I pathway through cleaving the IPS-1 protein, which is essential for effective antiviral signaling (Loo et al. 2006). Furthermore, NS3 actively engages with cellular signaling pathways, showcasing its versatility in influencing various cellular processes. By interacting with protein kinase K and contributing to the delocalization of sMaf, NS3 has the capacity to regulate and modify an array of cellular signaling cascades. This dynamic interaction allows NS3 to impact cellular responses and contribute to the intricacies of viral-host interactions (Borowski et al. 1997).

1.1.6.6 NS4A

NS4A serves as a cofactor for the NS3 protease, facilitating its activity. NS4A contains three domains: an N-terminal hydrophobic domain for transmembrane alpha-helix formation, a central region for NS3 folding and a C-terminal acidic domain regulating NS5A hyperphosphorylation and viral replication. The central region of NS4A plays a key role in mediating the interaction with NS3 and activating its protease function. Additionally, the C-terminal transmembrane domain (TMD) of NS4A anchors the NS3-4A complex firmly within the ER membrane, providing a stable environment for their collaborative functions (Zhu and Briggs, 2011; Kim et al. 1997). Furthermore, NS4A is essential for the phosphorylation of NS5A, adding another layer of significance to its role in the viral life cycle (Asabe et al. 1997).

1.1.6.7 NS4B

NS4B is a protein with a molecular weight of 27 kDa, which contains four transmembrane domains (TMDs) that serve as anchors that secure it to the ER membrane. Its primary and vital function involves inducing the formation of the membranous web, a unique cellular structure formed by the restructuring of ER membranes and their interaction with LDs (Hügle et al. 2001). An essential role of NS4B is its indirect interaction with NS3 and NS5A through its association with NS4A, leading to the assembly of the HCV replication complex (RC) within the membranous web (Egger et al. 2002).

1.1.6.8 NS5A

NS5A is a phosphoprotein with two phosphorylation forms: hypophosphorylated form with a size of 56 kDa and a hyperphosphorylated form with a size of 58 kDa (Moradpour et al. 2007). NS5A is essential for viral replication, interacting with cellular and viral proteins and regulating cell signaling pathways and immune responses (Ashfaq et al. 2011; Zayas et al. 2016). NS5A is hydrophilic and consists of three domains, with an amphipathic α-helix at the N-terminus, enabling attachment to the ER membrane (Brass et al. 2002). Domain I contains a zinc binding

motif essential for RNA replication, while Domain II contributes to viral replication and Domain III is involved in infectious particle assembly (Appel et al. 2008; Ross-Thriepland et al. 2013).

In HCV-infected hepatocytes, the NS5A protein is located in the endoplasmic reticulum, where it forms virus-induced multiple-membrane vesicles. This is referred to as the membranous web and serves as the host for RNA replication complexes. Later on, viral RNA is transported from the replication complex to LDs, where particle assembly takes place (Ploen et al. 2013). NS5A, together with core protein, interact with lipid droplets, therefore playing a role in disruption of lipid metabolism contributing to steatosis (Shi et al. 2002). NS5A is also involved in targeting NS4B protein to lipid droplets (Riva et al. 2021). Additionally, NS5A induces lipid accumulation via the AMPK/SREBP-1c pathway (Meng et al. 2019). Human apolipoprotein E (apoE) was established to be crucial in HCV infectivity and assembly. C-terminal α-helix domain of apoE was found to be responsible for its interaction with NS5A leading to the targeting of NS5A to LDs (Cun et al. 2010).

NS5A possesses an interferon-α-sensitivity-determining region (ISDR) that represses the antiviral protein kinase R (PKR) induced by interferon (Gale et al. 1997). The phosphorylation forms of NS5A act as a switch between viral replication and viral particle assembly/release. The basal form may facilitate replication, while hyperphosphorylation is required for assembly and release (Goonawardane et al. 2017). The hyperphosphorylation of NS5A is dependent on the NS3-mediated autocleavage between NS3 and NS4A, followed by its release from the NS4A-5A polyprotein (Chiang et al. 2020). NS5A can modulate the MAPK pathways involved in hepatocyte transformation and HCC formation, affecting apoptosis, cell growth, ROS-dependent pathways and the PI3K pathways (Macdonald et al. 2004). It also mediates the recruitment and activation of c-Raf kinase, essential for viral replication through the MEK/ERK signaling pathway (Bürckstümmer et al. 2006; Himmelsbach et al. 2009).

1.1.6.9 NS5B

NS5B, with a molecular weight of 65 kDa, serves as the RNA-dependent RNA polymerase (RdRp) in the HCV life cycle. It plays a primary role in catalyzing the synthesis of viral RNA. An α-helix structure at its C-terminus acts as an anchor, attaching NS5B firmly to the ER membrane, enhancing its stability and function (Moradpour et al. 2007). NS5B utilizes plus-strand RNA as a template and actively generates complementary minus-strand RNA, which serves as a template for new plus-strand genomes. This direct synthesis allows for rapid amplification of viral RNA in infected cells (Ashfaq et al. 2011). However, errors can occur during replication due to the lack of a proofreading function, leading to the generation of diverse genetic variants called quasispecies (Martell et al. 1992; Tsukiyama-Kohara and Kohara 2017). This provides mutations, which enables HCV to adapt and evade the host immune response. NS5B is a major target for antiviral agents aimed at inhibiting HCV propagation and disease, due to its role in viral replication (Ashfaq et al. 2011). Targeting NS5B effectively offers a promising approach for developing antiviral therapies to combat HCV infection.

1.1.7 Life cycle of HCV

1.1.7.1 Entry and uncoating HCV

Upon primary infection, HCV particles circulate in the bloodstream until they encounter the surface of hepatocytes. The entry process (Figure 3) is orchestrated through interactions with several cell receptors, including glycosaminoglycans (GAGs) present on heparan sulfate proteoglycans (HSPGs), low-density-lipoprotein receptor (LDLR), Cluster of Differentiation 81 (Tetraspanin-28) (CD81), (scavenger receptor class B member 1 (SCARB1), the tight junction proteins claudin-1 (CLDN1), the tight junction proteins claudin-6 (CLDN6), the tight junction

proteins claudin-9 (CLDN9), (the receptor tyrosine kinases epidermal growth factor receptor (EGFR) and ephrin receptor A2 (EphA2), the cholesterol transporter Niemann-Pick C1-like 1 (NPC1L1), transferring receptor 1 (TfR1) and the cell death-inducing DFFA-like effector b (CIDEB), C-type lectins liver/lymph node-specific intercellular adhesion molecule-3-grabbing integrin (L-SIGN, dendritic cell-specific intercellular adhesion molecule-3-grabbing nonintegrin (DC-SIGN) (Albecka et al. 2012; Martin and Uprichard 2013; Alazard et al. 2019). The scavenger receptor class B member 1 (SRB1) plays a critical role in HCV entry (Rice 2011). Upon initial contact with the host cell, SRB1 interacts with ApoE and LDL lipoproteins present in the HCV virion. This exposes the CD81 binding site on the E2 glycoprotein initiating the entry process. Additionally, the endopeptidase calpain-5 (CAPN5) and the ubiquitin ligase Casitas B-lineage lymphoma proto-oncogene B (CBLB) form a complex with CD81, supporting HCV entry (Scarselli et al. 2002; Dubuisson 2007). Following attachment, the viral particles move laterally to tight junctions and interact with CLDN1. The formation of a CD81-CLDN1 co-receptor complex is critical for downstream processes during viral entry, including Rho GTPase signaling, protein kinase A (PKA) and the Ras/MEK/ERK pathway, which are promoted by the signaling of epidermal growth factor receptor (EGFR) or ephrin type A receptor 2 (EphA2) (Douam et al. 2015; Alazard, et al. 2019). The tight junction protein OCLN is also essential for viral entry, although its involvement is believed to occur at a later stage. Following successful attachment and interaction with the host cell surface, the HCV particles are internalized into the host cell via clathrin-dependent endocytosis. Clathrin-coated vesicles mediate the internalization of the virus particles, facilitating their transport into the cell (Benedicto et al. 2009). Once internalized, the viral particles are transported along actin filaments through a process known as reverse actin transport. This transport mechanism facilitates the movement of the virus particles toward Rab5-positive early endosomes. Subsequently, a fusion process occurs, leading to the release of the capsid harboring the RNA into the cytoplasm (Dubuisson 2007).

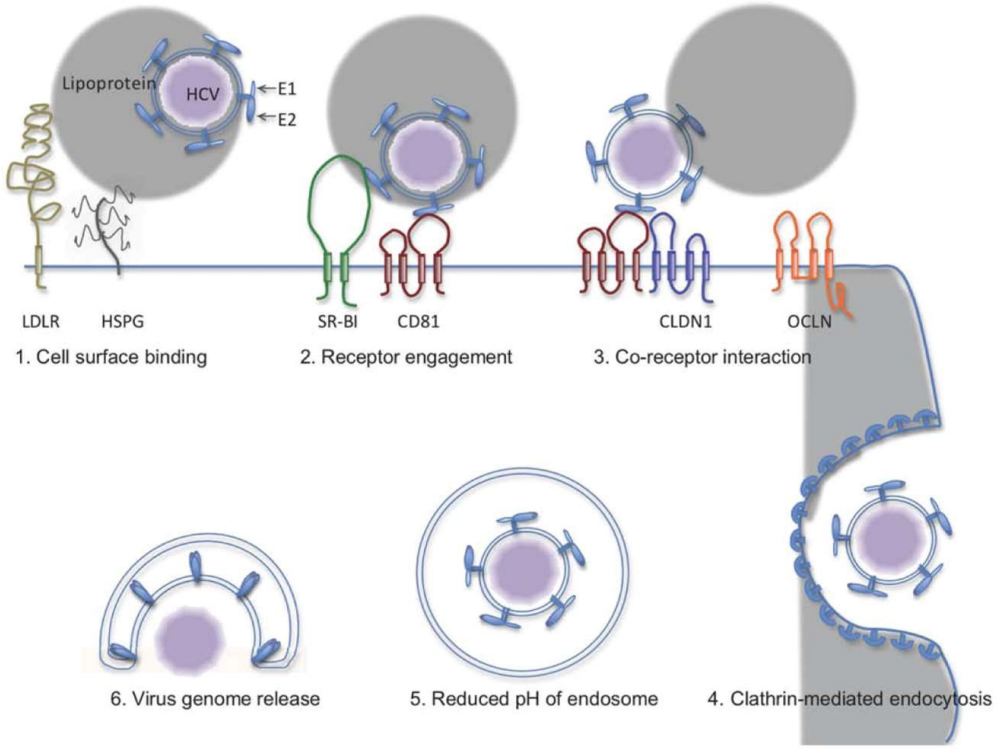

Figure 3. The HCV Entry Process (Wong-Staal et al. 2010). HCV entry into host cells begins with the contact of lipoproteins with LDLR and HSPG and attachment of the viral envelope glycoprotein E2 to specific receptors on the cell surface, including CD81 and scavenger receptor class B type I (SR-BI). This attachment allows the fusion of the viral membrane with the host cell membrane, enabling clathrin-mediated endocytosis and the release of the

viral RNA into the cytoplasm where replication and viral protein production occur, ultimately leading to the establishment of an HCV infection.

1.1.7.2 RNA translation and replication

The translation of viral RNA through IRES occurs at the rough ER, where the viral polyprotein is synthesized. Afterwards, the polyprotein is cleaved into ten mature proteins, consisting of both structural proteins (core, E1 and E2) and nonstructural proteins (p7, NS2, NS3, NS4A, NS4B, NS5A, NS5B) (Bartenschlager et al. 2004; Lindenbach and Rice 2005). The cleavage process is carried out by cellular proteases, which target the structural proteins and p7, while viral proteases are responsible for cleaving the nonstructural proteins (Lorenz 2010; Zephyr et al. 2021; Welbourn and Pause 2007). To support the replication process, host cell factors and viral proteins induce modifications to the cellular membranes, leading to the formation of a specialized structure known as the membranous web. This membranous web contains membranes derived from the ER, LDs and double-membrane vesicles (DMVs) (Figure 4.) (Romero-Brey et al. 2012; Blanchard and Roingeard 2018). The NS4B protein plays a crucial role in forming the scaffold for the membranous web, while NS5A induces the formation of DMVs through its interaction with the phosphatidylinositol-4-kinase-III (PI4KIII) (Stoeck et al. 2018; Tabata et al. 2020). The PI4KIII not only promotes the accumulation of phosphatidylinositol-4-phosphate (PI4P) within the membranous web, but it also induces the accumulation of cholesterol and other lipids in the membranes, which increase replication and assembly efficiency. To ensure the establishment of cholesterol-enriched DMVs, the virus manipulates lipid transfer proteins (Avula et al. 2021; Strating and Jm van Kuppeveld 2017). The regulation of HCV replication can be achieved by manipulating the cholesterol biosynthetic pathway and the replication rate of HCV can be effectively suppressed through the administration of lipid-lowering drugs (Kim and Chang 2013). Lipid droplets serve as intracellular storage organelles for excess fatty acids, cholesterol esters and triacylglycerides (TAG) surrounded by a phospholipid monolayer, coated with several proteins. They can form through the fusion of existing LDs or by accumulating neutral lipids in the ER membrane within the bilayer, leading to the formation of lens-like structures (Cohen 2018; Olzmann and Carvalho 2019; Lee et al. 2019). The budding of mature lipid droplets from the ER and the formation of their monolayer membrane requires proteins from the FIT (fat storage-inducing transmembrane protein) family, which are also involved in HCV replication and morphogenesis (Choudhary et al. 2015; Hayes et al. 2017). The interaction of nonstructural proteins with LDs, facilitated by Rab18, promotes viral replication (Salloum et al. 2013). Additionally, the tail-interacting protein of 47kDa interacts with NS5A and, along with Rab9, is involved in transporting viral RNA from the replication complex to LDs, where particle assembly takes place (Ploen et al. 2013). The replication process of the viral genome relies on the RNA-dependent RNA polymerase NS5B, which needs other non-structural proteins and host cell factors like cyclophilin B and the liver-specific microRNA miR-122. MiR-122 plays a crucial role in viral replication and, in conjunction with entry factors, contributes to HCV's host tropism. MiR-122 binds to the 5'-UTR of the HCV genome, leading to the recruitment of Argonaut 2 (Alazard et al. 2019, Joping 2012). This recruitment stabilizes the genome and shields it from the exonuclease Xrn1 (Kunden et al. 2020). Furthermore, cyclophilin B interacts with NS5B, enhancing the enzyme's RNA-binding activity (Moradpour et al. 2007). During the replication process, the (+)RNA genome functions as a template for NS5B to synthesize a negative-oriented RNA strand. This newly synthesized strand, in turn, serves as a template for generating several (+)RNA strands. These strands are utilized for translation, replication, or packaged into virions (Bartenchlager et al. 2013). Early during infection, HCV activates mTOR, which functions as an antiviral response by the host cells, leading to a decreased viral RNA level (Johri et al. 2020; KE et al. 2011; Stöhr et al. 2017). mTORC1, in turn, restricts HCV replication through ULK1, which modulates the levels of miR-122 and contributes to a balance between viral replication, virion packaging and release. Additionally, miR-22, supported by

glycogen synthase kinase 3 (GSK3), enhances viral replication, further affecting the dynamics of the infection process (Saleh et al. 2018).

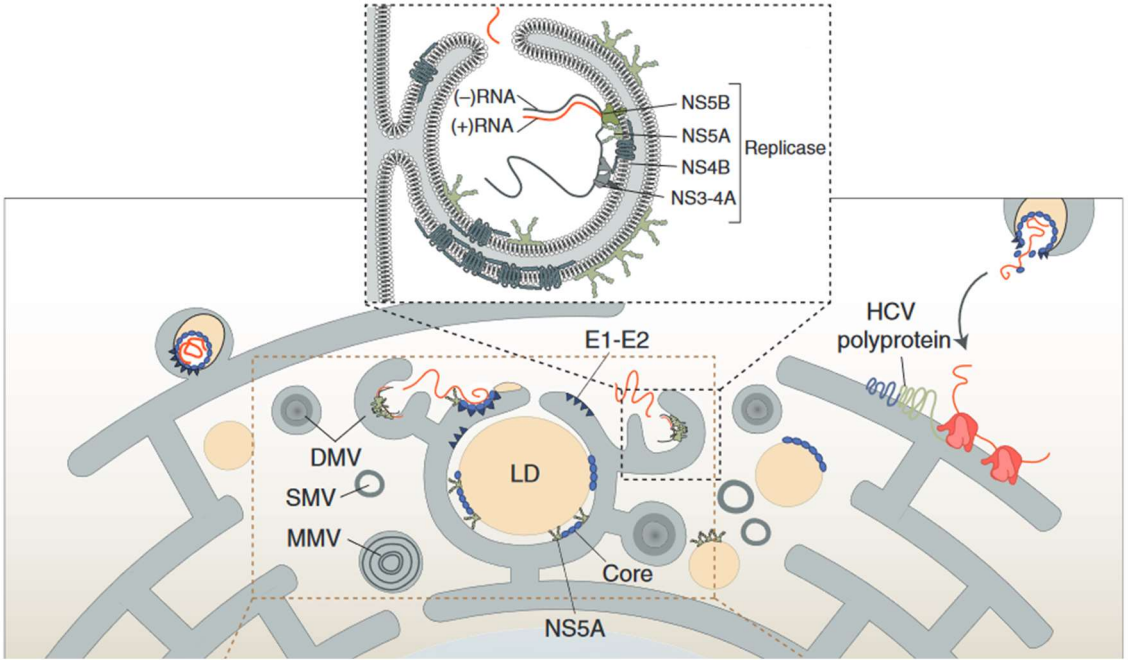

Figure 4. Replication machinery of HCV (Tabata et al. 2020). Upon the entry of the HCV genome into the host cell, it undergoes translation and the resulting polyprotein is processed. Afterwards, viral proteins interact with host factors to induce modifications in the cell's membranes, leading to the formation of different types of vesicles: single-membrane vesicles (SMVs), multimembrane vesicles (MMVs) and double-membrane vesicles (DMVs). These vesicles are closely associated with lipid droplets (LDs). Non-structural viral proteins reside on the surface of these LDs, playing a crucial role in the replication process. The RNA is delivered to nearby assembly sites by NS5A and NS3, which are enriched with core protein and E1-E2 envelope glycoprotein complexes.

1.1.7.3 Assembly and release

Hepatitis C virus (HCV) assembly is a crucial stage in the viral life cycle and it occurs in close proximity in detergent-resistant membranes (DRMs) of the ER or the mitochondrial-associated ER membranes (MAMs). The replication and assembly sites of HCV are interconnected with cytosolic lipid droplets (cLDs), which serve as essential platforms for the accumulation of viral components (Tabata et al. 2020). Cellular proteins DGAT1 and PLA2G4 transport Core protein to cytosolic LD surfaces (Herker et al. 2011). Core binds viral RNA, forming the nucleocapsid near the ER membrane where E1 and E2 accumulate. Local accumulation of E1E2 complexes is controlled by NS2, p7 and SPCS1 (Popescu et al. 2011; Suzuki et al. 2013). The capsid is sequestered into the ER lumen, acquiring a lipid bilayer with enriched E1E2 complexes (Huang et al. 2007). AP2M1 transports the core protein from LDs to the stalling site (Neveu et al. 2012).

Once the assembly is completed, the newly formed virions undergo further maturation before they become fully infectious. This maturation process involves forming LVPs through fusion or binding to lipoproteins, characterized by their low buoyant density (Gastaminza et al. 2006; Gastaminza et al. 2008) and the transfer of ready virions through the Golgi compartment, where they undergo finalization (Morozov and Lagaye 2018). The Golgi apparatus acts as a crucial organelle in modifying and processing the viral particles, preparing them for release. The release of mature virions occurs through the very-low-density lipoprotein (VLDL) pathway, which relies heavily on the presence of apolipoprotein B. This pathway facilitates the transport of the virions to the plasma membrane, where they can be released from the infected cell into the extracellular space to infect new host cells (Morozov and Lagaye 2018). HCV also induces

a decrease in α-taxilin (Elgner et al. 2016), which promotes the formation of the SNARE complex and facilitates the release of viral particles.

1.1.8 Model systems

Early efforts to isolate and culture HCV using traditional cell-based approaches were unsuccessful, as the virus could only replicate in specific cells, such as human or chimpanzee fetal liver cells and hepatocytes, or human peripheral blood mononuclear cells. Unfortunately, these cells were difficult to obtain and had a limited lifespan in culture, making them impractical for research (Kato et al. 1995; Lanford et al. 1994; Carcamo and Nguyen 2012). HCV replicon model was established in 1999 (Blight et al. 2000; Lohmann et al. 1999). Although the replicon could replicate autonomously within the cell, it was incapable of producing infectious viruses (Duverlie et al. 2007; Bartenschlager et al. 2013). The HCV replicon system is based on subgenomic replicons, allowing replication in hepatic cell cultures like the Huh 7 cell line. This replicon is a bicistronic RNA that expresses an antibiotic resistance gene under the control of the HCV IRES. Additionally, it contains the HCV nonstructural proteins NS3-NS5B under the control of a second IRES. The use of antibiotic selection on RNA-transfected Huh7 cells leads to the establishment of stable cell lines capable of low-level HCV replication. Another model, the HCV pseudotyped viral particles model, was developed in 2003 (Bartosch et al. 2003). This model utilized lentiviral vectors, with a reporter gene and HCV envelope proteins. The HCV pseudoparticles (HCVpp) enabled advanced studies on HCV receptors and the structure and function of the HCV envelope proteins.

A major breakthrough in HCV research occurred in 2005 when a genotype 2a HCV strain (JFH-1) from a patient with fulminant hepatitis C was obtained (Wakita et al. 2005). Utilizing the knowledge gained from studying the HCV subgenomic replicon, HCVcc (cell-culture-derived HCV) in the Huh 7 cell line was established. This in vitro experiment provided a comprehensive understanding of the complete lifecycle of HCV and the virus obtained from the cell cultures proved highly infectious in chimpanzees and immunodeficient mice with partial human livers (Lindenbach et al. 2006). Another relevant aspect was the identification of the Huh-7 subclone, Huh-7.5.1 with defects in innate response. This allowed efficient virus propagation and provided a tool for the analysis of the interactions between virus and host (Zhong et al. 2005).

Afterward, various chimeras were developed (Figure 5.). One such chimera combined the NS3-NS5B region of the JFH1 isolate with the core-NS2 region from another genotype 2a isolate (J6) (Pietschmann et al. 2006). This resulted in two distinct chimeras: J6/JFH1, with a genotype breakpoint between NS2 and NS3 and Jc1, with a breakpoint within NS2 (Lindenbach et al. 2006; Pietschmann et al. 2006). The JFH1 region allowed efficient in vitro replication and infection, while the J6 region enhanced the production of viral particles. Based on the Jc1 construct, a bicistronic luciferase reporter virus was developed, where enzyme activity was directly proportional to viral replication (Koutsoudakis et al. 2006). To serve as a negative control, a replicon deficient virus by introducing a point mutation in the catalytic motif of the RNA-dependent RNA polymerase NS5B, changing GDD to GND (Wakita et al. 2005) was developed. Figure 5 illustrates the different HCV constructs.

Figure 5. Overview of HCV constructs (Elgner 2016, modified). The replication-deficient mutant GND was derived from the JFH1 isolate (genotype 2a). The chimera Jc1 consists of the structural proteins p7 and segments of NS2 from the J6 isolate (genotype 2a), along with the remaining non-structural proteins from JFH1. In the bicistronic reporter virus Jc1-Luc, an IRES-dependent luciferase is positioned upstream of the Jc1 sequence.

Chimpanzees were the primary animal model for HCV research due to their close genetic similarity to humans. However, ethical considerations, cost and the lack of cirrhosis development in chronically infected chimpanzees led to the exploration of alternative small animal models, such as the tree shrew and a chimeric human liver mouse, those animals also do not develop cirrhosis (Xie et al. 1998; Mercer et al. 2001).

To address the limitations of existing mouse models, human hepatocellular factors using a recombinant adenovirus expression system were introduced into mice. These genetically manipulated mice expressed human CD81, scavenger receptor type B class 1, claudin 1 and OCLN genes, which made them susceptible to HCV infection. This immunocompetent small animal model provided valuable insights into HCV co-receptor biology and served as a useful tool to evaluate antiviral drugs and neutralizing antibodies (Ploss et al. 2009; Wang 2013). All these animal models provide valuable insight, but those systems are still limited an no model system can fully replicate human HCV infection. Table 1. presents summary of HCV models.

Table 1. Summary of in vitro and in vivo models for hepatitis C virus (Wang 2013).

In vitro and in vivo models	Established year	Advantages	Deficiencies
In vitro			
Cultivation of HCV	1993-1999	Achieved cultivation of HCV in human foetal liver cells, human hepatocytes or PBMC. Illustrated HCV is quite species selective and has a narrow range of hosts	Requires specific cellular factors to support viral lifecycle. Primary human and chimpanzee hepatocytes or highly differentiated cells dependent. Most of them have yielded limited success. Poor reproducibility and low levels of HCV replication.
HCV replicon	1995-2000	Provided a cell-based model for the study on HCV genome replication	
HCV VLP	1998-1999	Rare evidence to support that HCV structural proteins core, E1 and E2 could form VLP	
HCVpp	2003	Provided a convenient and feasible tool for studies on viral entry, HCV receptor, neutralizing antibody, etc.	
HCVcc	2005	A break through in production of infectious hepatitis C virus in tissue culture	
In vitro			

In vitro and in vivo models	Established year	Advantages	Deficiencies
In vitro			
Chimpanzee	1979	The only recognized animal model for HCV study, played a critical role in HCV discovery and play an essential role in defining the natural history of HCV	Chimpanzees differ from humans in their course of infection, that chronic carriers do not develop cirrhosis or fibrosis, limited availability, cost performance and public resistance
Tree shrew	1998	Might be a succedaneum for chimpanzees	Persistent HCV infection could not be established and only 25% of infected animals developed transient or intermittent viremia. Germ line was not available to a small animal model
Chimeric human liver mouse	2001	Exhibited prolonged infection with high viral titers following inoculation with HCV isolated from human serum. HCV can be transmitted horizontally. Drug evaluation	Since the mice were immunodeficient, they were not appropriate models to study HCV pathogenesis
Genetically humanized mouse	2011	Represents the first immunocompetent mice model for HCV study. Allows for the studies of HCV coreceptor biology in vivo	Operation is difficult

HCVpp: Hepatitis C virus (HCV) pseudotyped viral particles; VLP: Virus like particle; HCVcc: Cell culture derived HCV.

1.2 Lipids as key factors in cellular membranes, energy storage and signaling pathways

Lipids play take part in cellular functions and their roles can be categorized into three general groups. Firstly, phospholipids, sphingolipids and cholesterol, function as central components of cellular membranes. These lipids contribute to the structural integrity and functional versatility of membranes. The environment of cellular membranes is primarily composed of amphipathic lipids, with both hydrophobic and hydrophilic segments. This amphipathic nature allows membranes to form spontaneously, when immersed in water. This ability to self-associate allowed for the segregation, not just from the outside environment, but of the cell's insides into different compartments called organelles. This compartmentalization brought numerous advantages, by separating chemical reactions, allowing each organelle to carry out its functions independently; limiting the spreading of reaction products, preventing unwanted interference between different cellular processes and led to a remarkable improvement in biochemical efficiency, as it concentrated essential components and enzymatic machinery in localized regions. Additionally, lipids participate in membrane dynamics in processes such as: budding, tubulation, fission and fusion are orchestrated by lipids, which enables cellular functions such as: cell division, biological reproduction and intracellular membrane trafficking. These dynamic processes ensure the proper distribution of cellular components, enable the exchange of essential molecules between compartments and facilitate intercellular communication (Horn and Jaiswal 2019; Casares et al. 2019).

Secondly, lipids are stored in LDs, which primarily consist of triacylglycerols (TAGs) and stearyl esters. Lipid reserves serve as an important energy source and during periods of high energy demand or nutrient scarcity, the stored lipids can be broken down to release energy and sustain cellular activities (Zhang et al. 2019; Casares et al. 2019). The significance of LDs and lipid storage goes beyond energy preservation. Additionally, LDs protect cells from lipotoxicity, by sequestering and storing lipids, what prevents potential damage caused by lipid overload (Nguyen and Olzmann 2017).

Finally, some lipids serve as signaling molecules in various cellular pathways. This includes: phosphatidic acid (PA), sterols, free fatty acids (FAs), glycerolipids and sphingolipids. Lipids are able to regulate and coordinate multiple cellular processes, maintain significant influence over cell growth, differentiation, apoptosis and response to external stimuli. In the process of signal transduction, lipids define membrane domains, providing the structural framework that allows proteins to aggregate and disperse. This organization of proteins then leads to the formation of secondary signaling or effector complexes, facilitating a cascade of events that mediate the cellular response. Additionally, lipids can function as both first and second messengers, initiating and amplifying signaling pathways. When amphipathic lipids undergo rupture, they generate bipartite signaling elements with diverse functions (van Meer G et al. 2017). These elements can be distributed within the membrane, thanks to the hydrophobic portions of the molecules and also travel through the cytosol via their soluble and polar regions, facilitating communication between different cellular compartments. The involvement of these specialized lipids in cellular signaling pathways highlights their flexibility and importance in orchestrating complex cellular responses (Hla and Dannenberg 2012; Breslow and Weissman 2010).

1.2.1 Cellular cholesterol homeostasis

Cholesterol is involved in maintaining membrane permeability, fluidity and takes part in signaling pathways. Its levels are dynamically regulated through de novo biosynthesis, exogenous uptake, storage and export. The intracellular cholesterol trafficking is depicted in the Figure 6. Cholesterol is involved in synthesizing steroid hormones, bile acids and vitamin D. Most cells can produce cholesterol, but the primary sites are hepatocytes and enterocytes (Afonso et al. 2018; Maxfield and van Meer G 2010).

1.2.1.1 Cholesterol Uptake

Cholesterol absorption involves several mechanisms, including solubility and sterol release from micelles. A protein Niemann-Pick-C1-like-1 (NPC1L1) regulates cholesterol absorption in the upper small intestine (Altmann et al. 2004). Inside enterocytes, cholesterol is esterified with a fatty acid by acyl-cholesterol acyl transferase (ACAT2) in the ER. The resulting cholesteryl ester is transported with chylomicrons, which are processed in the Golgi apparatus and then secreted into circulation via the thoracic duct. Some free cholesterol is also excreted back into the intestinal lumen through transporters like ATP-binding cassette transporters sub-family G members 5 and 8 (ABCG5 and ABCG8) (Nguyen et al. 2012). Liver X Receptor (LXR), a nuclear receptor, is a key factor in regulating cholesterol uptake and secretion in the intestine. LXR inhibits NPC1L1 and activates ABCG5 and ABCG8. Furthermore, LXRs increase cholesterol efflux from enterocytes by upregulating ABCA1 expression. LXR's effects prevent cholesterol buildup in enterocytes. It is important to note that both dietary cholesterol and de novo synthesized cholesterol are essential for maintaining intestinal integrity (Alfonso et al. 2018; Luo et al. 2019; Duan et al. 2022; Shi et al. 2022).

1.2.1.2 Cholesterol Biosynthesis and Uptake

Cholesterol biosynthesis and uptake are tightly regulated through negative feedback mechanisms that sense cholesterol and oxysterol levels. The transcription factor SREBP-2 (Srebf2) is an important factor in controlling key genes involved in cholesterol synthesis (HMGCR, HMGCS, MVK) and uptake (LDLR) (Brown et al. 2018). SREBP-2 is located on the ER membrane, with its NH2- and COOH-terminal domains facing the cytosol. When cholesterol levels drop, the SCAP-SREBP complex dissociates from Insig-1, leading to Insig-1's degradation and the subsequent sorting of the complex into COPII-coated vesicles. These vesicles transport the SCAP-SREBP complex from the ER to the Golgi, where SREBP is cleaved, releasing its active NH2-terminal domain. This domain enters the nucleus and

activates the transcription of target genes involved in cholesterol synthesis and uptake (Sun et al. 2005). Aside from regulating cholesterol synthesis and uptake genes, SREBP-2 also inhibits cholesterol efflux by binding to the ABCA1 promoter's E-box region, reducing cholesterol release from cells. Additionally, miR-33, a microRNA co-transcribed with SREBF2, suppresses cholesterol trafficking and export, rapidly restoring intracellular cholesterol levels (Rayner et al. 2011). Under conditions of cholesterol abundance, the Insig1-SCAP-SREBP2 complex remains anchored to the ER due to conformational changes in SCAP that favor its binding to Insig-1. Cholesterol or 25-hydroxycholesterol in the ER membrane prevents the assembly of COPII-coated vesicles, further trapping the complex in the ER. This process is regulated by the MELADL sequence in SCAP, which becomes inaccessible when Insig-1 binds, blocking the binding site for coat proteins and inhibiting vesicle assembly. Additionally, cholesterol binding to SCAP's luminal loop 1 displaces its binding to loop 7, promoting an open conformation that facilitates Insig-1-SCAP binding and restricts COPII protein access to the MELADL sequence. Recent findings indicate that SREBP2's transcriptional activity can be repressed by the ubiquitin E3 ligase Rnf145, induced by LXR, another cholesterol regulator (Cook et al. 2017). Rnf145 ubiquitinates SCAP, hindering its transport to the Golgi and contributing to cholesterol homeostasis (Alfonso et al. 2018).

1.2.1.3 The LDLR and Cholesterol Uptake

LDL particles belong to the lipoprotein family and are responsible for transports of lipids within an organism. Examples of lipoproteins include chylomicrons, VLDL, IDL and HDL. Each particle has a lipophilic core with unique lipid composition, enveloped by a phospholipid membrane and accessory proteins [294,295]. The LDLR binds to LDL particles and undergoes endocytosis, leading to LDL degradation in lysosomes (Goldstein and Brown 2009). Cholesterol negatively regulates LDLR expression through SREBP-2, reducing LDL uptake when intracellular cholesterol is high and inducing it when cells are cholesterol-deprived. Proprotein convertase subtilisin/kexin type 9 (PCSK9) further regulates LDLR levels at the plasma membrane by directing it to lysosomes for degradation. Mutations in PCSK9 can cause autosomal-dominant hypercholesterolemia (Poirier et al. 2009). LXR ligands decrease LDL particle binding and uptake through the inducible degrader of LDLR (IDOL), which ubiquitinates and degrades LDLR. Oxidized LDL contributes to atherosclerosis by transport of the cholesterol to arterial wall macrophages through receptors including LOX-1, CD36, SR-A and SR-B1, which leads to to the formation of lipid-laden cells (Hong et al. 2010). Cholesterol efflux, facilitated by HDL, is essential in preventing atherosclerosis, as it transports excess cholesterol from peripheral tissues to the liver for excretion, in reverse cholesterol transport (RCT) (Karathanasis et al. 2017; Alfonso et al. 2018).

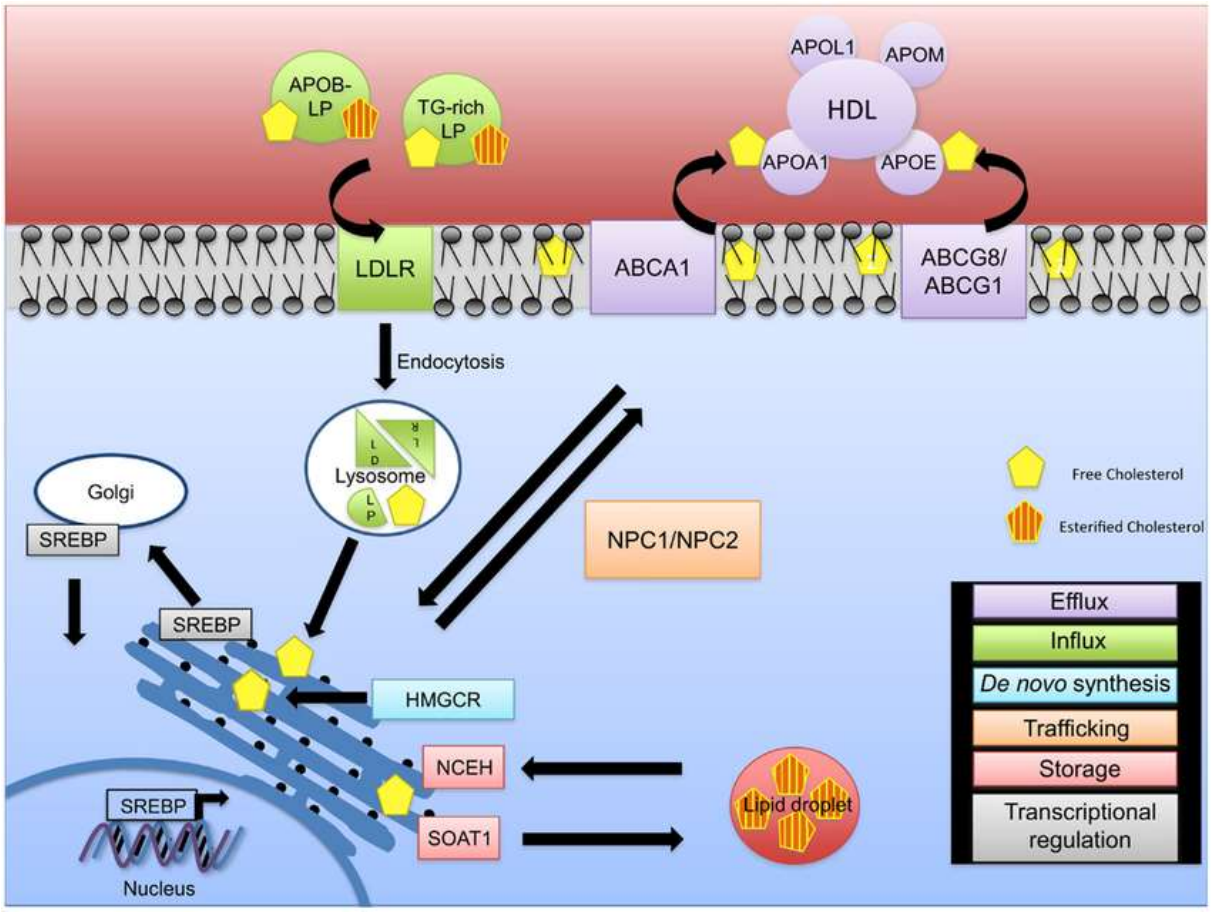

Figure 6. Intracellular cholesterol trafficking (Merscher et al. 2014). Cholesterol homeostasis is tightly regulated through various mechanisms. Free cholesterol is produced through de novo synthesis (blue), which involves the key enzyme HMGCR located in the ER. In situations where cellular cholesterol levels are low, cholesterol influx occurs (green) with the help of APOB-rich lipoproteins and triglyceride-rich lipoproteins. These lipoproteins are internalized via endocytosis and transported to the lysosome for degradation, releasing LDL and VLDL remnants and afterwards, free cholesterol. Since excess free cholesterol can be harmful, it is transported to the plasma membrane using NPC1/2 and then transported from the cell through an ABCA1-ApoAI/L1- or ABCG1/8-HDL-mediated mechanism (purple). Alternatively, the excess free cholesterol can be converted into cholesteryl esters via SOAT1, leading to the formation of cholesterol-enriched lipid droplets (red). These cholesteryl esters can later be converted back to unesterified (free) cholesterol through NCEH. The regulation of cholesterol pathways also occurs at the transcriptional level (grey). When there is a shortage of cholesterol, SREBP is transported to the Golgi apparatus and undergoes cleavage, allowing it to enter the nucleus and regulate the expression of cholesterol-related genes. This finely orchestrated network of mechanisms ensures the maintenance of cholesterol levels within the cell.

1.2.1.4 Cholesterol modulating drugs

Cholesterol metabolism's precise regulation presents clinical opportunities for achieving specific outcomes by reducing cholesterol levels in patients with hypercholesterolemia or cholestasis. Various lipid-lowering drugs act through different mechanisms to achieve this goal. The discovery of cholesterol-lowering drugs began with Fibrates in the late 1950s, exemplified by Clofibrate, which led to the development of derivatives like Bezafibrate, Fenofibrate and Gemfibrozil. These drugs activate PPARα, suppressing bile acid synthesis and resulting in reduced serum cholesterol (Horinouchi et al. 2023; Post et al. 2001). In the early 1970s, Statins emerged as more selective cholesterol-lowering agents. Drugs such as Pravastatin, Fluvastatin, Atorvastatin and Simvastatin inhibit HMGCR, which decreases intracellular cholesterol and systemic cholesterol levels (Day et al. 1997; Tanaka et al. 1994). A third group of compounds, including Lecimibid or Avasimibe, interferes with cholesterol storage in LDs by

targeting ACAT. However, they were not adopted for clinical use (Delsing et al. 2001). Novel approaches to lower systemic cholesterol involve larger molecules such as cyclosporin A-derivatives, hormones, or antibodies. PSC833 inhibits ABC-transporters, leading to increased cellular cholesterol levels (Nagao et al. 2013). NGM282, acting as a hormone, inhibits CYP7A1-expression, altering cholesterol detoxification. Monoclonal antibodies Evolocumab and Alirocumab offer another strategy (Friche et al. 1992; Sabatine et al. 2015). They bind PCSK9, preventing LDLR degradation and increasing LDL uptake for clearance from serum (Chaudhary et al. 2017). In summary, these compounds aim to reduce serum cholesterol, but they differ in their effects on intracellular cholesterol levels. While statins decrease cholesterol synthesis, others like Fibrates, Avasimibe, PSC833, FGF19 and Alirocumab either increase cholesterol uptake or retain it within cells (Hirschfield et al. 2019; Zhou et al. 2019).

1.2.2 HCV exploits lipids for its life cycle

Hepatitis C virus relies on reprogramming lipid metabolism at various stages of its life cycle to ensure its successful replication and propagation within host cells (Figure 7). The virus interferes with key pathways of lipid synthesis and insulin signaling, impacting lipid metabolism within infected cells (Chang 2016). Insulin resistance can arise from elevated levels of free fatty acids, elevated ROS levels, as well as increased suppressor of cytokine signaling 3 and tumor necrosis factor alpha (TNF-α) levels (Elgretli et al. 2013; Uysal et al. 1997). These factors lead to the downregulation of insulin receptor substrate signaling 1. Consequently, increased insulin production causes accumulation of glucose. With an accumulation of lipogenic substrates (glucose and free fatty acids) and high lipogenic hormone levels (hyperinsulinemia), lipogenesis becomes overstimulated, ultimately leading to hepatic steatosis (McCullough 2004).

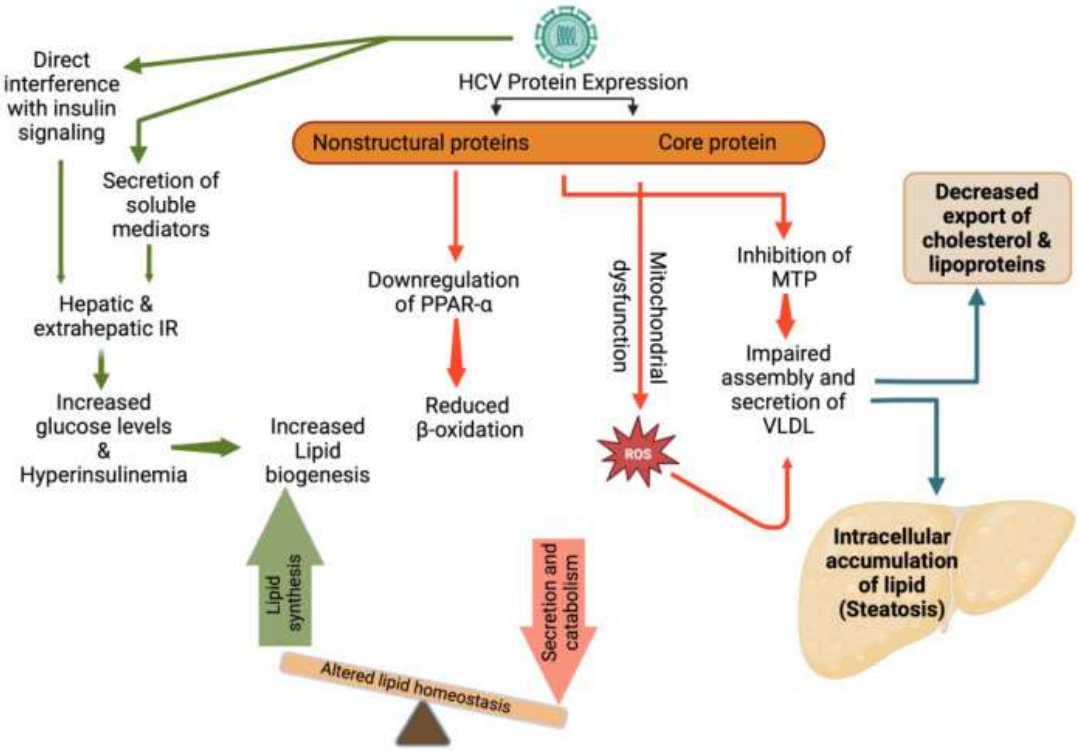

Figure 7. HCV causes changes in lipid metabolism and steatosis (Elgretli et al. 2023). HCV is associated with insulin resistance (IR) and affects peroxisome proliferator-activated receptor-α (PPAR-α), reactive oxygen species (ROS), microsomal triglyceride transfer protein (MTP) and very-low density lipoproteins (VLDL).

The initial step of the HCV life cycle, virus entry, is already heavily dependent on lipids as described in 1.1.7.1. A critical entry factor, the cholesterol transporter Niemann-Pick C1-like 1 (NPC1L1), is located on the surface of hepatocytes. HCV particles exploit cholesterol regulation to indirectly enter hepatocytes by reabsorbing biliary cholesterol secreted in the bile, thereby establishing a connection between cholesterol transport and viral entry (Popescu et al. 2014). In typical physiological conditions, LDLr facilitates the internal transportation of cholesterol-rich LDL via clathrin-mediated endocytosis. Given the competitive relationship between HCV and LDL for LDLr, it has been proposed that higher levels of apoB-associated cholesterol, like LDL, could serve as a potential predictor for HCV treatment response (Elgretli et al. 2013; Sorrentino et al. 2013).

Upon infection with HCV, a notable consequence is the induction of increased lipogenesis, leading to the excessive production of lipids. Simultaneously, HCV disrupts the export and degradation of these lipids, resulting in their accumulation within the host cell. The virus achieves this by interfering with mitochondrial lipid β-oxidation, which contributes to the altered lipid homeostasis observed during HCV infection (Chang 2016). HCV RNA replication further highlights the virus's reliance on high lipid content. To facilitate this step, the replication organelle must acquire a means of transferring cholesterol and sphingolipids along the endosomal-lysosomal pathway. Here, the non-structural protein NS5A hijacks cholesterol lipid transfer proteins to create a favorable environment for viral genome replication. HCV viral particles are packaged into endoplasmic reticulum luminal lipid droplets along with VLDL cholesterol precursor. These lipoviral particles are then secreted into circulation through the VLDL-dependent pathway. This disruption of lipoprotein homeostasis by HCV infection impairs the VLDL-releasing pathway, contributing to hepatic steatosis (Yoshimura and Oppenheim 2008; Chaudhari et al. 2021). HCV manipulates the host factor diacylglycerol acyltransferase-1 to facilitate the creation of lipid droplets. Additionally, NS5A binds to PAT proteins, family of lipid droplet proteins that regulate cellular lipid stores, to enable targeting of LDs (Vogt et al. 2013). LTPs like the oxysterol-binding protein (OSBP) and the glycosphingolipid transfer protein four-phosphate adaptor protein 2 (FAPP2) work in conjunction with NS5A to increase cholesterol concentration at the ER, the site of viral replication. These proteins catalyze the transfer of unesterified cholesterol from the ER to the Golgi compartment, where they exchange cholesterol for phosphatidylinositol-4-phosphate (PI4P), an essential component for HCV replication (Stoeck et al. 2017).

Similar to other positive-sense RNA viruses, HCV, triggers host membrane modifications known as the membranous web to support its replication. The virus can efficiently replicate and package, while also evading the host's innate immune defenses, by gathering replication factors within the MVBs. The formation of the HCV membranous web is a complex process that relies on a collaborative interplay between HCV nonstructural proteins and a growing array of host factors, as well as numerous lipids (Wang and Tai 2016; Zhang et al. 2019). Viral Replication Complexes (VRCs) can be classified morphologically into two types: invagination-type or protrusion-type, depending on whether the donor membrane curves away from or into the cytoplasm, respectively (Figure 8A). A negative membrane curvature results in membrane invagination away from the cytoplasm, creating an environment where viral replication proteins and viral RNA synthesis take place inside the VRCs (Figure 8B). In contrast, positive membrane curvature leads to the protrusion of membranes into the cytoplasm, facilitating viral RNA synthesis on the surface of the VRCs (Figure 8C). Most of the Flaviviruses, like ZIKV, DENV and WNV, have an invagination type VRCs, but HCV has a protrusion type VRC. These protrusion VRCs may also form double-membrane vesicles, providing a protected environment for viral replication (Romero-Brey and Bartenschlager 2014; Strating and van Kuppeveld 2017; Zhang et al. 2019).

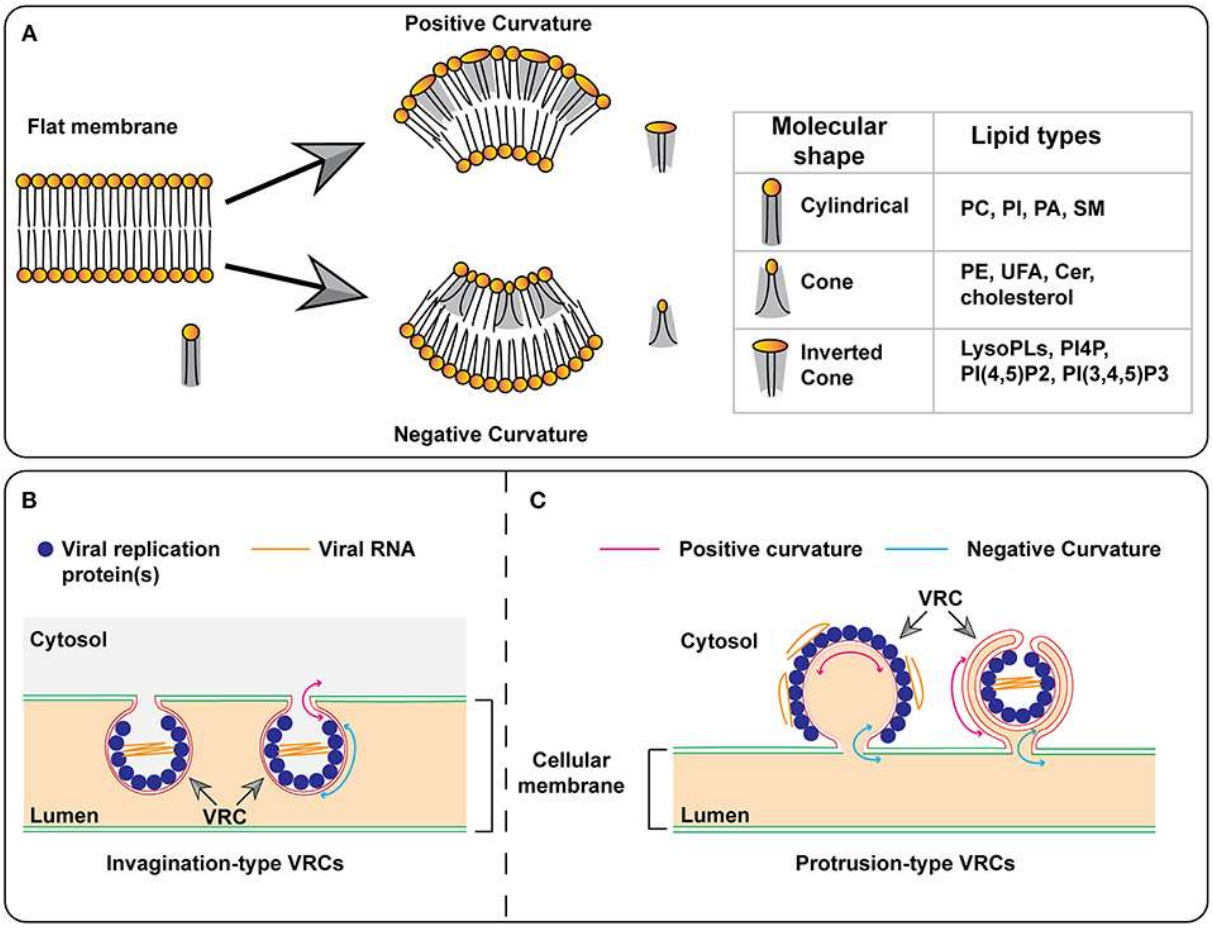

Figure 8. Models for the formation of membrane curvature and viral replication complexes (Zhang et al. 2019). (A) The introduction of specific lipids with either cone or inverted-cone shapes induces negative or positive membrane curvature, respectively. (B, C) Illustrations depicting the mechanisms behind invagination-type and protrusion-type replication complexes. In the protrusion-type model, the VRC on the right illustrates the formation of a double-membrane vesicle (DMV). PC, phosphatidylcholine; PI, phosphatidylinositol; PI4P, phosphatidylinositol-4-phosphate; $PI(4,5)P_2$, phosphatidylinositol-4,5-bisphosphate; $PI(3,4,5)P_3$, phosphatidylinositol-3,4,5-trisphosphate; PA, phosphatidic acid; SM, sphingomyelin; PE, phosphatidylethanolamine; UFA, unsaturated fatty acid; Cer, ceramide; VRC, virus replication complex.

Moreover, additional lipid transfer proteins have been identified to selectively impact HCV replication. Among them are steroidogenic acute regulatory protein-related lipid transfer domain protein 3 (STARD3), oxysterol-binding protein-related protein 1A and -B (OSBPL1A and -B) and Niemann-Pick-type C1 (NPC1). HCV also exploits NPC1 to recruit unesterified cholesterol from regions of high cholesterol content to the sites of viral replication, further highlighting the virus's capacity to manipulate host lipid metabolism for its benefit (Stoeck et al. 2017).

As the viral life cycle progresses, HCV assembly sites emerge as critical hubs for lipid metabolism reprogramming. LDs are cellular deposits rich in cholesterol esters and triacylglycerides and play a crucial role in HCV particle assembly; without them, the formation of infectious viral particles cannot take place. An important host cofactor called TIP47 binds to the HCV protein NS5A, initiating a complex interaction that facilitates the integration of LDs into membranous webs, where viral replication occurs. Even after viral release, the association with TIP47 persists, underscoring its significance in HCV replication and particle release (Ploen et al. 2013). Furthermore, viral particle assembly relies heavily on its association with apolipoproteins. The maturation process follows a pathway similar to that of Very Low-Density

Lipoprotein (VLDL) maturation. This association ensures the formation of mature and infectious viral particles, enabling HCV to exploit the host's lipid machinery to efficiently propagate and infect other cells (Popescu et al. 2014).

HCV life cycle involves complex interactions with host lipid metabolism at multiple stages. The virus effectively manipulates lipid pathways to establish infection, promote replication and generate infectious particles. Understanding these mechanisms is crucial for developing targeted antiviral therapies aimed at disrupting the virus's reliance on lipid metabolism, offering promising strategies to combat HCV infections effectively. These connections are relevant for HCV-associated pathogenesis and a significant global health concern.

1.2.3 HCV and oxidative stress

1.2.3.1 Implications for Insulin Signaling and Metabolism

Infection with HCV has a negative effect on liver cells, particularly in terms of inducing oxidative stress. Infection leads to elevated levels of 8-hydroxydeoxyguanosine (8-OHdG) and reactive aldehydes (for example 4-Hydroxy-2-nonenal) produced by lipid peroxidation (Fujita et al. 2008). The imbalance between reactive oxygen species (ROS) or reactive nitrogen species (RNS) production and the cell’s ability to neutralize them leads to potential damage and disruption of cells normal metabolic processes. The primary sources of ROS and RNS, such as: superoxide anions (O2 •−), hydroxyl radicals (HO•), hydrogen peroxide (H2O2), nitric oxide (NO), nitrogen dioxide (NO2) and nitrate (NO3), are the mitochondria, ER, peroxisomes and other organelles. These cellular organelles become major contributors to the increased oxidative stress observed during HCV infection (Rebbani and Tsukiyama-Kohara 2016; Ivanov et al. 2013).

The elevated levels of ROS caused by HCV infection have a negative impact on insulin-dependent signaling pathways in liver cells. The activation of c-Jun N-terminal kinase and the resulting activation of serine/threonine phosphorylation of IRS1/2 mediates the inhibition of insulin receptor signaling in a ROS-dependent manner (Gastaldi et al. 2017). Additionally, the excess ROS interfere with the functions of AMP-activated kinase (AMPK) through the activation of protein phosphatase 2A (PP2A). Moreover, liver biopsies from CHC patients showed an increased expression of peroxisome proliferator-activated receptor-gamma co-activator 1α (PGC-1α) in HCV-infected cells (Shlomai et al. 2012). PGC-1α is a transcriptional co-activator of genes involved in gluconeogenesis initiation (Lin et al. 2005) and is implicated in insulin resistance induction in response to oxidative stress (Kumashiro et al. 2008). ROS-mediated elevation of PGC-1α transcript levels corresponded with up-regulation of glucose-6 phosphatase (G6Pase) and increased glucose production (Shlomai et al. 2012). This disruption leads to a state of insulin resistance, where liver cells become less responsive to insulin's regulatory signals.

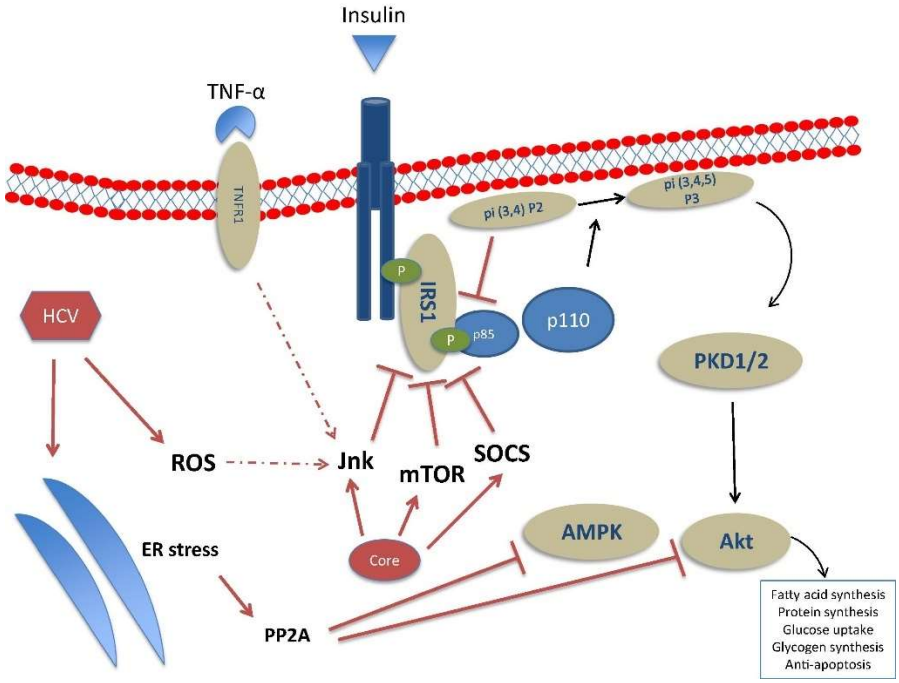

Figure 9. Various interactions between HCV and the hepatocyte insulin signaling pathway (Gastaldi et al. 2017). HCV core can directly activate inhibitors of insulin signaling, including mammalian target of rapamycin (mTOR), suppressor of cytokine signaling (SOCS)-3 and c-Jun N-terminal kinase (JNK). Additionally, HCV induces ER stress, leading to the activation of protein phosphatase 2A (PP2A), which inhibits Akt and AMP-activated kinase (AMPK), crucial regulators of gluconeogenesis. Other abbreviations: PKD1/2 (protein kinase D1/2) and p85/p110 (subunits p85 and p110 of phosphatidylinositol 3-kinase).

As a consequence, insulin resistance induces the sterol regulatory element binding transcription factor 1 (SREBF1), which is a transcription factor responsible for promoting the expression of genes involved in fatty acid biosynthesis. Resulting increase in the synthesis of fatty acids in liver cells, contributes to the development of fatty liver disease. Increased fatty acid biosynthesis causes inhibition of liver regeneration and impacts overall health of the liver. The liver's ability to repair and regenerate itself is crucial for maintaining its normal physiological functions and disruption caused by HCV-induced oxidative stress can prevent liver regeneration (Clément et al. 2009; Kim et al. 2007).

In conclusion, infection with HCV induces oxidative stress in liver cells, resulting in elevated levels of reactive oxygen and nitrogen species. Oxidative stress negatively impacts insulin-dependent signaling pathways, leading to insulin resistance and subsequent activation of SREBF1, which further promotes fatty acid biosynthesis. As a consequence, liver regeneration is inhibited, compromising the liver's ability to repair and maintain its optimal function. Aftermath of impaired liver regeneration can lead to liver fibrosis, cirrhosis and hepatocellular carcinoma (Jindal et al. 2021; Allaire and Gilgenkrantz 2018). Understanding these mechanisms is essential for developing effective strategies to mitigate the consequences of HCV infection on the liver and overall health (Rebbani and Tsukiyama-Kohara 2016).

1.2.3.2 Intracellular membrane rearrangement, mitochondrial dysfunction and ER stress

The hepatitis C virus impacts the intracellular environment of host cells, what leads to massive rearrangements of intracellular membranes. These changes are primarily orchestrated by HCV's non-structural proteins, which disrupt the normal protein homeostasis of both the mitochondria and the ER. One of the critical factors in this process is the HCV core protein, which is believed to contribute to increased ROS production within the mitochondria (Korenaga et al. 2005; Ivanov et al. 2013; Paracha et al. 2013). By binding to the outer mitochondrial

membrane (OMM), the core protein renders the mitochondria more susceptible to calcium ion (Ca^{2+}) influx. Consequently, this abnormal Ca^{2+} influx triggers the opening of the mitochondrial permeability transition pore (mPTP), leading to the release of cytochrome c; a component of the mitochondrial electron transport chain (Brault et al. 2013; Williamson and Colberg-Poley 2009; Brookes et al. 2004).

Moreover, the HCV infection promotes the phosphorylation of Drp1 (Dynamin-1-like protein), which plays a role in promoting mitochondrial fission (Kim et al. 2014; Li et al. 2021). This fission process concludes in the induction of Parkin-dependent mitophagy, a selective degradation process that eliminates damaged or dysfunctional mitochondria through autophagy. Interestingly, this mitochondrial degradation supports the release and propagation of the virus, aiding in the virus's survival and replication within the host cell (Kim et al. 2014).

In addition to affecting the mitochondria, HCV replication induces calcium ion Ca^{2+} overload in the endoplasmic reticulum, leading to the release of Ca^{2+} from the ER into the cytoplasm. This disruption in ER Ca^{2+} homeostasis triggers the unfolded protein response (UPR), a cellular stress response aimed at restoring protein-folding equilibrium in the ER. However, the continuous disturbance caused by HCV can overwhelm the UPR and lead to further dysfunction of the ER (Zhao et al. 2023; Panda et al. 2021; Medvedev et al. 2017; Mekahli et al. 2011). Additionally, the HCV core protein inhibits the sarcoplasmic/endoplasmic reticulum calcium ATPase (SERCA), which is responsible for transport of Ca^{2+} from the cytosol back into the sarcoplasmic reticulum. As a result, Ca^{2+} homeostasis is disrupted, contributing to increased Ca^{2+} stress within the cell. The dysregulation of Ca^{2+} signaling can lead to the disruption of the electron transport chain in the mitochondria. The electron transport chain perturbation further enhances the production of ROS, leading to a significant increase in ROS levels within the cell (Jin et al. 2021; Medvedev et al. 2016).

1.2.3.3 Keap1-Nrf2-ARE signaling pathway in HCV infection

To neutralize the damaging effects of oxidative stress caused by various factors, including chronic HCV infection, cells have evolved antioxidant defense strategies that developed to maintain redox homeostasis and protect the cell from oxidative stress. Antioxidants are molecules, which serve the purpose of support in defense mechanisms in neutralizing reactive oxygen species and maintaining redox balance and can be categorized into two groups: endogenous and exogenous. The endogenous antioxidants consist of enzymatic compounds, such as peroxiredoxins and glutathione peroxidase, which directly scavenge and detoxify ROS. Additionally, non-enzymatic, exogenous antioxidants, neutralize free radicals and protect cellular structures from oxidative damage. This includes examples: like vitamin C, vitamin E and glutathione (Zhu et al. 2023). Patients with chronic HCV infection exhibit lower levels of antioxidant defense enzymes. This includes for example glutathione peroxidase and glutathione reductase. Such a deficiency in antioxidant enzymes can lead to an imbalance in redox homeostasis, making cells more vulnerable to oxidative stress-induced damage (Ivanow et al. 2013).

One crucial defense mechanism against oxidative stress is the Nrf2/Keap1 signaling pathway. Nrf2 (NF-E2-related factor 2) is a transcription factor that plays a key role in triggering the expression of cytoprotective genes. All Nrf proteins share a common feature, the DNA binding basic region-leucine zipper (bZip) domain, which is crucial for their activity. When activated, these transcription factors can form heterodimers with one of three small Maf proteins (MafG, MafF, MafK). The resulting heterodimers possess the ability to bind to the Maf recognition sequence, found in the promoters of target genes involved in the antioxidant response element (ARE) called as well, EpRE (electrophile-response element). As a result, the expression of target genes is triggered in response to oxidative stress (Ohtsuji et al. 2008). Under normal

physiological conditions, Nrf2 is bound to its inhibitor, Keap1 (Kelch-like ECH-associated protein 1), constantly ubiquitinated and degraded in the proteasome in cytosol. Upon activation due to oxidative stress, or other factors like: inflammation, growth factor, the Nrf2-Keap1 complex dissociates, allowing Nrf2 to translocate into the nucleus (Sengoku et al. 2022; Silvestro and Mazzon, 2022). Nrf2 forms a heterodimer with small Maf proteins (sMafs) and binds to a conserved sequence in the antioxidant response element (ARE). This binding initiates the expression of detoxifying enzymes and other cytoprotective genes, which help combat the harmful effects of oxidative stress (Figure 10.) (O'Connell and Hayes 2015; Harder et al. 2015).

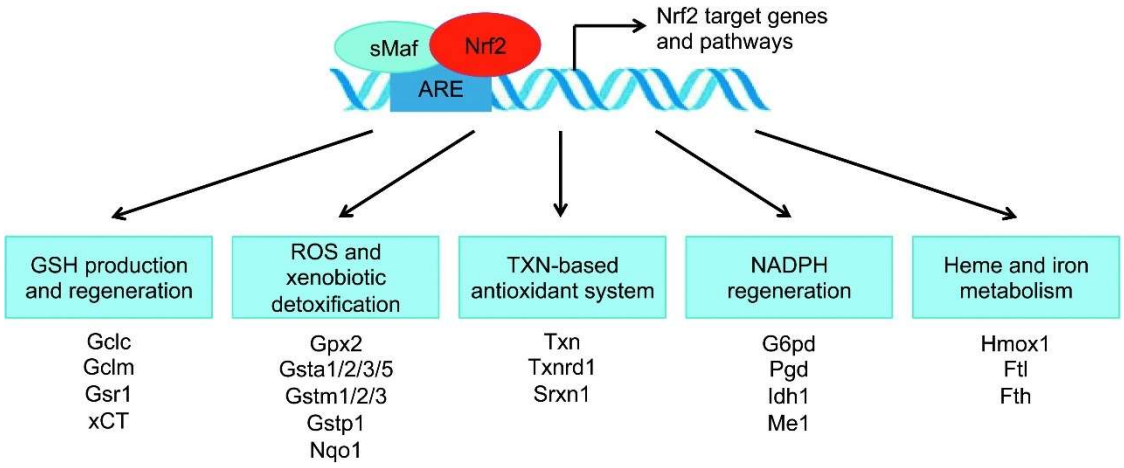

Figure 10. The cytoprotective defense system regulated by Nrf2 (Tonelli et al. 2018). Nrf2 regulates among others: GSH and TXN production, utilization and regeneration, NADPH regeneration, heme and iron metabolism, ROS and xenobiotic detoxification, Nrf2 provides the main cytoprotective defense system in the cell.

However, HCV replicating cells exhibit impaired Nrf2/ARE signaling, primarily due to the withdrawal of sMaf proteins from the nucleus. In HCV-infected cells, sMafs bind to the NS3 protein located on the cytoplasmic side of the ER, as an integral part of the viral replicon complex. This interaction prevents sMafs from translocation into the nucleus and forming the Nrf2-sMaf complex necessary for Nrf2's dependent activation of antioxidant response genes. As a consequence, the impaired Nrf2/ARE signaling contributes to the preservation of elevated ROS levels in HCV-infected cells, further exacerbating oxidative stress (Zhou et al. 2022; Bender and Hildt 2019; Shin et al. 2013).

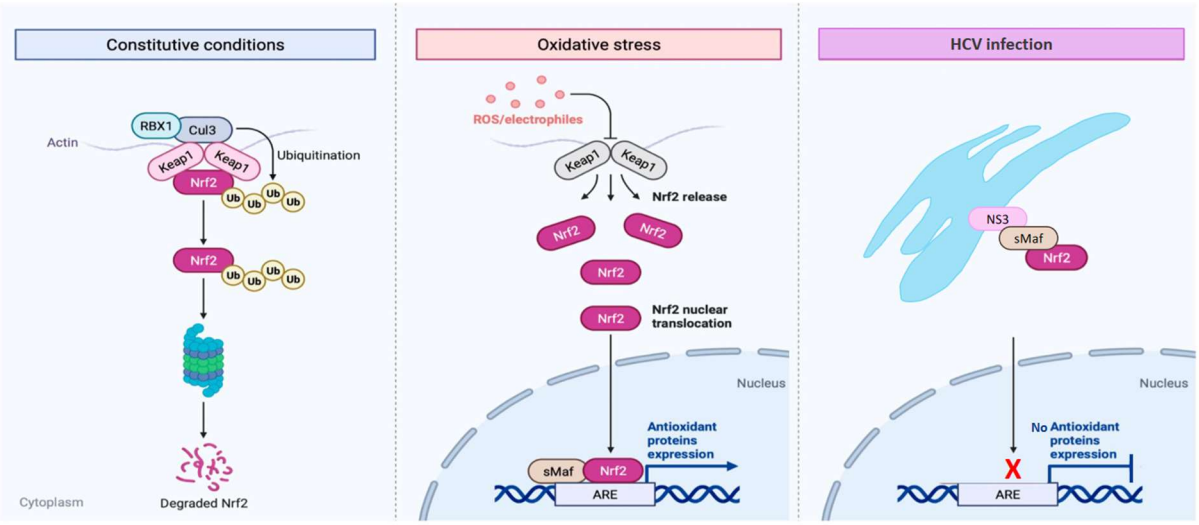

Figure 11. Schematic picture of Nrf2 under constitutive, oxidative stress conditions and HCV infection (Hammad et al. 2023, modified). Chronic Hepatitis C virus infection results in oxidative stress in the liver cells. One mechanism to protect against oxidative stress is the Nrf2/Keap1. Under basal conditions, NRF2 is constantly ubiquitinated through KEAP1 and degraded in the proteasome in cytosol. Under stress conditions, KEAP1-NRF2 interaction is stopped and free NRF2 translocates into nucleus. Then, NRF2 forms heterodimers with sMaf and binds to ARE antioxidant response elements sites to trigger transcription of cytoprotective genes. Nrf2/ARE signaling is impaired in HCV replicating cells, due to withdrawal of sMaf proteins from nucleus and binding to NS3 on the cytoplasmic site of the ER, as the integral part of replicon complex. The NS3-bound sMaf proteins bind to Nrf2, prevents Nrf2 from entering the nucleus to trigger the expression of the genes responsible for protection against oxidative stress.

Moreover, constantly elevated ROS levels may induce autophagy as a protective response. One of the factors that have been identified as a regulator of autophagy gene expression is the Nrf2/ARE signaling pathway. Nrf2 activation has been shown to regulate autophagy-related genes, enhancing the cell's ability to clear damaged cellular components and reduce oxidative stress (Medvedev et al. 2016). HCV infection triggers autophagy in host cells and this induction involves multiple pathways, including ER stress activation and oxidative stress induction. HCV can directly induce autophagy through the protein activity, for example NS3, NS4B and the NS3/NS5B nonstructural polyproteins. Additionally, NS4B promotes Rubicon expression, inhibiting autophagosome-lysosome fusion (Chu and Ou, 2021). HCV infection induces the accumulation of autophagosomes in cells. The delayed maturation of autophagosomes in HCV-infected cells is attributed to the temporal regulation of Rubicon and UVRAG proteins, ultimately favoring HCV replication in the early stage of infection. Induced autophagy and impaired degradation of MVBs leads to increased exosome release. TSPAN-CD63 is involved in mediating the degradation of MVBs through autophagic endosomal fusion in the HCV model. In summary, HCV hijacks autophagy for viral release via MVBs (Aydin et al. 2021, Chu and Ou, 2021; Medvedev et al. 2016).

1.3 Nuclear factor erythroid 2-related factor 1 (Nrf1)

1.3.1 Nrf1 processing

Another significant element in maintaining cellular redox homeostasis is the ubiquitously expressed transcription factor Nrf1 (Nuclear factor erythroid 2-related factor 1), also known as nuclear factor erythroid-2-like 1 (NFE2L1) of the Cap´N´Collar family (Xiang et al. 2018). Nrf1 undergoes complex and dynamic process of post-translational modifications and proteolytic cleavages, leading to the generation of multiple isoforms with distinct functionalities. Nrf1 is composed of nine structural domains; NTD (N-terminal domain), AD1, NST, AD2, SR, Neh6L,

CNC, bZIP and Neh3L; each responsible for various roles. Table 2 presents a summary of the main functions of the Nrf1 domains (Zhang and Xiang 2016; Qiu et al. 2022).

Table 2. Major Nrf1 structural domains (Zhang and Xiang 2016).

Domain	Function	Amino acids
AD1	(acidic domain 1) functions as the major TAD (transactivation domain) in Nrf1. This domain contains the PEST1 sequence, the Neh2L subdomain, the CPD (Cdc4 phosphodegron) and the Neh5L subdomain.	125–298
AD2	(acidic domain 2) contributes to transactivation activity of Nrf1 and is particularly important for the short Nrf1*β*/LCR-F1 isoform. This domain includes an acidic-hydrophobic amphipathic region and SDS1 (serine/aspartate/serine motif 1) that contains the *β*-TrCP-binding degron.	403-455
bZIP	Basic region-leucine zipper binding DNA	624-730
CNC	(cap'n'collar) The CNC family includes C. elegans Skn-1, the four vertebrate activators NF-E2 p45 subunit, Nrf1 (including its long form TCF11 and short form Nrf1*β*/LCR-F1), Nrf2 and Nrf3 and two distantly related repressors Bach1 and Bach2.	581–624
CRAC	(cholesterol-recognition/amino acid consensus motif) adjoins membrane-associated segments to enable interaction of the protein with membrane lipids. CRAC1 and CRAC2 are located close to the TM1 region within the NTD (N-terminal domain) of Nrf1. CRAC3 lies immediately adjacent to the DIDLID/DLG element (situated on the border between Neh2L and PEST1).	CRAC1 (62–70) CRAC2 (74–82) CRAC3(171-186)
Neh1L	(Nrf2–ECH homology 1-like) region contains both CNC and bZIP domains and functions as the DBD (DNA-binding domain).	581-730
Neh2L	(Nrf2–ECH homology 2-like) subdomain is situated in the center of AD1 in Nrf1. It is overlapped N-terminally by the PEST1 sequence and is flanked C-terminally by the CPD and Neh5L regions. Importantly, the Neh2L contains DLG and ETGE motifs, but these do not target Nrf1 for the Keap1-mediated proteasomal degradation. The DLG motif overlaps with the DIDLID element; both are integrated together and therefore referred to as the DIDLID/DLG element.	171–186
Neh3L	(Nrf2–ECH homology 3-like) region, also called the C-terminal domain, includes a CRAC5 that lies adjacent to TMc (C-terminal transmembrane region) and a putative arginine-enriched ER retention signal.	730–741
Neh4L	(Nrf2–ECH homology 4-like) acts as a TAD in TCF11, but not in Nrf1. It is lost in Nrf1 by alternative splicing.	125–298
Neh5L	(Nrf2–ECH homology 5-like) subdomain functions as an essential TAD. It shares homology with the DIDLID/DLG element and an amphipathic region of the AD2 region.	409–428
Neh6L	(Nrf2–ECH homology 6-like) domain is situated between the SR (serine-repeat) domain and the DBD and contributes to the negative regulation of Nrf1. The N-terminal region of Neh6L that overlaps with the PEST2 sequence, contains a core SDS2 (serine/aspartate/serine motif 2) and also is adjacent to CRAC4/TMp (a proline-kinked hinge structure folded).	497-525
NHB1	(N-terminal homology box 1) comprises aa11–30 in the NTD (aa1–124) that negatively regulates Nrf1. The ER-targeting NHB1 sequence is highly conserved in equivalents in TCF11, Nrf3, CncC and Skn-1 and they are therefore proposed to be grouped together as the 'NHB1–CNC' subfamily of membrane-binding transcription factors.	11-30
NHB2	(N-terminal homology box 2) comprises aa81–106 in the NTD of Nrf1, which is conserved with equivalents in TCF11, Nrf3 and CncC, but does not exist in Skn-1. Although the amphipathic NHB2 sequence is identified to act as an ER-luminal anchor, if being repositioned on the cyto/nucleo-plasmic sides of membranes, it is predicted to function as a putative degron targeting to the ERAD pathway. This process is monitored	81–106

Domain	Function	Amino acids
	possibly by a spacer region (such as CRAC1/2) between NHB1 and NHB2.	
NST	(asparagine/serine/threonine) situated between AD1 and AD2. It exists as a glycodomain in the ER and has the capability to function as a bona fide TAD, which would be exerted only after it is repartitioned out of membranes into the cyto/nucleo-plasm. This process appears to be controlled by the TMi glycopeptide and additional CPD.	299–400
PEST	(proline/glutamate/serine/threonine) sequence acts as a degron that targets the protein for either proteasome-dependent or -independent proteolysis pathway. Besides the PEST1 sequence in the N-terminal one-third of AD1, the PEST2 sequence covers the entire SR domain aa454–488 (as an inducible TAD), the SDS2 motif (aa497–506) and the CRAC4/TMp core region (aa508–519).	PEST1 141-170 PEST2 456-519

Initially located in the endoplasmic reticulum Nrf1 undergoes selective processing upon cellular stimulation (Figure 12). The processing steps involve several modifications such as N-glycosylation, O-GlcNAcylation, deglycosylation, phosphorylation, ubiquitination, degradation and proteolytic cleavage, ultimately leading to the translocation of shorter, transcriptionally active, isoforms to the nucleus. Upon stimulation, Nrf1 undergoes N-glycosylation and O-GlcNAcylation in the ER, resulting in the formation of an inactive 120 kDa glycoprotein known as Nrf1α/TCF11 (Chen at al. 2015). Afterwards, this glycoprotein is cleaved into deglycoprotein B(-) with a size of 95 kDa. In some instances, an unstable partial deglycoprotein B of 105 kDa may also be detected. Further processing occurs through proteolytic cleavage proteasomes, leading to the generation of distinct proteoforms termed C (90 kDa) and D (85 kDa). This step involves the removal of a major N-terminal polypeptide of approximately ~12.5 kDa, as described (Xiang et al. 2018). The active 85 kDa form of Nrf1 is no longer an integral part of the membrane and can undergo additional proteolysis, leading to the creation of a shorter 55 kDa proteoform known as LCR-F. LCR-F1, is a dominant-negative inhibitor of ARE-driven genes, but can function as an activator as well (Wang et al. 2019; Kim et al. 2016; Wang et al. 2007). It can also be processed to produce even shorter isoforms of 46 kDa, 36 kDa and 25 kDa (Zhang et al. 2014; Zhang and Hayes 2013). These various Nrf1 isoforms exhibit distinct functionalities. They are key players in maintaining redox homeostasis by controlling the expression of antioxidant response element (ARE)-driven target genes, which are crucial in defense against oxidative stress, regulate hepatic fatty and amino acid metabolism and participate in maintaining proteostasis by controlling the expression of proteasomal subunits (Cui et al. 2021; Baird et al. 2017; Zhang and Hayes 2013). Mice with somatic inactivation of the nrf1 gene in the liver developed hepatic cancer. Prior to the onset of cancer, the mutant livers showed signs of steatosis, apoptosis, necrosis, inflammation and fibrosis (Xu et al. 2005; Hirotsu et al. 2012). The synergistic effects of NRF1 and NRF2 together are significantly more effective in combating hepatic stress compared to either factor alone. While deficiency in NRF1 or NRF2 individually had modest effects, the combined deficiency of both resulted in severe steatohepatitis, hepatic cholesterol overload, crystallization, elevated triglyceride storage, body weight loss and even led to lethality (Akl et al. 2023).

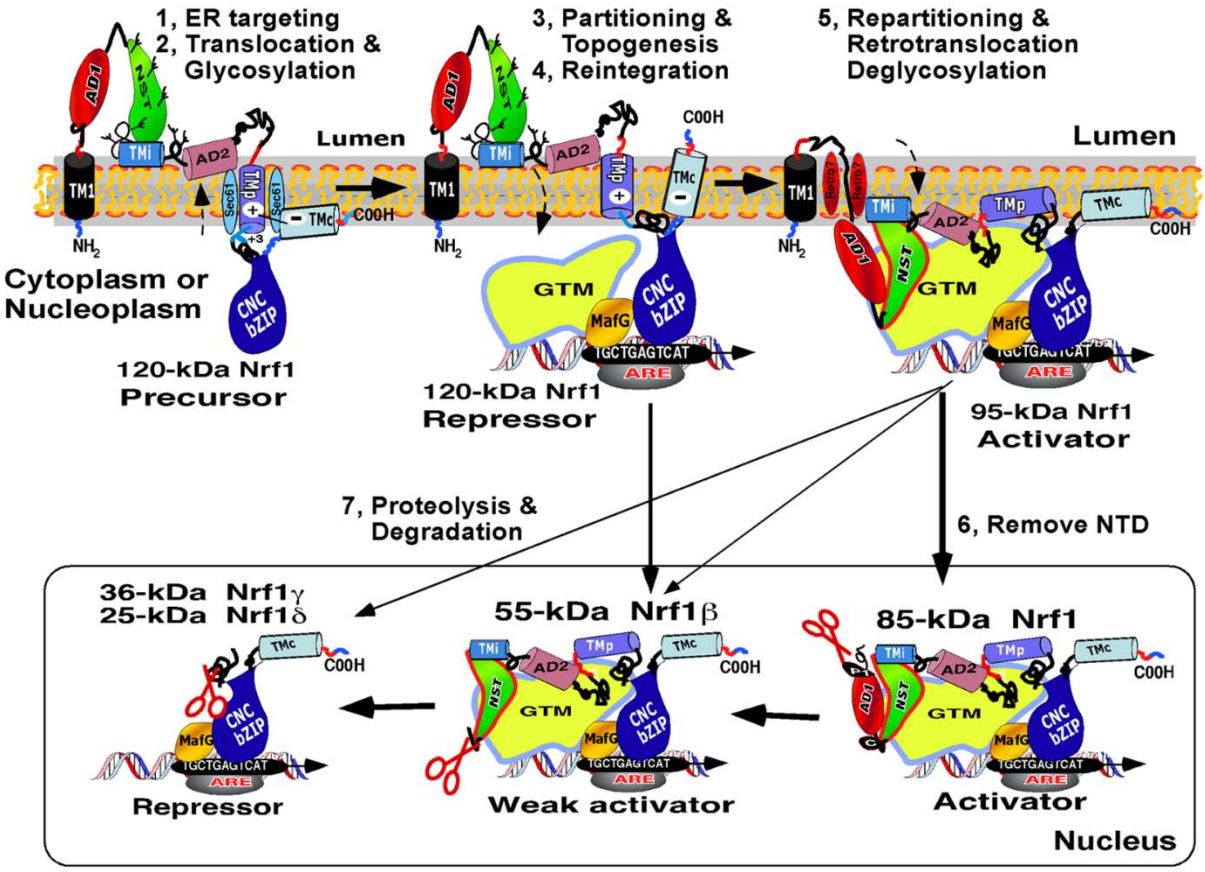

Figure 12. The model of the molecular mechanisms that regulate Nrf1 (Zhang et al. 2014). The model involves seven stages: I) Nrf1 is targeted to the ER and anchored in the membrane through TM1. II) The NST-adjoining TADs in Nrf1 are temporarily translocated into the lumen, where they are glycosylated to form a 120-kDa glycoprotein. III) During topogenesis, the TMi-adjacent amphipathic regions are tethered to the luminal leaflet of the membrane. TMp dynamically associates within membranes and PEST2 and Neh6L may be partitioned into distinct compartments. The basic CNC-bZIP domain is retained in the cyto/nucleoplasm, while the connecting TMc region is possibly left in the cytoplasm or integrated into membranes. IV) Once the TMi region is liberated from the restraint of its flanking glycopeptides, it is reintegrated into membranes. This enables repartitioning of AD2 and SR out of membranes to function as a TAD. V) When needed, the luminal NST and AD1 are repartitioned across the membrane into the cyto/nucleoplasm, leading to deglycosylation of Nrf1 and producing the 95-kDa active transcription factor that up-regulates genes through its TADs. VI) An 85-kDa cleaved isoform of Nrf1 is generated by removing the NTD, allowing it to be released into the nucleus and transactivate ARE-driven genes. VII) Distinct degrons trigger proteolysis of Nrf1, resulting in the 55-kDa Nrf1β/LCR-F1 isoform (a weak activator) and/or the dominant-negative 36-kDa Nrf1γ and 25-kDa Nrf1δ isoforms. Abbreviations: GTM - general transcriptional machineries; 'Retro?' - unidentified retrotranslocon complex.

1.3.2 Nrf1 is a cholesterol sensor

Recent studies have revealed that Nrf1 is a cholesterol sensor, that plays a role in protecting the liver against the damaging effects of excess cholesterol while simultaneously suppressing inflammation (Figure 13). When the cellular cholesterol levels surpass the ER carrying capacity, the excess cholesterol binds to a specific domain in Nrf1 known as the CRAC domain. This interaction allows Nrf1 the removal of excess cholesterol from the cellular environment (Widenmaier et al. 2017). Furthermore, oxysterols, which are derivatives of cholesterol, are also essential in maintaining cholesterol homeostasis as they act as ligands for Nrf1. Together, these molecules, namely cholesterol and oxysterols, mediate cholesterol transport via the LXR pathway. Upon activation, LXR forms heterodimers with the retinoid X receptor and this activation triggers the stimulation of target genes, including ATP-binding cassette transporters (ABC) ABCA1 and ABCG1. These transporters play a crucial role in increasing cholesterol excretion from the liver (Röhrl and Stangl 2018). Additionally, it was observed that NRF1 and

NRF2 cooperatively regulate genes involved in cholesterol elimination, inflammation mitigation and protection against oxidative damage. NRF1 and NRF2 have complementary roles in gene programming, effectively countering the progression of cholesterol-associated fatty liver disease (Akl et al. 2023).

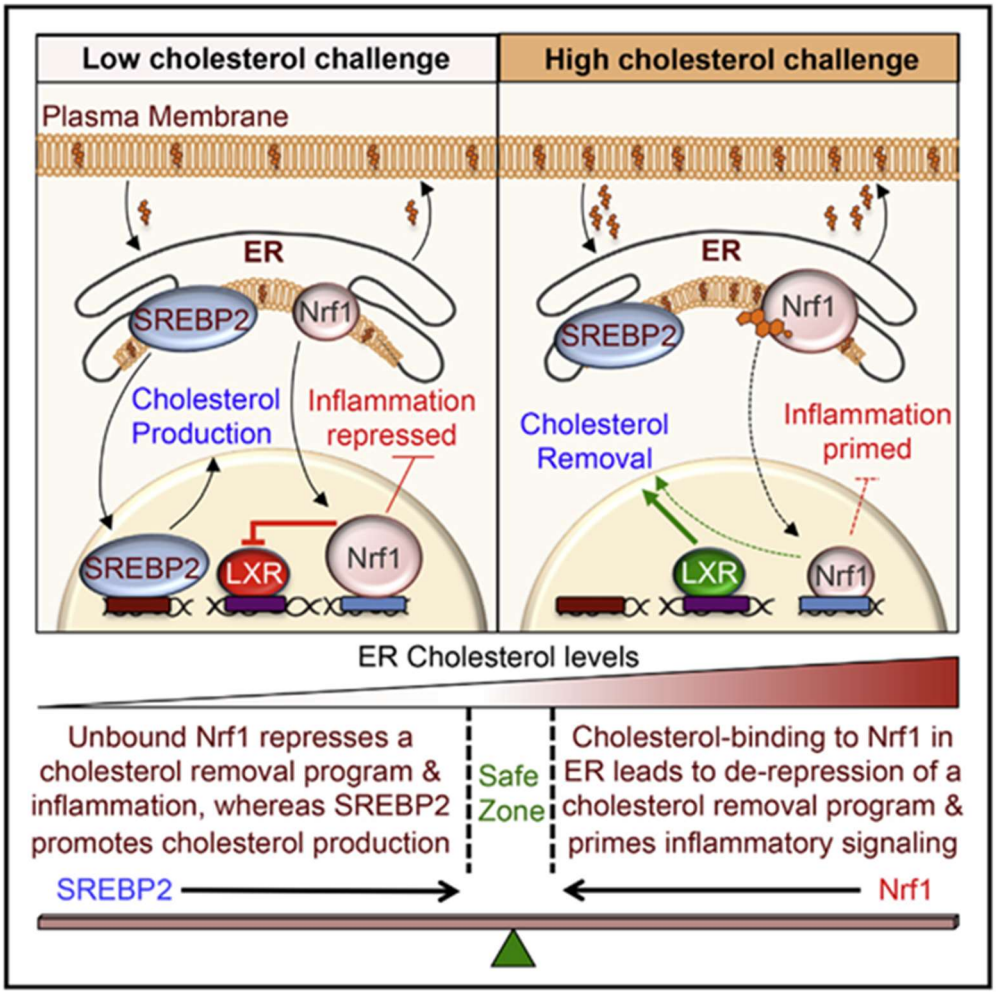

Figure 13. Nrf1 is an ER cholesterol sensor (Widenmaier et al. 2017). Under conditions of low cholesterol challenge, Nrf1 functions as a repressor, thereby inhibiting cholesterol removal and dampening the inflammatory response. Conversely, during high cholesterol challenge, Nrf1 binds to cholesterol within the ER, resulting in the suppression of cholesterol removal mechanisms and priming inflammation. In parallel, the sterol response element binding protein 2 (SREBP2) also acts as a cholesterol sensor and responds to cholesterol levels in an opposing manner. This creates a feedback loop that is coupled to an adaptive response, working in defense against excessive cholesterol accumulation.

By functioning as a cholesterol sensor and being part of regulatory pathways, Nrf1 controls liver cholesterol homeostasis and protects the cell from damage of excess cholesterol. It affects complex regulatory pathways, like the LXR pathway and ABC transporters to efficiently transport and excrete cholesterol, thereby protecting the liver and promoting overall cellular health. Recent studies highlight the crucial protective role of Nrf1 in liver physiology and offer promising directions for further research on therapeutic approaches targeting Nrf1 and its associated pathways to address cholesterol-related liver disorders (Widenmaier et al. 2017; Akl et al. 2023).

2 Aim of this study

The complex interactions between redox homeostasis, lipid metabolism and HCV infection, and the functions of Nrf1 and Nrf2 are poorly understood. Understanding those interactions is essential to the development of a specific antiviral treatment. Therefore, the primary objective of this research was to examine the impact of HCV on Nrf1 in several aspects. The aim of study was to examine if HCV infection affects the protein levels of Nrf1 and its subcellular localization. Interesting was also if there was an effect on Nrf1 activity in regulating the antioxidant response and cholesterol sensing process.

Furthermore, the study aimed to clarify HCV's possible impact on above mentioned processes to enhance replication and assembly. HCV life cycle is tightly connected to the lipid metabolism with the HCV viral particle released as lipoviroparticle. Therefore, the regulation of lipid metabolism and lipid droplet formation is an interesting area of study. A complete understanding of these mechanisms is crucial. The results of this study might have implications in the context of persistent HCV infection and its associated impact on autophagy, MVB degradation and exosome release. Better understanding of lipid-related processes may show new perspectives on the interaction between HCV infection and cellular mechanisms.

3 Materials

3.1 Cells

3.1.1 Prokaryotic cells

Strain	Genotype	Source
E. coli DH5α	F- endA1 glnV44 thi-1 recA1 relA1 gyrA96 deoR nupG purB20 φ80dlacZΔM15Δ (lacZYA-argF)U169, hsdR17(rK-mK+), λ-	Invitrogen, DE

3.1.2 Eukaryotic cells

Strain	Description	Source
Huh7.5	Human hepatoma cell line derived from Huh7 cells	Blight et al. 2002

3.2 Plasmids

Plasmid	Description	Source
GND	Replication-deficient HCV-JFH1 mutant due to a point mutation in NS5A	Pietschmann et al. 2006
pFK-Jc1	Chimera of the HCV genotype 2a isolates JFH1 and J6 producing higher titers of infectious particles	Pietschmann et al. 2006
pFK-Luc-Jc1	Encodes a bicistronic reporter constructs of the full-length Jc1 genome	Pietschmann et al. 2006
EGFP-N1	Encodes a green fluorescent protein from Aequorea coerulescens, this vector allows expression of a protein of interest as an N-terminal fusion to EGFP	Clontech, USA
Δa1pEGFP-N1 (pJo23)	Empty expression vector, served as control	Invirtogen, DE
85kDa-Nrf1	Encodes an 85kDa fragment of Nrf1 protein with an N-terminal fusion to EGFP	This study
25kDa-Nrf1	Encodes an 25kDa fragment of Nrf1 protein with an N-terminal fusion to EGFP	This study
sMafG-NES	Encodes a sMafG protein with a nuclear export signal fusion to mCherry	This study
sMafG-NLS	Encodes a sMafG protein with a nuclear localisation signal fusion to mCherry	This study
pGreenFire1-LXRE	Co-expresses a destabilized copepod GFP and luciferase from the Liver X Receptor (LXR) response elements (LXREs) and neighboring regions in the LXRα promoter	IBA Lifesciences, DE
pNQO1luc	Luciferase reporter construct harboring the AREs from NAD(P)H-dependent quinone oxidoreductase 1	Sabine Werner, ETH Zürich

3.3 Oligonucleotides

3.3.1 RT-qPCR-Primer

Description	Sequence (5' → 3')
RPL-fwd	AAAGCTGTCATCGTGAAGAAC
RPL-rev	GCTGCTACTTTGCGGGGGTAG

Description	Sequence (5' → 3')
JFH1-fwd (R6-260-R19)	ATGACCACAAGGCCTTTCG
JFH1-rev (R6-130-146)	CGGGAGAGCCATAGTGG
Nrf1-fwd	GCTGGACACCATCCTGAATC
Nrf1-rev	CCTTCTGCTTCATCTGTCGC
LXR-fwd	CCTTCAGAACCCACAGAGATCC
LXR-rev	ACGCTGCATAGCTCGTTCC
Random hexamer primers	-

3.3.2 Cloning primers

Description	Sequence (5' → 3')
85kDa-fwd	AAAAAGCTTATGGTTCACCGAGACCCAGAGG
25kDa-fwd	AAAAAGCTTATGATGGCACCCAGTGCCCTG
Nrf1-rev	AAAGGTACCCTTTCTCCGGTCCTTTGGCTTC
sMaf-NLS-fwd	AAATCTAGAGGAGGCGGATCTATGGTGAGCAAGGGCGAGGAGGATAACA
sMaf-NLS-rev	AAAGAATTCCTACTTGTACAGCTCGTCCATGCCGCCGGTG
sMaf-NES-fwd	AAACCTGACGGGATTAGGTCGTTCATCTCATCGTTACCCAGCGGCAGCCC CTTATCGTCAATCTTCTCGAGGATTGGGGACCCTGGTGGTAGCACGACCC CCAATAAAGGAAACAAGG
sMaf-NES-rev	AAAAAGCTTCTATTACACGCCCAGGGCGCTG

3.3.3 Sequencing primers

Description	Sequence (5' → 3')
CMV-fwd	GAGGTCTATATAAGCAGAGCTC
EGFP-rev	GACACGCTGAACTTGTGGCC

3.3.4 siRNA

siRNA	Target	Manufacturer
Nrf1 siRNA, SMARTPool M-019733-01-0010 (10 µM stock solution in RNase-free H_2O)	Nrf1	GE Healthcare Dharmacon, Inc., USA
Scrambled RNA, sc-37007 (10 µM stock solution in RNase-free H_2O)	Unspecific control	Santa Cruz Biotechnology, Inc., USA

3.4 Antibodies

3.4.1 Primary antibodies

Antibody	Species, clonality	Dilution (WB/IF)	Manufacturer
Anti-NRF1	Rabbit, polyclonal	1:500 / 1:200	Cell Signaling, USA
Anti-Nrf1	Mouse, monoclonal	1:200 / 1:150	Santa Cruz Biotechnology, Inc., USA
Anti-HCV core	Mouse, monoclonal	1:1000 / 1:200	Invitrogen, USA
Anti-NS3	Mouse, monoclonal	1:1000 / 1:500	BioFront Technologies, USA
Anti-NS3	Mouse, monoclonal	1:500 / 1:50	Virostat Inc., USA
Anti-NS5A	Rabbit, polyclonal	1:1000 / 1:200	-
Anti-sMaf G/F/K	Rabbit, polyclonal	- / 1:80	Santa Cruz Biotechnology, Inc., USA
Anti-β-actin	Mouse, monoclonal	1:10 000 / -	Sigma-Aldrich, USA

3.4.2 Secondary antibodies

Antibody	Species, clonality	Dilution WB/IF	Manufacturer
Anti-mouse IgG-Alexa488	Donkey, polyclonal	- / 1:1000	Thermo Fisher Scientific, DE
Anti-mouse IgG-Alexa546	Donkey, polyclonal	- / 1:1000	Thermo Fisher Scientific, DE
Anti-mouse IgG-Alexa633	Donkey, polyclonal	- / 1:1000	Thermo Fisher Scientific, DE
Anti-mouse IgG-Cy3	Donkey, polyclonal	- / 1:400	Jackson ImmunoResearch Europe Ltd., UK
Anti-mouse IRDye680RD	Donkey, polyclonal	1:10.000 / -	LI-COR Biosciences GmbH, DE
Anti-mouse IRDye800CW	Donkey, polyclonal	1:10.000 / -	LI-COR Biosciences GmbH, DE
Anti-rabbit IgG Cy3	Donkey, polyclonal	- / 1:400	Jackson ImmunoResearch Europe Ltd., UK
Anti-rabbit IgG-Alexa488	Donkey, polyclonal	- / 1:1000	Thermo Fisher Scientific, DE
Anti-rabbit IgG-Alexa546	Donkey, polyclonal	- / 1:1000	Thermo Fisher Scientific, DE
Anti-rabbit IgG-Alexa633	Donkey, polyclonal	- / 1:1000	Thermo Fisher Scientific, DE
Anti-rabbit IRDye680RD	Donkey, polyclonal	1:10.000 / -	LI-COR Biosciences GmbH, DE
Anti-rabbit IRDye800CW	Donkey, polyclonal	1:10.000 / -	LI-COR Biosciences GmbH, DE

3.5 Fluorescent dye

Dye	Dilution IF	Manufacturer
DAPI (1 mg/ml stock in PBS)	1:1000	Carl-Roth, DE
Filipin III (10 mg/mL stock in DMSO)	1:200	Sigma-Aldrich, USA
AUTODOT™ Lipid Droplets Visualization Dye (0,1 M stock in DMSO)	1:1000	Abcepta, Inc., USA

3.6 Molecular weight markers

3.6.1 DNA markers

Description	Manufacturer
Gene Ruler™ 1 kB Plus DNA ladder	Thermo Fisher Scientific, DE

3.6.2 Protein markers

Description	Manufacturer
PageRuler™ Prestained Protein Ladder	Thermo Fisher Scientific, DE
PageRuler™ Plus Prestained Protein Ladder	Thermo Fisher Scientific, DE

3.7 Enzymes

Enzyme	Manufacturer
AseI	NEB, DE

XbaI	NEB, DE
MluI	NEB, DE
RevertAid H Minus Reverse Transcriptase	Thermo Fisher Scientific, DE
RQ1 RNase-Free DNase	Promega, USA
T7 RNA-Polymerase	Biozym, DE

3.8 Inhibitors

Inhibitor	**Target**	**Manufacturer**
Protease inhibitors		
Aprotinin	Serine protease	Sigma Aldrich, DE
Leupeptin	Serine and cysteine protease	Sigma Aldrich, DE
Pepstatin	Acid-, aspartatic proteases	Sigma Aldrich, DE
PMSF	Serine protease	Carl-Roth, DE
RNase inhibitors		
RiboLock RNase Inhibitor	RNase	Thermo Fisher Scientific, DE
ScriptGuard RNase Inhibitor	RNase	Biozym, DE
Protein synthesis inhibitor		
Cycloheximide (CHX)	The translocation step in protein synthesis	Sigma Aldrich, DE

3.9 Reagents for cell culture

Reagent	**Manufacturer**
DMEM (Dulbecco's Modified Eagles Medium) 4.5 g/l glucose	Merck, DE
OptiMEM medium	Thermo Fisher Scientific, DE
PBS without Ca^{2+} and Mg^{2+}	Paul-Ehrlich-Institut, DE
FCS (fetal calf serum)	Bio&SELL, DE
L-glutamine	Biochrom GmbH, DE
Penicillin/Streptomycin	Paul-Ehrlich-Institut, DE
Puromycin	Sigma Aldrich, DE
Trypsin/EDTA	Paul-Ehrlich-Institut, DE

3.10 Chemicals

Chemicals	**Manufacturer**
dNTPs	Thermo Fisher Scientific, DE
10x T7-Scribe transcription buffer	Biozym, DE
25-hydroxycholesterol (25-HCH)	Cayman Chemicals, USA
3-Amino-9-ethylcarbazole (carbazole)	Carl Roth, Germany
4',6-diamidino-2-Phenylindole (DAPI)	Sigma Aldrich, DE
5x Reaction buffer for RT	Thermo Fisher Scientific, DE
6-Aminohexanoic acid	Carl-Roth, DE
Acetic acid (glacial)	Carl Roth, DE
Acetone	Carl-Roth, DE
Agarose	Genaxxon, DE
Ampicillin	Carl-Roth, DE
APS (Ammoniumperoxodisulfate)	Carl-Roth, DE
Bradford reagent	Sigma Aldrich, DE
Bromphenol blue	Merck, DE

Chemicals	Manufacturer
BSA (Bovine serum albumin)	PAA, AT
Chloroform	Carl-Roth, DE
DMSO (Dimetyl sulfoxide)	Genaxxon, DE
EDTA (Ethylendiaminotetraacetic acid)	Paul-Ehrlich-Institut, DE
Ethanol	Carl-Roth, DE
Ethidiumbromide	AppliChem, DE
Filipin III	Sigma Aldrich, DE
FuGENE® HD Transfection Reagent	Promega, USA
Immobilon Western HRP Substrate	Merck Milipore, DE
Isopropanol	Carl-Roth, DE
Maxima Probe SYBR Green qPCR Master Mix	Thermo Fisher Scientific, DE
MDH (Monodansylpentane) AUTODOT™	Abcepta, Inc., USA
Methanol	Carl-Roth, , DE
Mowiol	Sigma Aldrich, DE
N-TER peptide	Sigma Aldrich, DE
NTP-Mix	Thermo Fisher Scientific, DE
Optiprep (Iodixanol)	Progen Biotechnik, DE
Phenol	Applichem, DE
Polyethylenimine (PEI)	Polysciences, DE
Random Hexamer Primer	Thermo Fisher Scientific, DE
RNA-Solv® Reagent	VWR, USA
Roti®-Block	Carl-Roth, DE
Rotiphorese Gel 40 (Acrylamide/bisacrylamide)	Carl-Roth, DE
RQ1 DNase stop solution	Promega, USA
RQ1 RNase-Free DNase 10x Reaction Buffer	Promega, USA
SDS 10%	Paul-Ehrlich-Institut, DE
Simvastatin	SantaCruz Biotechnology,DE
Skim milk powder	Carl-Roth, DE
Sodium acetate	Paul-Ehrlich-Institut, DE
Sodium desoxycholat	Carl-Roth, DE
Sucrose	Carl-Roth, DE
TEMED	Carl-Roth, DE
Trichlormethan/Chloroform	Carl-Roth, DE
Tris	Paul-Ehrlich-Institut, DE
Tris-HCl	Paul-Ehrlich-Institut, DE
Triton-X-100	Fluka, DE
Tween20	Genaxxon, DE
β-Mercaptoethanol	Sigma-Aldrich, DE
Formaldehyde 37.5%	Carl-Roth, DE
1,4-diazabicyclo[2.2.2]octane (DABCO)	Merck, DE
NEBuffer 3.1	NEB, DE

3.11 Kits

Kit	Manufacturer
Cellscript T7-Scribe™ Standard RNA IVT Kit	Biozym, DE
LightCycler Multiplex RNA Master Mix	Roche Diagnostics, DE
LightMix Modular Hepatitis C Virus Kit	TIB Molbio, DE
Maxima™ SYBR Green qPCR Kit	Thermo Fisher Scientific, DE
QIAamp Viral RNA Mini Kit	Qiagen, Hilden, DE
Qiagen Plasmid Maxi Kit	Qiagen, Hilden, DE

Kit	Manufacturer
siPORT™ NeoFX™ Transfection Agent	Thermo Fisher Scientific, DE

3.12 Buffers and solutions

Buffer	Composition
Anode buffer I	20% Ethanol (v/v) 300 mM Tris
Anode buffer II	20% Ethanol (v/v) 25 mM Tris
Cathode buffer	20% Ethanol (v/v) 40 mM 6-Aminohexanoic acid
DNA loading dye (6x)	10 mM Tris-HCl 0.03% Bromphenol blue 0.03% Xylene Cyanol 60% Glycerol 60 mM EDTA pH 7.6
Luc lysis buffer	25 mM Tris-HCl 2 mM DTT 2 mM EGTA 10% Glycerol 0,1% Triton-X 100 pH 7.5
Luc substrate buffer	20 mM Tris-HCl 5 mM MgCl2 0,1 mM EDTA 33,3 mM DTT 470 µM Luciferin 530 µM ATP pH 7.8
Lysogeny broth medium (LB)	1% Trypton (w/v) 0.5% Yeast extract (w/v) 1% NaCl (w/v)
Mounting medium (Mowiol)	10% Mowiol (w/v) 25% Glycerol (w/v) 2.5% DABCO 100 mM Tris/HCl pH 8.5
Phosphate buffered saline (PBS) 10x	137 mM NaCl 2.7 mM KCl 8.1 mM Na_2HPO_4 1.5 mM KH_2PO_4 ad 1 L ddH2O pH 7.4
Radioimmunoprecipitation assay buffer (RIPA)	50 mM Tris-HCl pH 7.2 150 mM NaCl 0.1% SDS (w/v) 1% Sodium desoxycholat (w/v) 1% Triton X-100
SDS loading buffer (4x)	4% SDS (w/v) 125 mM Tris-HCl pH 6.8 10% Glycerol (v/v) 10% ß-Mercaptoethanol (v/v) 0.02% Bromphenol blue (w/v)

Buffer	Composition
SDS running buffer (10x)	0.25 M Tris-HCl 2 M Glycin 1% SDS (w/v) pH 8.3
Separation gel buffer	1.5 M Tris-HCl 0.4% SDS (w/v) pH 8.8
Stacking gel buffer	0.5 M Tris 0.4% SDS (w/v) pH 6.8
TAE-Puffer (50x)	2 M Tris 1 M Acetic Acid 50 mM EDTA pH 8.0
TBS-T (10x)	200 mM Tris-HCl 1.5 M NaCl 0.5% Tween pH 7.8

3.13 Devices

3.13.1 Electrophoresis

System	Manufacturer
Horizontal electrophoresis system HE33	GE Healthcare Europe GmbH, DE
Mighty small multiple gel caster SE200	GE Healthcare Europe GmbH, DE
Mighty small II vertical electrophoresis system SE 250	GE Healthcare Europe GmbH, DE
Standard power pack P25	Biometra GmbH, DE
TE77 ECL semi dry transfer unit	GE Healthcare Europe GmbH, DE

3.13.2 Microscopy

Mircoscope	Manufacturer
Confocal Laser Scanning Microscope TCS SP8	Leica Microsystems, DE

3.13.3 Imaging

Imaging system	Manufacturer
ImageQuant800 CCD Imager	Cytiva, USA
INTAS-Imaging System	Intas, DE
Odyssey CLx Imaging System	LI-COR, DE

3.13.4 PCR-Cycler

PCR Cycler	Manufacturer
LightCycler® 480 Instrument II	Roche, DE

3.13.5 Centrifuges

Centrifuge	Manufacturer
Heraeus Multifuge 1S-R	Thermo Fisher Scientific, DE
Microcentrifuge	Carl-Roth, DE

3.13.6 Other devices

Device	Manufacturer
Accujet® pro	Brand GmbH & Co. KG, DE
Electroporator Gene Pulser MXcellTM	BioRad, USA
Incubator BBD 6220	Heraeus, DE
Incubator Innova 44	New Brunswick Scientific, USA
Infinite M1000	Tecan, CH
NanoDrop™ One C	Thermo Fisher Scientific, DE
Neubauer chamber	Marienfeld, DE
Orion II Microplate Luminometer	Titerek, DE
Pipettes	Eppendorf, DE
RCT Classic magnetic stirrer	IKA, Staufen, DE
Rocking Plattform	Biometra, DE
S20 – SevenEasy™ pH	Mettler Toledo, DE
Sartorius analytical balance	Sartorius, DE
Sartorius balance LP 6000 200S	Sartorius, DE
SterilGardRIII Advance	The Baker Company, USA
Stuart roller mixer SRT9	Bibby Scientific, UK
Thermomixer 5436	Eppendorf, USA
Thermomixer compact	Eppendorf, DE
Vortex®Genie 2	Scientific Industries, USA
Waterbath 1228-2F	VWR, DE

3.14 Relevant materials

Material	Manufactuer
Cell culture flasks (T25, T75, T175)	Greiner Bio-One, DE
Cell culture plates (6, 12, 24, 96 wells)	Greiner Bio-One, DE
Cell scrapers	A. Hartenstein, DE
Coverslips, 18mm	Carl Roth, DE
Electroporation cuvettes, 4 mm	VWR, DE
Falcon tubes (15 ml, 50 ml)	Greiner Bio-One, DE
Filter tips (20 µl, 100 µl, 300 µl, 1 ml)	Sarstedt, DE
Graduated pipettes (5, 10, 25 ml)	Greiner Bio-One, DE
Microscope slides SuperFrost	Carl Roth, DE
Parafilm	Bemis, Bonn, DE
Phase Lock Gel Heavy, 2 ml	5 PRIME GmbH, DE
Pipette tips (2,5 µl, 20 µl, 100 µl, 1 ml)	Sarstedt, DE
Roti®-Fluoro PVDF membrane	Carl Roth, DE
RotiLabo® syringe filter 0,22 µm	Carl Roth, DE
RotiLabo® syringe filters (0,22 / 0,45 µm)	Carl Roth, DE
Safe-lock micro test tubes (1.5 ml, 2 ml)	Sarstedt, DE
Syringes (10 ml, 20 ml)	B. Braun, DE

3.15 Software

Software	Manufacturer
Citavi 5	Swiss Academic Software GmbH, CH
GraphPad Prism 9.5.1	GraphPad, USA
i-control 1.8	Tecan, CH
Image Studio	LI-COR, DE
Image Studio Lite 5.2	LI-COR, DE

ImageJ Fiji	Open source, USA
INTAS GDS	Intas, DE
LAS X	Leica, DE
LightCycler 480 SW 1.5	Roche Diagnostics, DE
MS Office	Microsoft, USA

4 Methods

4.1. Cell biology

4.1.1. Prokaryotic cell culture

E. coli DH5α strain from glycerol stocks were cultivated in LB medium at 37°C and 200 rpm in Erlenmeyer flasks for 16 hours. To select for transformed bacteria, 100 µg/ml ampicillin was added to the LB medium. To create new glycerol stocks, 10 ml of the overnight culture was centrifuged and the pellet was mixed with 50% glycerol (v/v) before being stored at -80°C.

4.1.2. Eucaryotic cell culture

The human hepatoma cell line, Huh 7.5 cells, were cultured in Dulbecco's modified Eagle's medium (DMEM) supplemented with 10% fetal calf serum, 2mM L-glutamine, 100U/ml of penicillin and 100µg/ml streptomycin (referred to as DMEM complete). For passaging adherent cells, 1X Trypsin/EDTA was used for a 5-minute treatment, following a wash with PBS. To stop trypsinization, 7 mL of DMEM complete was added to the cells. Afterwards, the cells were seeded at low density with fresh medium and cultured in a humidified atmosphere containing 5% CO2 at 37°C. All experiments involving infectious HCV were conducted under S3 safety conditions.

4.1.3. Electroporation of Huh7.5 cells

Two days prior to electroporation, cells were passaged and cultivated until they reached 80 to 90% confluence. Cells were trypsynized, washed twice with ice-cold D-PBS and then resuspended in D-PBS to a final concentration of 5×10^6 cells/ml for the electroporation. Next, a mixture of 10µg of in vitro transcribed RNA, derived from plasmids containing HCV genomes, was combined with 800µl of the cell suspension in a 4mm cuvette (PeqLab cell projects, UK). Electroporation was immediately performed using the Gene Pulser Xcell from Bio-Rad, delivering a single pulse at 0.3kV and 950 µF. Following electroporation, the cells were diluted into 12ml of DMEM complete medium and plated into cell culture flasks (T175). At 4 hours post-electroporation (pe), the medium was modified and cells were cultivated for around 3 weeks.

4.1.4. Transfection of Huh7.5 cells

One day prior to transfection, the cells were seeded at a density of 3×10^5 cells/well in 6-well plates. Huh7.5, GND and Jc1 cells that underwent electroporation were subsequently transfected using either linear polyethyleneimine (PEI) (1 mg/ml) from Polysciences or FuGENE® HD Transfection Reagent from Promega.

For PEI transfection, 1-2µg of Plasmid-DNA were resuspended in 200 µl of PBS and 12 µl of PEI per µg of Plasmid-DNA were added. The mixture was then gently inverted for 10 seconds.

On the other hand, for FuGENE transfection, 1.5µg of Plasmid-DNA was resuspended in 200 µl of Opti-MEM® I Reduced Serum Medium from Life Technologies and 4.5µg of FuGENE was added. The solution was mixed by gently inverting it for 10 seconds.

After a 10-minute incubation at room temperature, the respective reaction mix was added dropwise to 2 ml of medium in each well of the 6-well plate. Following 8 hours for PEI transfection and 24 hours for FuGENE transfection, the medium was modified. The cells were harvested 48 hours after the transfection process.

4.1.5. Silencing of gene expression

To prepare the transfection mix, 0.2 µL of Nfe2l1 siRNA (Dharmacon) or scrambled RNA (both at a concentration of 10 µM) was mixed with OptiMEM medium (Thermo Fisher) using the siPORT overlay protocol (Thermo Fisher). The mixture was then incubated for 15 minutes at room temperature.

Next, 100 µL of the transfection mix was pipetted into each well of a 12-well plate and evenly dispersed. Afterwards, Huh7.5 cells stably electroporated with HCV-Jc1 at a cell density of 1x10^5 cells were added over the transfection mix in each well.

4.1.6. Cell harvest and lysis

To prepare Western blot lysates, supernatant was aspirated and cells were washed once with PBS. After that, cells were lysed on ice for 5 minutes using 100 µl of RIPA buffer supplemented with protease inhibitors. Lysed cells were then scraped from the cell culture plate and transferred into a 1.5 ml Eppendorf tube. Lysates, were then sonicated for 10 seconds at 30% power to disrupt the cells. Afterwards, the lysates were centrifuged for 10 minutes at full speed and 4°C to remove cell debris from the samples.

Supernatant was aspirated and cells were washed once with PBS to prepare luciferase lysates. Afterwards, cells were lysed on ice for 5 minutes using 200µl of luciferase lysate buffer. Later on, the lysates were centrifuged for 10 minutes at full speed and 4°C to remove cell debris from the samples.

4.1.7. Treatments

Cells were initially seeded in growth medium and treated 24 hours after seeding. Serum-free DMEM supplemented with a final concentration of 25 µM 25-HC (dissolved in 96% v/v ethanol) or 5 µM Simvastatin (dissolved in DMSO) for 24 hours was used as a treatment.

During the treatment with 25-HC, 1% v/v ethanol was present. For the experimental controls serum-free DMEM was supplemented with equal volumes of 2% v/v ethanol or 0.1% v/v DMSO, respectively. These served as the control treatments for comparison.

4.2 Molecular biology

4.2.1. Agarose gel electrophoresis

Plasmid DNA and RNA samples were subjected to agarose gel electrophoresis. A 0.7% (w/v) agarose gel was used for DNA and 1% (w/v) agarose gel was used for RNA. Appropriate amount of agarose was dissolved in 1x TEA buffer. Once the agarose solution cooled and became liquid, it was poured into a horizontal gel chamber and 0.1 µg/ml ethidium bromide was added to the gel to visualize nucleic acids. Solidified gel was then placed in an

electrophoresis chamber containing 1x TAE buffer. Samples were mixed with 6x loading buffer and loaded into the gel pockets. Electrophoresis was performed at 90 volts, allowing the nucleic acids to migrate through the gel. Finally, the separated nucleic acids were visualized using UV-light (254/365 nm) at the INTAS imaging system.

4.2.2. Determination of nucleic acid concentration

Nanophotometer was used to determine the concentration of nucleic acids and the absorbance (A) of the aromatic nucleobases was measured at a wavelength (λ) of 260 nm. Additionally, absorbance was measured at λ=230 nm to account for solvents and at λ=280 nm for proteins to assess the purity. Pure DNA samples should have a ratio of A260/280=1.8. Similarly, RNA samples should have the ratio of A260/280=2.0. Additionally, both DNA and RNA samples are considered pure when the ratio A260/230 falls within the range of 2.0-2.2.

4.2.3. Isolation of plasmid DNA

Plasmid DNA was extracted from E. coli DH5α using the QIAGEN Plasmid Maxi Kit following the manufacturer's protocol. The extraction was performed from a 500 ml bacterial overnight culture.

4.2.4. Generation of competent bacteria

To generate chemically competent bacteria E. coli DH5α cells were inoculated and placed in shaking incubator at 37°C and 200 rpm for 12-16h. Then, 1 mL of ON culture was added to 100 mL of fresh LB medium and shake incubated at 37°C and 150rpm for 3-4 hours or until OD reached 0.6. Bacteria were then placed on ice for 20 min, centrifuged at 4°C at 5000 rpm for 5 minutes. Bacteria pellet was resuspended with 2,7mL ice-cold 0,1 M $CaCl_2$ and incubated on ice for 30 min. Bacteria was again centrifuged at 4°C at 4000rpm for 10 minutes, supernatant was discarded and pellet was combined by resuspending in 2,3mL ice-cold 0,1M CaCl2 with 50% glycerol. Competent bacteria were flash frozen in liquid nitrogen and stored in -80°C.

4.2.5. Transformation of competent bacteria

Chemically competent E. coli DH5α cells were transformed using 100 ng of plasmid DNA. 100 µl of competent cells was added to a plasmid solution and the mixture was incubated on ice for 30 minutes. Following this, a heat shock was performed for 90 seconds at 42°C and the cells were placed back on ice for 2 minutes. Next, 400 µl of LB medium was added to the cells and the mixture was incubated at 37°C with shaking at 700 rpm for 1 hour. Subsequently, the cell suspension was transferred into an Erlenmeyer flask containing 250 µl of LB medium with ampicillin and incubated overnight at 37°C and 200 rpm to allow for transformation and colony growth.

4.2.6. Phenol/chloroform extraction of nucleic acids

A phenol/chloroform extraction method was used to extract nucleic acids. Obtained aqueous solution was mixed with 0.1 volume of 3 M sodium acetate (pH 5.2) and one volume of phenol/chloroform and transferred into a Phase lock tube. After centrifugation for 5 minutes at 17,000 g and 4°C, chloroform was added and the sample was centrifuged again. The upper aqueous solution, containing the extracted nucleic acids, was then carefully transferred into a new reaction tube. To precipitate DNA, the solution was mixed with 2.5 volumes of ice-cold

ethanol, while for RNA precipitation, 0.7 volumes of isopropanol were used. After centrifugation for 60 min at 17,000 g and 4°C, the supernatant was discarded and the nucleic acid pellet was washed with 70% ethanol. Subsequently, the pellet was air-dried and resuspended in water. Distilled (dH2O) was used for DNA or DEPC-treated water (DEPC-H2O) for RNA.

4.2.7. *In vitro* T7 transcription

Isolated, linearized and purified plasmid DNA with a T7 promoter was used to generate HCV genome by T7 transcription. The T7 Scribe™ Standard RNA IVT Kit was used and reaction mixed according to the manufacturer's protocol.

4.2.8. RNA isolation

For intracellular RNA isolation, cell culture supernatant was aspirated at the time of harvesting and cells were washed twice with PBS at room temperature. Cells were lysed by using RNA-Solv® Reagent and RNA was isolated according to the manufacturer's instructions. Air-dried RNA pellets were resuspended in ddH_2O supplemented with 0.1 % DEPC.

For extracellular viral RNA isolation, 140 µl of supernatant collected from the plate were used. RNA was isolated with the QIAamp Viral RNA Mini Kit (spin protocol) according to the manufacturer's instructions. For elution of viral RNA, 60 µl elution buffer was used.

4.2.9. cDNA synthesis

10 µg of isolated intracellular RNA was first incubated with 1 U DNase and the corresponding buffer in a reaction volume of 10 µl for 60 minutes at 37 °C. 1 µl DNase Stop-Solution was added to the mixture to stop the reaction and the solution was incubated at 65 °C for 10 minutes. Afterwards, 1 µl Random Hexamer Primer was added to the RNA and incubated at 65 °C for 15 minutes. The cDNA synthesis was performed by adding the master mix shown in Table. The reaction mixture was first incubated at room temperature for 10 minutes and then at 42 °C for 60 minutes. Heating of the samples to 72 °C for 10 minutes stopped the reaction. The cDNA was stored at -20 °C until analysis by RT-qPCR.

Table 3. Master mix for cDNA synthesis

Master mix for first strand cDNA synthesis	
5x RT buffer	4 µl
dNTP mix (10 mM)	2 µl
RevertAid™ H Minus RT (200 U/µl)	1 µl
Nuclease-free water	1 µl

4.2.10. Real-Time qPCR

Analysis of gene expression was performed using the synthesized cDNA. Real-time qPCR on the LightCycler 480 system was carried out: for this 3 µl of diluted cDNA was mixed with specific primers and 2x Maxima SYBR Green qPCR Master mix, as detailed in the table underneath. Each sample was then duplicated while kept on ice.

Table 4. RT-qPCR sample composition.

Component	**Volume (per sample)**
Diluted cDNA	3 µl
Forward primer (10 µM)	0.25 µl
Reverse primer (10 µM)	0.25 µl
2x Maxima SYBR Green Master Mix	5 µl

Nuclease-free water	1.5 µl

A fluorescent dye, SYBR Green, was used for the detection of cDNA. SYBR Green intercalates with complementary DNA during the qPCR reaction. The fluorescence intensity of dye directly correlates to the quantity of amplified DNA and is measured at the end of each cycle. The RT-qPCR program is shown in table 5.

Table 5. RT-qPCR program for intracellular RNA aplification.

Program	Temperature (°C)	Hold time (sec)	Slope (°C/sec)	Cycles
Denaturating	95	600	20	1
Cycling	95	15	20	45
	56	30	20	
	72	30	5	
Melting	95	60	20	1
	60	30	20	
	95	0	0.1	
Cooling	40	30	20	1

Results for RNA quantification were calculated as n-fold titers using the $2^{-\Delta Cp}$ method.

To quantify extracellular viral genomes, the LightMix® Modular HCV Virus Kit was used, following the protocol provided by the manufacturer. This kit contains a reverse transcriptase, a DNA-directed DNA polymerase, dNTPs, specific primers targeting HCV and a labeled hydrolysis probe for detection at 530 nm. After preparing the master mix, it was combined with the isolated extracellular viral RNA in a 1:1 ratio. Subsequently, the qPCR program detailed in Table 6 was executed using the LightCycler 480.

Table 6. RT-qPCR program for extracellular RNA aplification.

Step	Temperature [°C]	Time [s]	Slope [°C/s]	Cycles
Reverse Transcription	50	600	4.4	1
Denaturation	95	30	4.4	1
Denaturation	95	5	1.1	
Annealing	60	30	2.2	45
Elongation				
Melting Curve	95	10	4.4	
	60	10	2.2	1
Cooling	40	2	2.2	

Results for extracellular viral RNA quantification were calculated as n-fold titers using the 2-ΔCp method.

4.2. Protein biochemistry

4.2.1. Protein quantification by Bradford assay

Quantification of the protein concentration was performed via the Bradford assay. 100µl of Bradford reagent containing the Coommassie dye was mixed with 5µl of lysate sample. As the assay is based on the colorimetric change in absorbance of the Coomassie dye, the dye shift was measured at 595nm in Tecan Reader and protein quantification was carried out following the manufacturer's guidelines (Bradford, 1976).

4.2.2. SDS-PAGE

Sodium dodecyl sulfate polyacrylamide gel electrophoresis (SDS-PAGE) was used to separate proteins based on their molecular weight (Laemmli, 1970). A stacking gel and a separation gel biuld the gel. The stacking gel, with a polymer concentration of 4% was used to concentrate proteins. The separation gel, with a concentration ranging from 8% to 14%, depending on the size of the target protein, was used to separate SDS-denatured proteins. Equal amounts of protein (75 to 150 µg) were denatured in 4x SDS loading buffer for 10 minutes at 95°C before being separated in a vertical chamber with an electric field strength of 90-120 V.

4.2.3. Western blot

After SDS-PAGE separation, proteins were transferred onto a PVDF membrane activated with methanol for 45s. To transfer the proteins a semi-dry blotting chamber applying an electric field of 1.3 mA/cm² for 1 hour was used. In order to prevent unspecific binding of antibodies, the membrane was blocked with 1x Roti®-Block or 5% skim milk in TBST buffer blocking solution at room temperature for 1 hour. The primary antibody was diluted in the blocking solution before incubating the membrane at room temperature for 1 hour or overnight at 4°C. Afterwards, unbound antibodies were removed through three 10-minute washing steps with TBS-T. Next, the membrane blocked in Roti-Block was incubated with a fluorophore-conjugated secondary antibody, diluted in the blocking solution, for 1 hour at room temperature while avoiding exposure to light. Afterward, the membrane was washed again with TBS-T to eliminate unbound secondary antibody. The signals for the specific proteins were detected using the Li-Cor Odyssey CLx imaging system. Next, the membrane blocked in milk was incubated with an HRP-conjugated secondary antibody, diluted in the blocking solution, for 1 hour at room temperature. In this case, the signals for the specific proteins were detected using

the ImageQuant800 CCD Imager imaging system and Immobillion Western HRP substrate. Densitometric quantification of the protein signals was performed using the Li-Cor Image Studio software.

4.2.4. Half-life determination

Cells were treated with growth medium supplemented with a final concentration of 142 µM CHX for 0 to 240 minutes to determine the half-life of the proteins. The medium supplemented with equal volumes of dH2O served as an experimental control. The cells were collected using RIPA buffer and subjected to analysis via western blot. The half-life was determined using the mean values' nonlinear regression equation.

4.2.5. Luciferase reporter assay

Lysate cleared by centrifugation was transferred into a white microtiter plate. Orion II Microplate Luminometer chemiluminometer was used to measure the chemiluminescence of each sample after adding the firefly-luciferase substrate for a duration of 10 seconds. Addition of the substrate follows automatically by a built-in liquid dispenser. To standardize the measured values, the relative protein concentration in the lysates was calculated using the above-mentioned Bradford test. Luciferase lysis buffer was used as a blank value in the Bradford assays.

4.2.6. End point dilution assays ($TCID_{50}$)

Cells were fixed with 4% formaldehyde, washed with PBS and incubated overnight at 4°C. Horseradish peroxidase–coupled donkey-α-rabbit IgG (NA934; GE Healthcare, Chicago, IL) was used as secondary antibody and subsequent stain was performed using 3-amino-9-ethylcarbazol (30 mM Na-acetate, 12 mM acetic acid, 0.05% w/v 3-amino-9-ethylcarbazol, 0.01% H_2O_2). Evaluation of viral titers in cell culture supernatants was achieved by subjecting collected supernatants to an end point dilution assay (EDPA). Huh 7.5 cells were seeded in a 96-well plate at a density of 1 x 10^4 cells/well. After 6 h cells were infected using a serial dilution of cell culture supernatant (5 steps, 1:5 ratio) in 6 replicates for 72 hours. At the time of harvesting, cells were fixed with 4% formaldehyde, washed with PBS and incubated overnight at 4°C. Blocking occurred by addition of 5% BSA in TBS-T for 1h at room temperature. NS5A-specific serum was used to detect HCV-replicating cells. Samples were further probed with HRP-conjugated secondary antibodies diluted in blocking buffer for 1h at RT. Subsequently, samples were washed with TBST at room temperature and HRP-dependent stain was achieved by incubation with sterile-filtered Carbazole stain solution for 2h at RT. Infected wells were identified via presence of a red precipitate with the help of a digital microscope. The resulting TCID50 was calculated based on the method of Spearman and Kärber.

4.2.7. Indirect immunofluorescence microscopy

4.5.1.1 Standard indirect immunofluorescence staining

A confocal laser scanning microscope (CLSM) at the CLSM TCS SP8 (Leica) was used to examine the localization and distribution of proteins in the cells. Cells were cultured on 18 mm cover slips in a 12-well plate and washed with PBS. 4% formaldehyde in PBS for 20 min at room temperature was used for fixation of the cells on the cover slips. Following fixation, cells were washed three times in PBS for five minutes each and subjected to permeabilization for 10 minutes at room temperature with 0.5% Triton X-100 in PBS. After permeabilization, cells were washed again three times for 5 minutes each with PBS and nonspecific antibody binding was blocked with 5% BSA in PBS for 15 minutes at room temperature. Unspecific antibody

binding was avoided by blocking for 15 minutes in 1% fresh prepared BSA in PBS at room temperature. PBS was used to wash the cells once. The cells were incubated with the primary antibodies for 1 hour at room temperature in a humid chamber before being rinsed three times in PBS for 5 minutes. The secondary antibodies were incubated under the same conditions and DAPI was used for nuclear staining. Nonspecifically bound antibodies were removed by washing three times with TBS-T for five minutes each. Finally, cover slips were mounted onto microscope slided by embedding in Mowiol. Stained samples were kept at 4°C and protected from light until they were analyzed via a confocal laser scanning microscope.

4.5.1.2 Filipin staining

For cholesterol and oxysterols staining by Filipin III, cells were fixed using 4% formaldehyde in PBS for 20 minutes at room temperature. Excess formalin was removed and cells were washed once with PBS. Formaldehyde-dependently formed Schiff-bases were quenched via addition of TBS for 5 min at RT. Afterwards, blocking and permeabilization occurred by addition of 5% BSA in TBS supplemented with 0.1 mg/mL Filipin III for 30 min at room temperature. Next, cells were incubated with 45 µl of primary antibody diluted in BSA for 1 hour at room temperature in a humid chamber without and addition of Filipin III with subsequent washing with TBS at room temperature. Afterwards, cells were incubated with 45 µl of fluorophore-labeled secondary antibody and Filipin III for 1 hour at room temperature, protecting from light. Any nonspecifically bound antibodies were removed by washing three times for 5 minutes each with TBS. Finally, the cover slips were mounted onto microscope slides using Mowiol. The stained cells were stored in the dark at 4°C until analysis using a confocal laser scanning microscope.

4.5.2 Immunohistochemistry

Paraffin-embedded human liver sections were subjected to the immunostaining. The samples were fixed in PBS with 4% formaldehyde. Following that, 4m thick paraffin liver sections were deparaffinized with xylene, followed by a graded series of ethanol treatments. To achieve proper antibody binding and antigen retrieval, the sections were heated in a 10 mM sodium citrate solution at pH 6.0 at 95°C for 30 minutes. An anti-Nrf1 primary antibody that targets the protein's N-terminus was used, as well as an anti-core antibody, to detect HCV infected cells. Anti-rabbit Alexa Fluor 488-conjugated and anti-mouse Alexa Fluor 546-conjugated antibodies were used as the secondary antibodies. DAPI (4,6-diamidino-2-phenylindole) staining was used to visualize the nuclei of the cells.

4.4 Microscopy

4.4.1 Confocal laser scanning microscopy

Mowiol-mounted samples on glass slides were subjected to analysis using a Confocal Laser Scanning Microscope Leica TCS SP8 System equipped with a DMi8 microscope at room temperature. The imaging was conducted using a 100x magnification oil immersion objective with a numerical aperture of 1.4. The pinhole was set to 1.3 AU, which resulted in a confocal section thickness of 0.895 µm.

Image acquisition and quantification were carried out using either the LAS X Control Software or FIJI Software. To quantify the protein amounts, the corrected total cell fluorescence (CTCF) was calculated using the formula: Corrected total cell fluorescence (CTCF) = integrated density - (area of selected cell x mean fluorescence of background readings). A minimum of 10 cells were analyzed for each sample during the quantification process. LDs analysis was performed using particle analysis feature in Fiji (Image J) software. Size of the particle was set as 0,01-infinity (inch^2). Circularity was set as 0.00-1.00. The total count, perimeter, ferret diameter and average size were measured.

4.5.1 Statistical analysis

The experiments were conducted under consistent and similar conditions throughout the study. The figure legends indicate the number of separate experiments represented in each figure. GraphPad Prism 9.2 software was used for statistical analysis and graphical data visualization. The mean standard error of the mean (SEM) is used to represent the results. The error bars in the figures reflect the standard error of the mean, which shows the precision of the mean values.

An unpaired t-test was performed to determine statistical significance, as shown in the figure legends. The following notation is used in the legends to signify the significance levels: "*" represents a significance level of p 0.05, "**" represents a significance level of p 0.01 and "***" represents a significance level of p 0.005.

5 Results

5.1 Decreased amount of Nrf1 in HCV replicating cells

Given the knowledge, that HCV infection induces oxidative stress, elevates cholesterol levels, and impairs Nrf2/Keap1 signaling it was interesting to explore the role of Nrf1 in the context of HCV infection. The quantitative polymerase chain reaction (qPCR) was used to measure Nrf1 transcripts in two types of cells: HCV-replicating cells (Jc1) and HCV-nonreplicating matching control cells (GND) to investigate the influence of HCV infection on Nrf1 expression. Considerable increase in Nrf1 mRNA in HCV-infected cells compared to HCV-negative cells was observed, which indicated that HCV infection upregulates Nrf1 gene expression (Figure 14 A).

Surprisingly, total cellular lysates derived from HCV-positive cells have lower amounts of full-length Nrf1 protein than lysates derived from HCV-negative cells, despite an increase in Nrf1 mRNA (Figure 14 B). Immunofluorescence analyses using HCV-core-, NS3-, NS5A- and Nrf1-specific antiserums demonstrate that in HCV negative cells the quantity of Nrf1 protein was reduced, but there were no changes in subcellular location (Figure 14 D); supporting the results observed in the Western blot analysis (Figure 14 B).

To further understand the effect of HCV infection on Nrf1 protein levels, cleaved Nrf1 fragments were analyzed using Western Blot method with an antibody targeting the protein's C-terminus. The data revealed a comparable pattern, with considerably lower amount of cleaved Nrf1 protein in HCV-positive cells as opposed to HCV-negative cells (Figure 14C). Furthermore, confocal laser scanning microscopy demonstrated that amount of the cleaved Nrf1 protein was reduced in the nuclei of HCV-positive cells compared to the negative control (Figure 14 D).

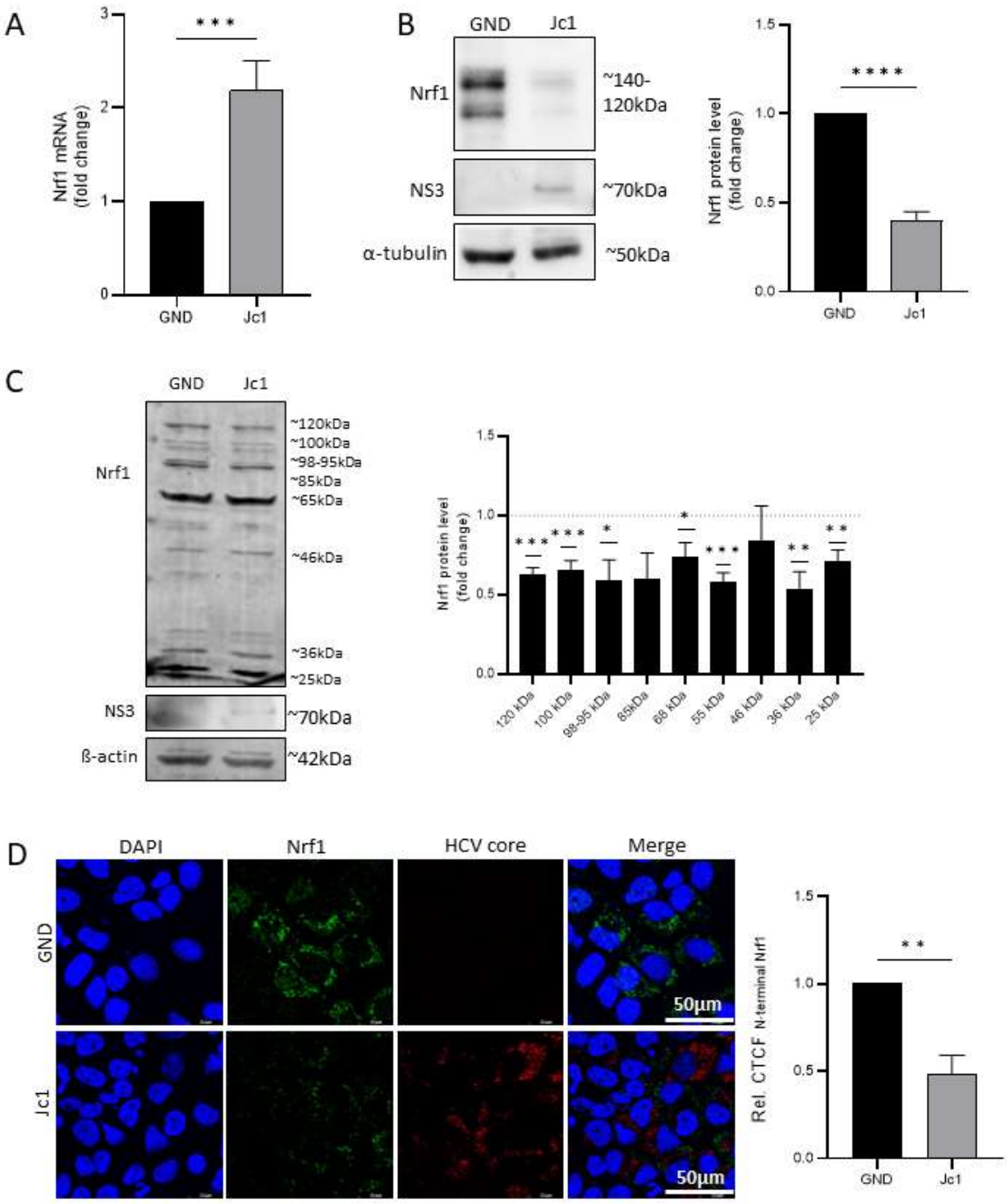
A
Nrf1 mRNA (fold change)
***
GND
Jc1
B
GND
Jc1
Nrf1
~140-120kDa
NS3
~70kDa
α-tubulin
~50kDa
Nrf1 protein level (fold change)
****
GND
Jc1
C
GND
Jc1
Nrf1
~120kDa
~100kDa
~98-95kDa
~85kDa
~65kDa
~46kDa
~36kDa
~25kDa
NS3
~70kDa
ß-actin
~42kDa
Nrf1 protein level (fold change)
120 kDa
100 kDa
98-95 kDa
85kDa
68 kDa
55 kDa
46 kDa
36 kDa
25 kDa
D
DAPI
Nrf1
HCV core
Merge
GND
Jc1
50µm
50µm
Rel. CTCF N-terminal Nrf1
**
GND
Jc1

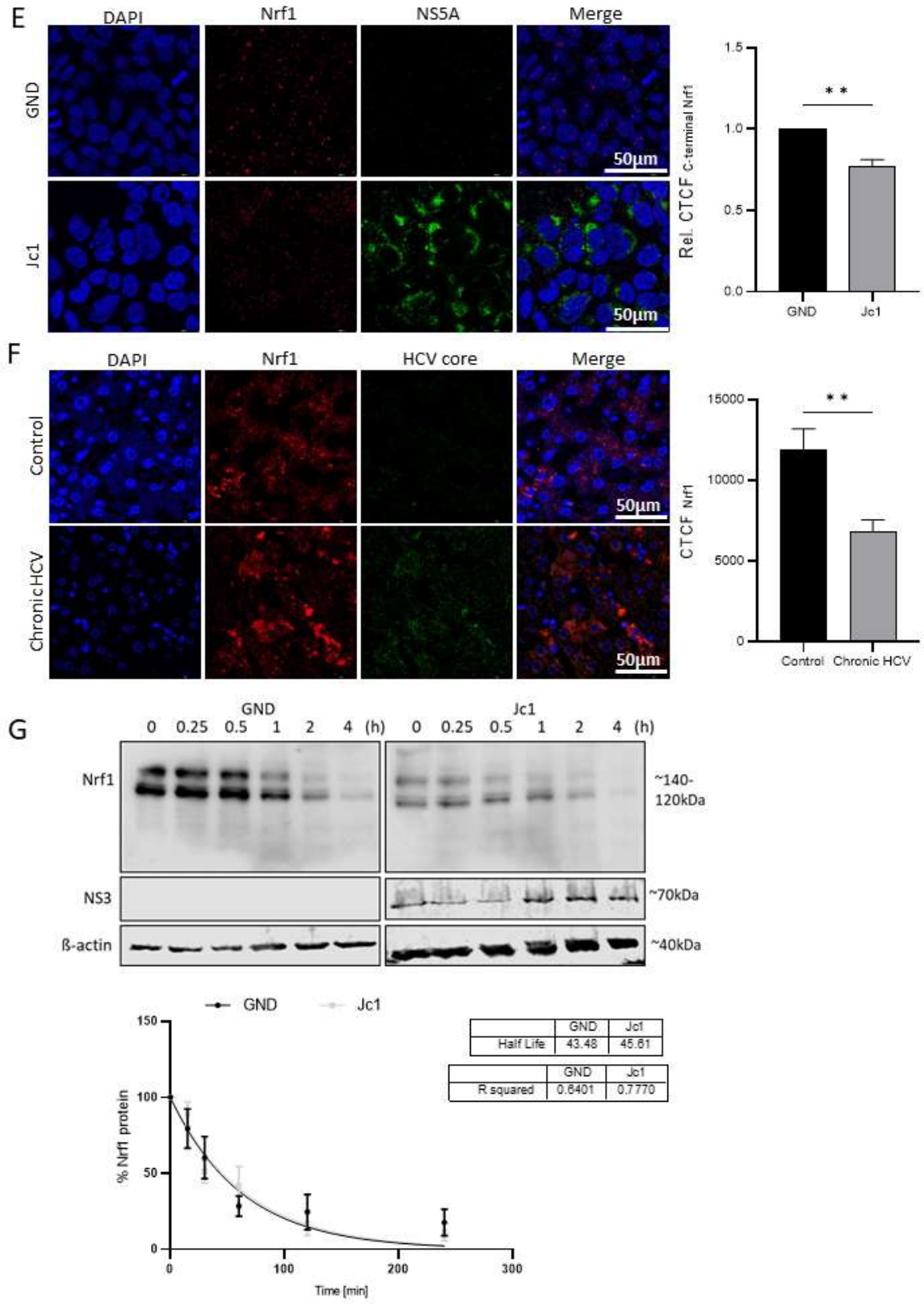

Figure 14. HCV has no effect on Nrf1 half-life. (A) Relative change in intracellular Nrf1 mRNA in uninfected or infected cells as assessed via RT-qPCR; values are referred to HCV-negative cells. (B) Representative Western blot of cellular lysates derived from HCV-positive (Jc1) or negative (GND) cells using an antibody that binds to the N-terminal part of Nrf1. In addition, NS3 was detected to confirm HCV replication. Detection of alpha-tubulin served as loading control. Quantification based minimum on 3 independent experiments for detection of Nrf1. The value for control cells (GND) was arbitrarily set as 1. (C) Representative Western blot of cellular lysates derived from HCV-positive (Jc1) or negative (GND) cells using an antibody that binds to the C-terminal part of Nrf1 for detection

of Nrf1-specific fragments. In addition, NS3 was detected to confirm HCV replication. Detection of alpha-tubulin served as loading control. Quantification based on minimum 3 independent experiments for detection of Nrf1-specific fragments. Relative change in Nrf1 signal intensity referred to GND cells. The respective values for control cells (GND) were arbitrarily set as 1 and shown as dotted line. (D) CLSM images of HCV-positive (Jc1) and HCV negative (GND) cells. For detection of Nrf1 an antibody binding to the N-terminal part was instrumental (green fluorescence) NS3 is visualized by the red fluorescence and nuclei were stained by DAPI (blue). Quantification of Nrf1-specific signal intensity expressed as relative CTCF. The respective values for control cells (GND) from each experiment were arbitrarily set as 1. (E) CLSM images of HCV-positive (Jc1) and HCV negative (GND) cells. For detection of Nrf1 an antibody binding to the C-terminal part was instrumental (red fluorescence) NS5A is visualized by the green fluorescence and nuclei were stained by DAPI (blue). Quantification of Nrf1-specific signal intensity in the nucleus expressed as relative CTCF. The respective values for control cells (GND) from each experiment were arbitrarily set as 1. (F) CLSM images of liver tissue derived from patients suffering from chronic HCV or non-infected patients. For detection of Nrf1 an antibody binding to the N-terminal part was instrumental (red fluorescence) HCV core is visualized by the green fluorescence and nuclei were stained by DAPI (blue). Quantification of Nrf1-specific signal intensity expressed as CTCF. (G) Representative Western blot of cellular lysates derived from HCV-positive (Jc1) or negative (GND) cells over the course of 0 to 240 min 142 µMCHX-treatment using an antibody that binds to the N-terminal part of Nrf1 for detection of Nrf1-specific fragments. In addition, NS3 was detected to confirm HCV replication. Detection of beta-actin served as loading control. Relative change in Nrf1 signal intensity in (G); values expressed as % of signal intensity at 0 min CHX-treatment; curve fitting applied as one-phase decay model with intercept set to 100 and decay set to reach 0 %.

To correlate these findings from the in vitro experiments with an in vivo situation, liver sections of chronically HCV infected patients were analyzed with respect to Nrf1 protein level in confocal laser scanning microscopy (Figure 14 F). Immunofluorescence staining of the liver sections revealed significantly lower protein level of Nrf1 protein in cells of livers with chronic HCV infection as compared with control.

Next, Nrf1 half-life was determined in both HCV-replicating and non-replicating cells to better understand the dynamics of Nrf1 transcription factor, regulation in the context of HCV infection (Figure 14 G). Surprisingly, Nrf1 protein half-life remains unaffected upon HCV infection and no significant changes between the HCV-replicating and HCV-nonreplicating cells was observed, what suggests that the reduction in Nrf1 protein levels observed in HCV-positive cells is likely not a result of altered protein degradation rates.

The results of these analyses demonstrate that HCV infection has an effect on Nrf1, resulting in increased mRNA expression and decreased protein levels. Overall, HCV infection affects Nrf1 expression at several levels, from mRNA transcripts to functional proteins, both in vitro and in vivo in infected patients.

5.2 Silencing of Nrf1 favours HCV life cycle

To further investigate the role of Nrf1 on HCV, Nrf1 protein knockdown was performed with Nfe2l1 siRNA human SMARTPool in HCV positive Huh 7.5 cells and overlay transfection protocol using siPORT. When comparing Nrf1 knockdown to scrRNA, an upward trend in HCV protein level was found. However, it is crucial to note that the observed increase did not achieve statistical significance (Figure 15 A - E). Similar upward trend to this of Western blot results was observed in intracellular and extracellular viral titers (Figure 15 F, G). Correspondingly, the effect of Nrf1 knockdown was tested on HCV replication using the Jc1 sequence containing a luciferase reporter gene, where a rise in HCV replication can be observed (Figure 15 H).

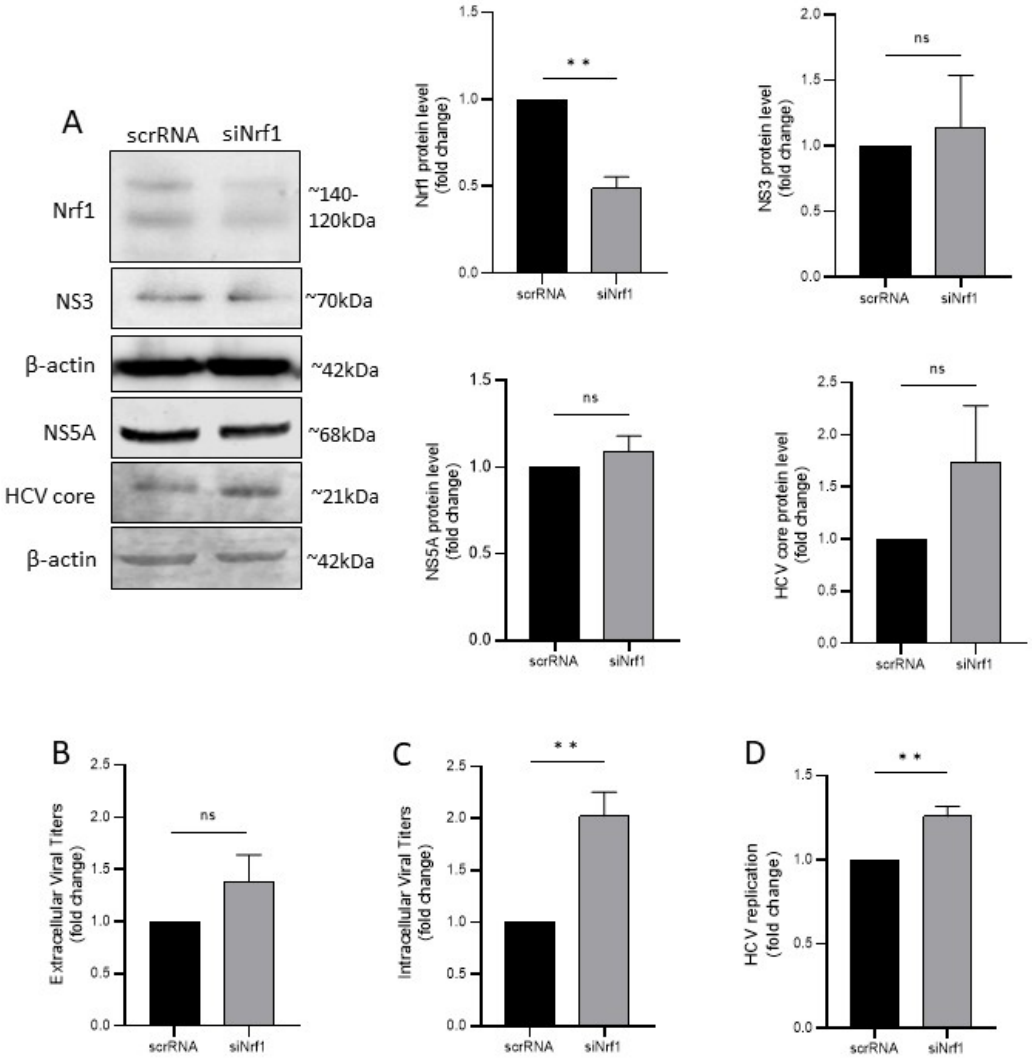

Figure 15. HCV infection regulates Nrf1. (A) Representative Western blot of cellular lysates derived from HCV-positive (Jc1) cells transfected with Nrf1-specific siRNA or as control with scrRNA using an antibody that binds to the N-terminal part of Nrf1. Cells were lysed 96 h after transfection. In addition, NS3, NS5A, core was detected. Detection of actin served as loading control. Quantification based on 3 independent experiments. The value for scrRNA transfected cells was arbitrarily set as 1. (B/C) Relative change in number of infectious intracellular viral particles of transfected and infected cells as assessed by determination of the TCID50. Values are referred to scrRNA transfected cells that were arbitrarily set as 1. Quantification based on 3 independent experiments. (D) Relative change in luciferase activity in scrRNA or siNrf1 transfected cells replicating an HCV-luc reporter virus (pFK-Luc-Jc1). Values are referred to scrRNA transfected cells that were arbitrarily set as 1. Quantification based on 3 independent experiments.

The first results caused concern about the data's reliability, because the effects might have been influenced by the low number of cells in which the knockdown occurred, as shown in the total lysate. In order to obtain more accurate results, the protein levels of HCV core and NS3 were investigated using a single-cell analysis technique called CLSM. Upon implementing Nrf1 knockdown, the effects on both HCV core and NS3 protein levels were carefully examined. Interestingly, the outcome of the single-cell analysis showed a significant increase in both HCV core and NS3 protein levels upon Nrf1 knockdown (Figure 16 A-F).

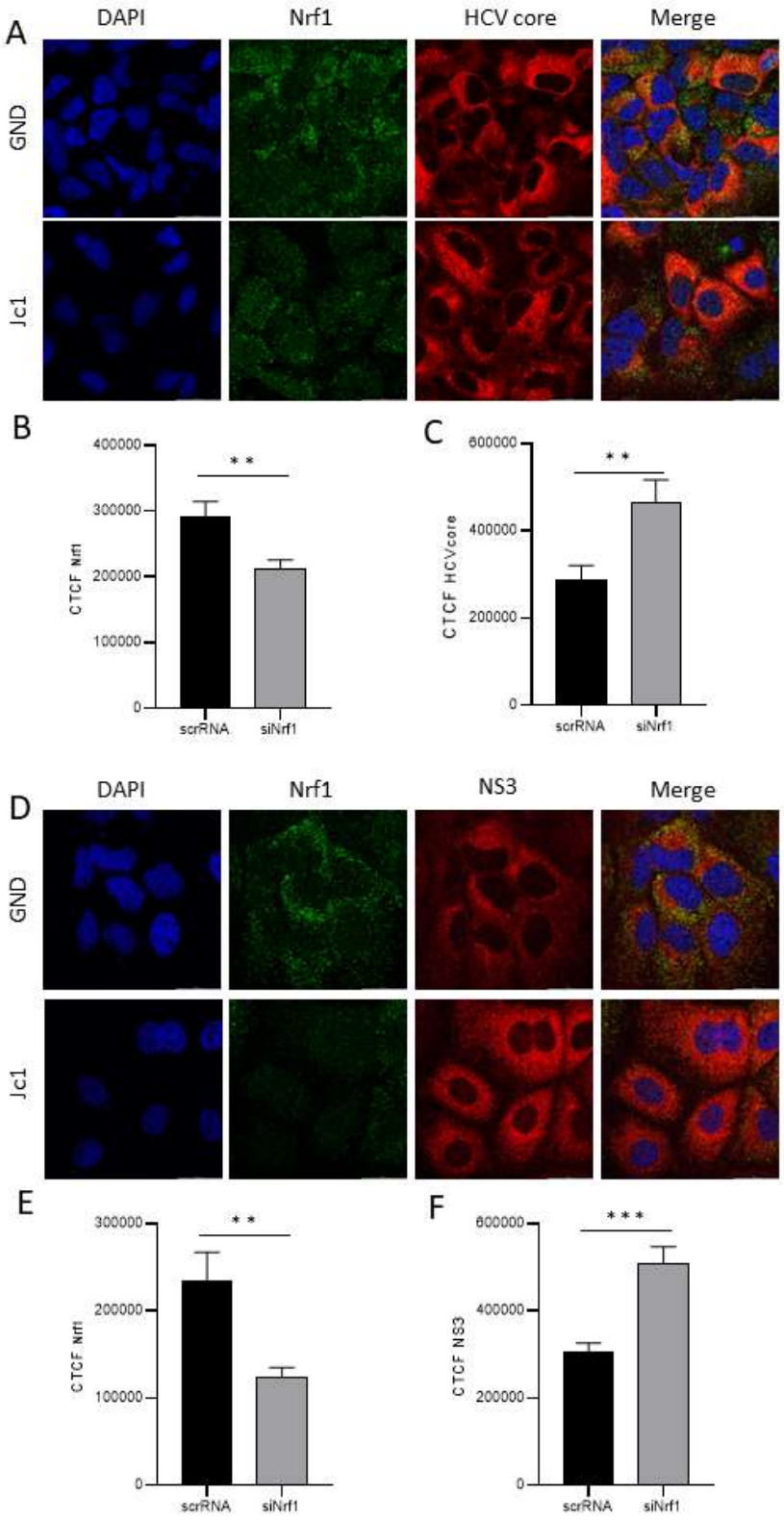

Figure 16. Nrf1 knockdown in single cells. (A/D) CLSM images of HCV-positive (Jc1) cells that were transfected either with scrRNA or Nrf1-specific siRNA. Cells were fixed 96 h after transfection. For detection of Nrf1 an antibody binding to the N-terminal part was instrumental (green fluorescence), NS3 and HCV core is visualized by the red fluorescence and nuclei were stained by DAPI (blue). Quantification of Nrf1-specific (E/R) core-specific (C) and (F) NS3-specific signal intensity is expressed as CTCF.

5.3 Overexpression of Nrf1 fragments restricts HCV replication, assembly and release

Two different fragments of Nrf1 protein, 25 kDa and 85 kDa, were used in the study to investigate the interaction between Nrf1 and HCV and their impact on structural and non-structural HCV proteins (Figure 17 A-D). Huh7.5 cells with an overexpression of Nrf1 25kDa and 85kDa fragments resulted in a strong decrease of amount of the non-structural NS5A protein and reflect an enhanced protein turnover (Figure 17 F, G, I). Moreover, overexpression of both the 25kDa and 85kDa Nrf1 fragments led to a reduction in the HCV core protein amount, similarly to NS5A protein (Figure 17 E, G, H). However, the effect was enhanced when using the 85kDa Nrf1 fragment compared to the 25kDa fragment.

To assess the impact of Nrf1 overexpression on HCV replication, the Jc1 sequence containing a luciferase reporter gene was used. In the analysis it was observed that the 85kDa Nrf1 fragment had a significant impact on HCV replication. However, the 25kDa Nrf1 fragment did not display the same effect (Figure 17 J).

Interestingly, an opposite effect concerning intracellular and extracellular viral genomes was observed. Both the 25kDa and 85kDa Nrf1 fragments caused an increase in the levels of intracellular viral genomes (Figure 17 K, L).

Furthermore, overexpression of both Nrf1 fragments greatly reduced the number of infectious intracellular viral particles (Figure 17 M), which shows that Nrf1 can impact viral particle formation or release within the cell. Surprisingly, overexpression of both Nrf1 fragments resulted in a reduction in the number of viral particles produced (Figure 17 N), what suggests that Nrf1 may play a role in restricting HCV particle dissemination to nearby cells.

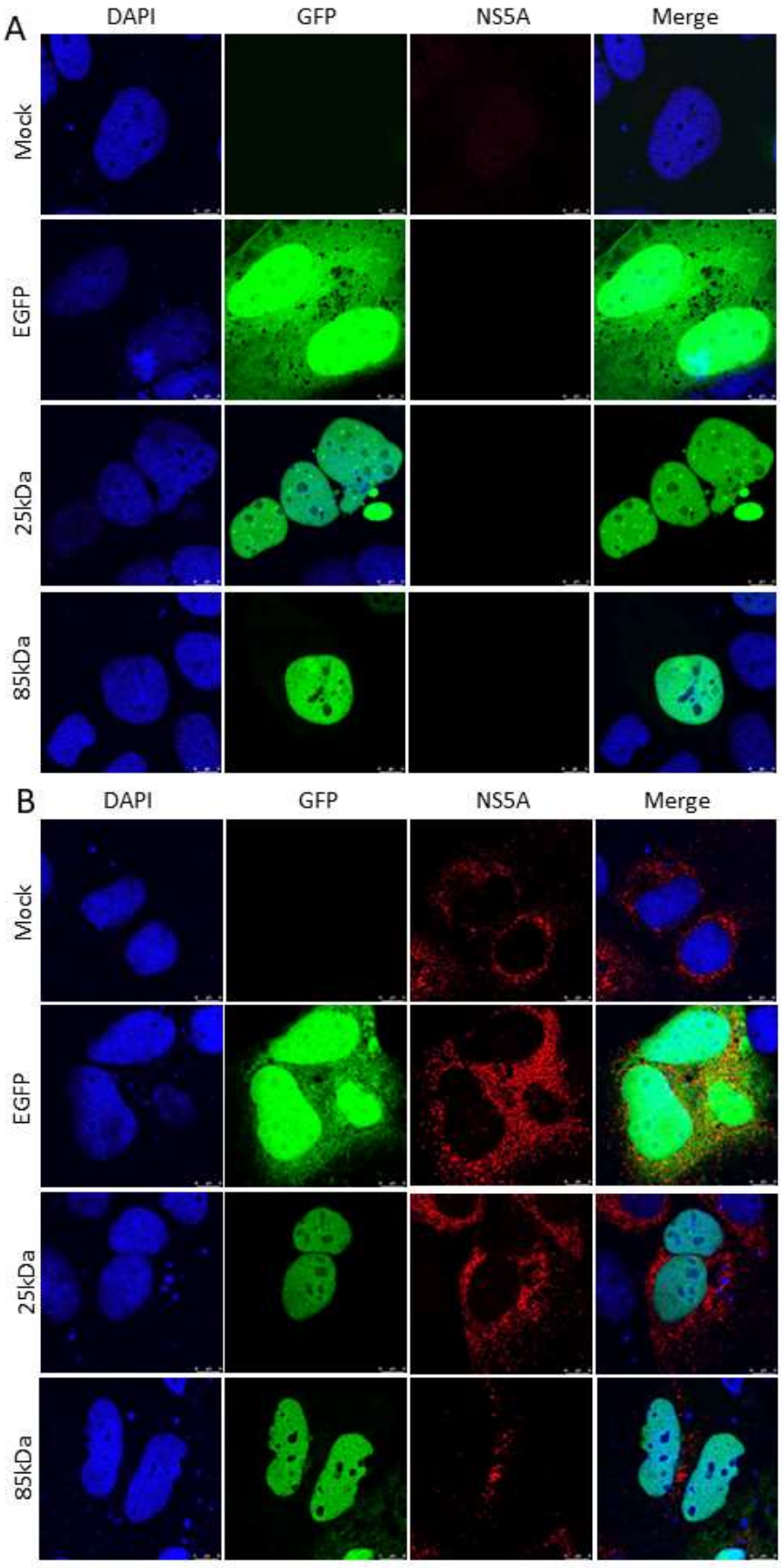
A
DAPI
GFP
NS5A
Merge
Mock
EGFP
25kDa
85kDa
B
DAPI
GFP
NS5A
Merge
Mock
EGFP
25kDa
85kDa

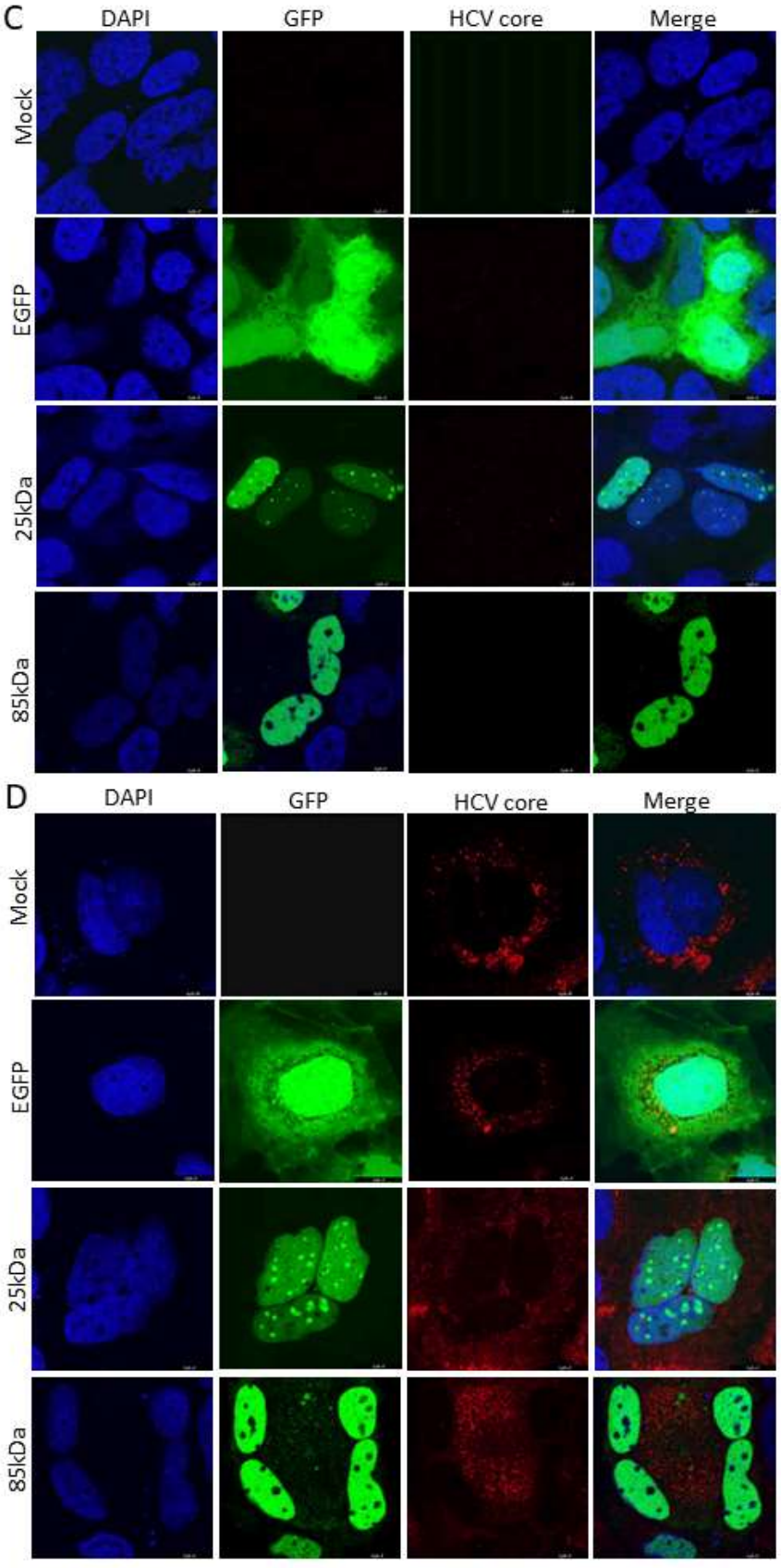
C
DAPI
GFP
HCV core
Merge
Mock
EGFP
25kDa
85kDa
D
DAPI
GFP
HCV core
Merge
Mock
EGFP
25kDa
85kDa

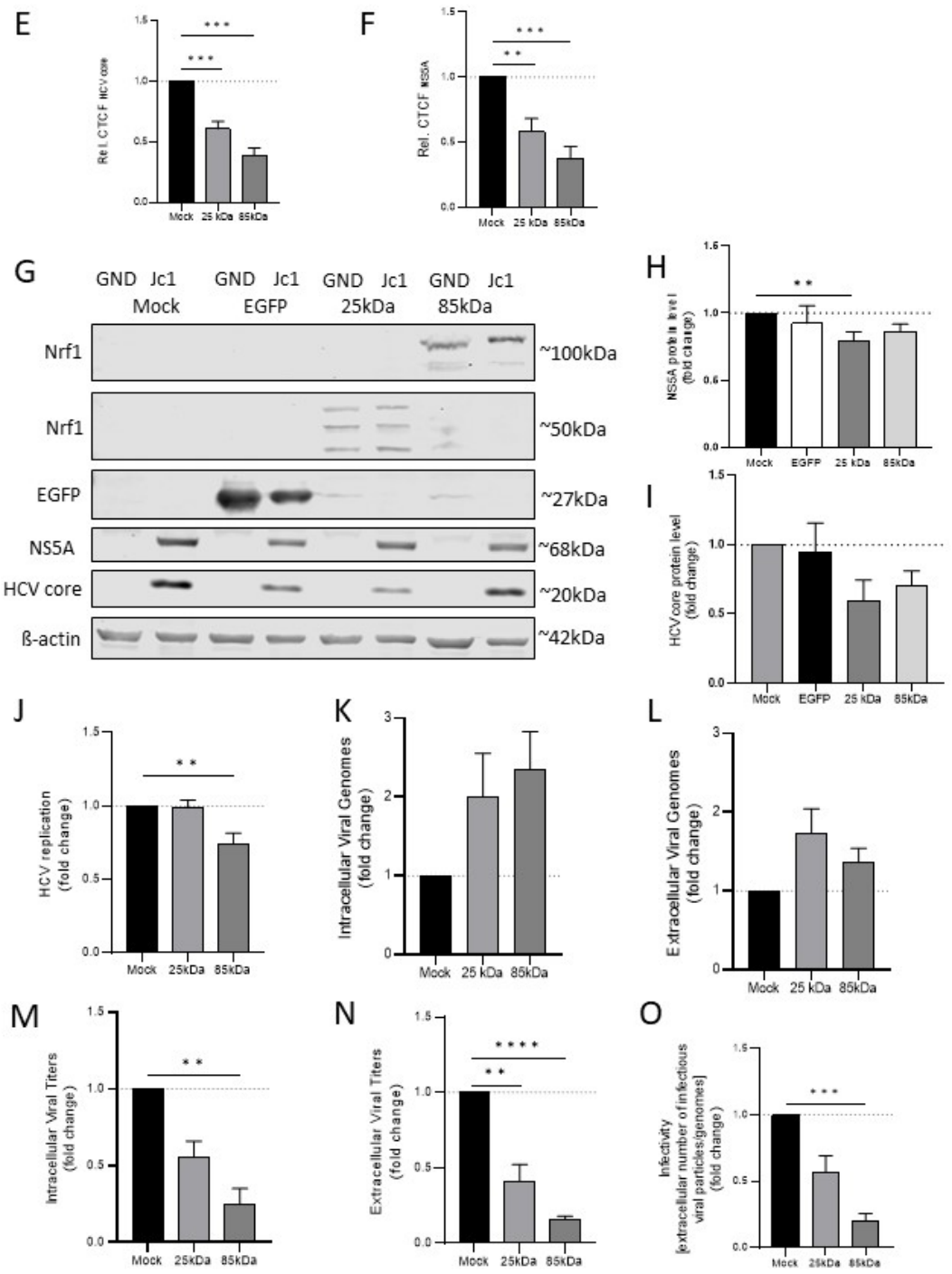

Figure 17. Overexpression of Nrf1 restricts HCV. (A-D) CLSM images of HCV-negative (GND) and HCV-positive (Jc1) cells that were either mock transfected or with an expression vector encoding a fusion protein of eGFP Nrf1-25 kDa or eGFP Nrf1-85 kDa. Cells were fixed 48 h after transfection. For detection of eGFP-Nrf1-25 kDa and eGFP-Nrf1-85 kDa the GFP-specific fluorescence was used. (A/B) NS5A (red fluorescence) and (C/D) core (red fluorescence) is visualized. Nuclei were stained by DAPI (blue). (E/F) Quantification of NS5A and core-specific signal intensity are expressed as CTCF. Values are referred to mock transfected cells that were arbitrarily set as 1. (G) Representative Western blot of overexpressed Nrf1 fragments, NS5A, HCV core and βActin in total lysates of uninfected or infected cells. (H) Relative change in NS5A signal intensity in (G); values referred to mock transfected, infected cells. (I) Relative change in HCV core signal intensity in (G); values referred to mock transfected, infected cells. (J) Relative change in HCV-promoter driven luciferase activity in transfected cells, values referred to mock transfected cells. (K/L) Quantification of (K) intracellular and (L) extracellular viral genomes by RT-PCR. Values are referred to mock transfected cells that were arbitrarily set as 1. (M/N) Relative change in number of infectious intracellular viral particles released by mock transfected cells or cells transfected with the expression vector

encoding eGFP-Nrf1-25 kDa and eGFP-Nrf1-85 kDa as assessed by determination of the TCID50. Values are referred to mock transfected cells that were arbitrarily set as 1. (O) Determination of the specific infectivity for the extracellular environment. Values are referred to mock transfected cells that were arbitrarily set as 1.

Taken together, these data demonstrate that the two distinct fragments of Nrf1, 25kDa and 85kDa, affect various aspects of HCV proteins. The available data supports the hypothesis that Nrf1-HCV interaction occurs throughout the HCV life cycle by proving how Nrf1 fragment overexpression impairs viral particle replication, release and accumulation of HCV.

5.4 Extranuclear sMaf proteins have the capacity to withdraw Nrf1 from the nucleus

The HCV infection causes delocalisation of sMaf proteins from the cell nucleus to the cytoplasmic site of the ER, where sMaf proteins bind to NS3 (Figure 18 A, B).

Interestingly, this effect can be artificially mimicked by expressing sMaf proteins containing a nuclear export signal (NES). When NES-containing sMaf proteins are expressed in the cells, regardless of whether the cells are infected with HCV or not, they localize outside of the nucleus (Figure 18 C, D). NES leads to the nuclear export, but not to localization on the ER surface, which demonstrates that the presence of the NES signal alone is sufficient to cause the delocalization of sMaf proteins. Furthermore, sMaf-NES proteins have the capacity to withdraw Nrf1 protein fragments out of the nucleus (Figure 18 C, D). This suggests that the interaction between sMaf-NES and Nrf1 fragments leads to their translocation from the nucleus to the cytoplasmic region.

Opposing effect can be observed when sMaf proteins containing a nuclear localization signal (NLS) are coexpressed with Nrf1 fragments. Both Nrf1 fragments and sMaf-NLS proteins localize in the nucleus, what suggest that the presence of the NLS signal facilitates the nuclear import of both Nrf1 and sMaf proteins (Figure 18 E, F).

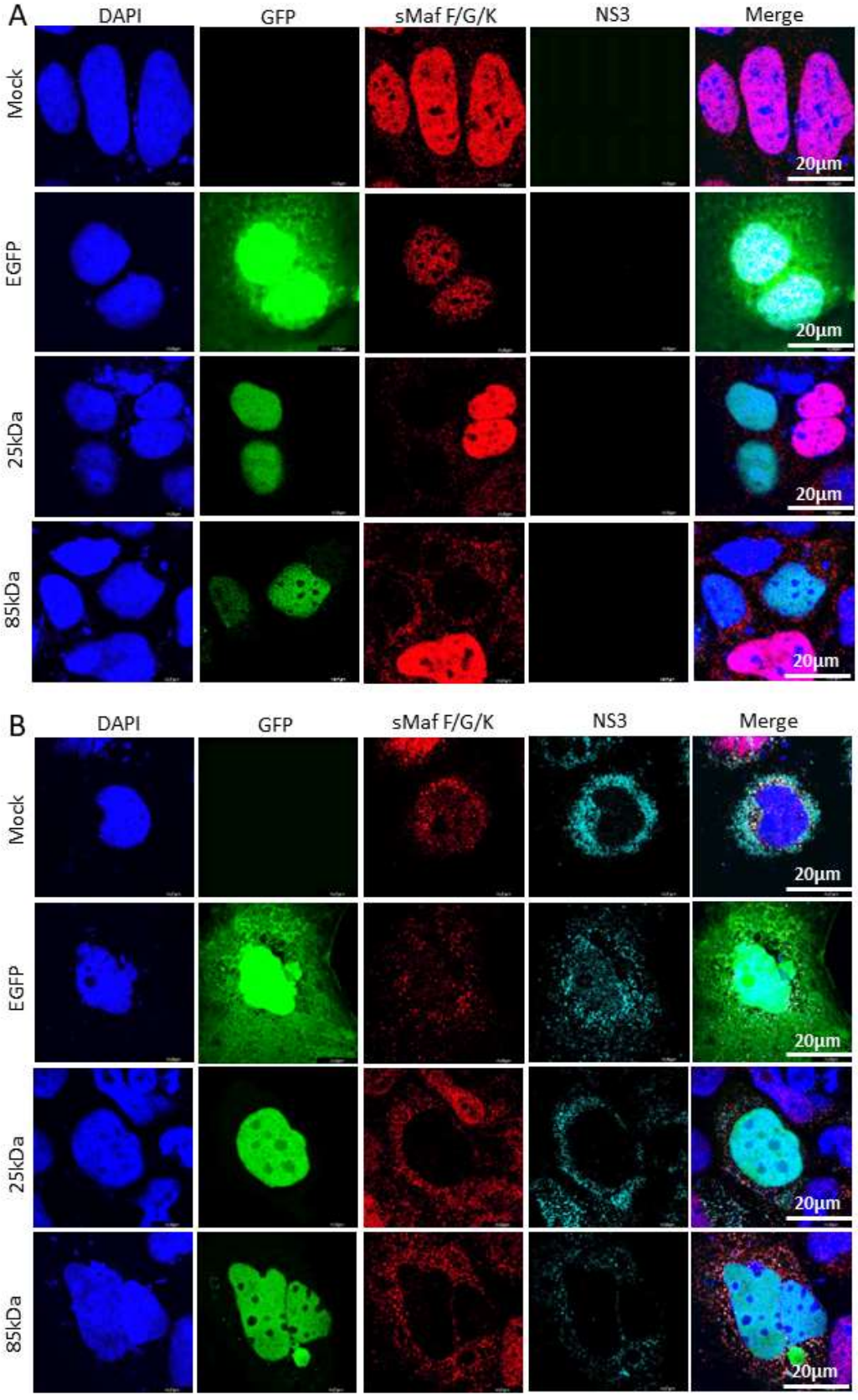
A
DAPI
GFP
sMaf F/G/K
NS3
Merge
Mock
EGFP
25kDa
85kDa
20μm
B
DAPI
GFP
sMaf F/G/K
NS3
Merge
Mock
EGFP
25kDa
85kDa
20μm

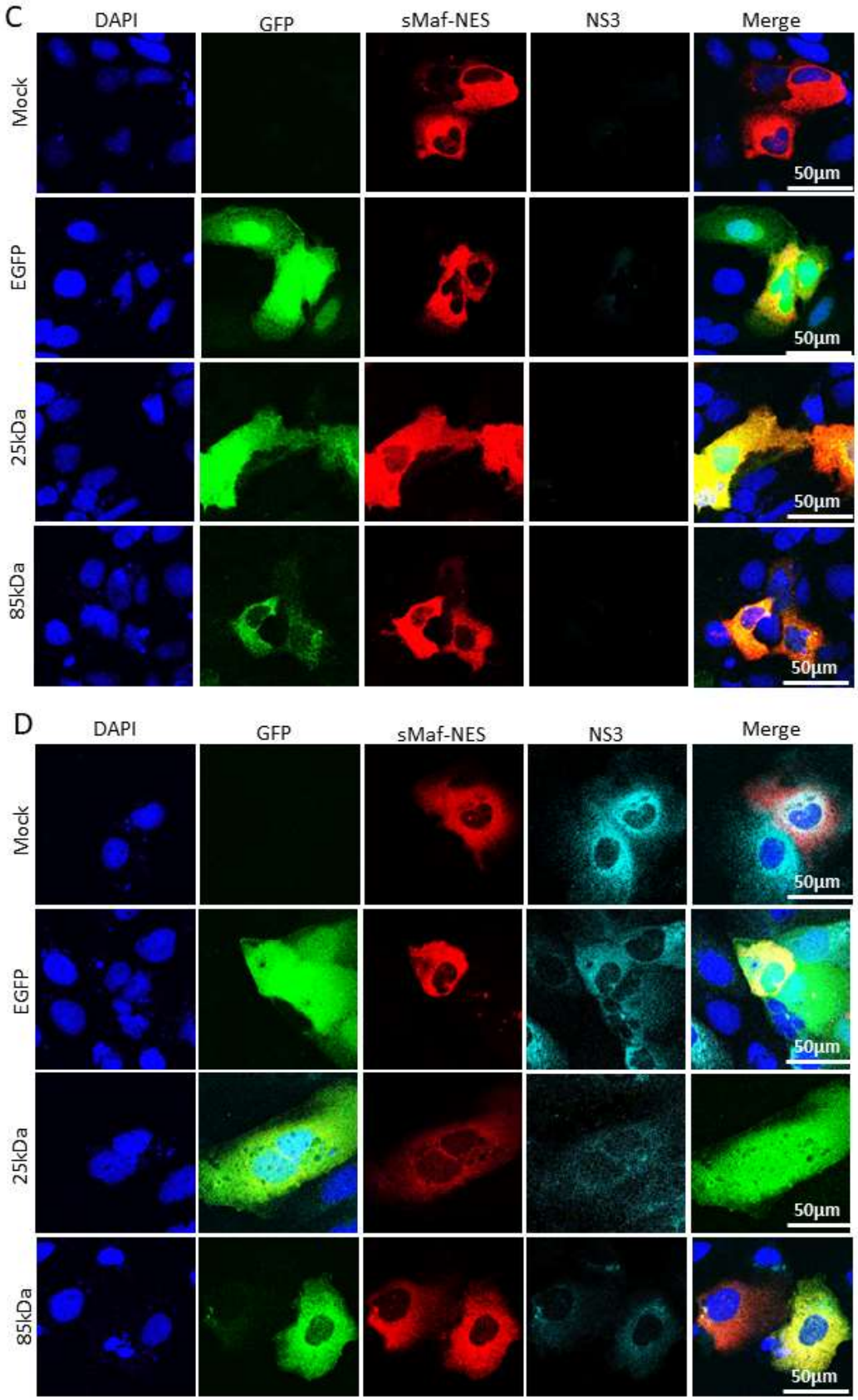
C
DAPI
GFP
sMaf-NES
NS3
Merge
Mock
EGFP
25kDa
85kDa
50μm
D
DAPI
GFP
sMaf-NES
NS3
Merge
Mock
EGFP
25kDa
85kDa
50μm

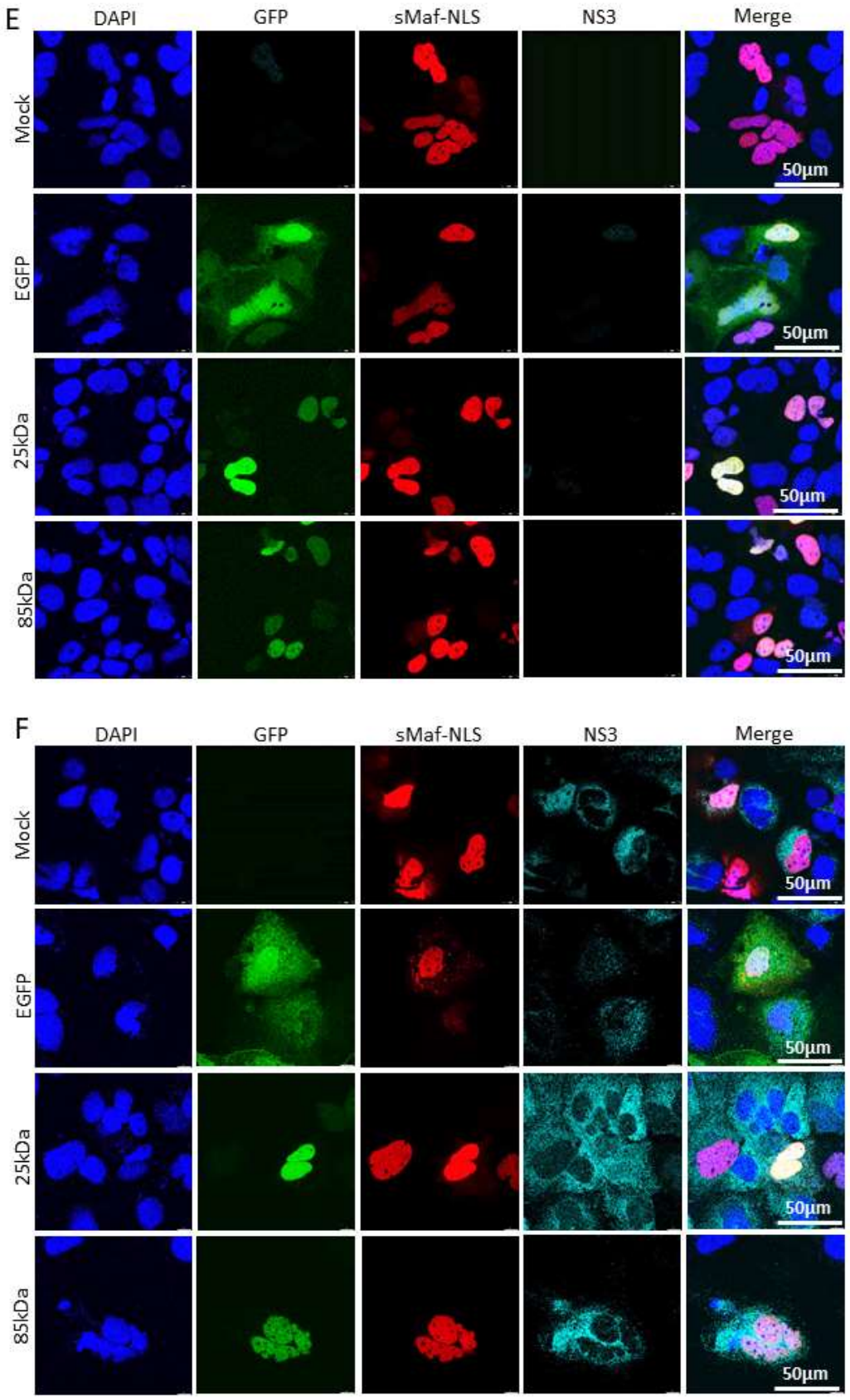

Figure 18. sMaf affects localization of Nrf1 fragments. Delocalization of Nrf1 by sMaf-NES fusion proteins (C/D) CLSM images of HCV-positive (Jc1) and HCV negative (GND) cells transfected with an expression vector encoding eGFP-Nrf1-25 kDa or eGFP-Nrf1-85 kDa (green). Cells were either mock transfected (A/B) or with an expression vector encoding a sMaf-NES-mcherry fusion protein (red) (C/D) or with an or with an expression vector encoding a sMaf-NLS-mcherry fusion protein (red) (E/F). NS3 is visualized in cyan and nuclei were stained by DAPI (blue).

5.5 Impaired activation of Nrf1/ARE-dependent gene expression by extranuclear sMaf-variant

To study the impact of Nrf1 fragments on ARE-dependent genes in the context of HCV infection, a luciferase reporter gene assay was performed using a reporter gene containing the ARE sequence derived from the promoter of NAD(P)H quinone oxidoreductase 1 (pLucNQO1). Firstly, there was a substantial decrease in the reporter gene's baseline expression in the presence of HCV infection. Furthermore, overexpression of the 85kDa Nrf1 fragment increased reporter gene promoter activity. This effect was observed both in HCV- negative as well as HCV-positive cells, however, the increase was less pronounced in HCV-positive cells (Figure 19).

Afterwards, an experiment was performed to investigate the involvement of sMaf proteins in modulating the Nrf1 fragment's effect on the ARE-dependent genes. Coexpression of sMaf proteins containing a nuclear export signal (NES) with the Nrf1 fragments led to a significant reduction in the activation of the reporter gene, in mock transfected cells, including both in HCV-positive as well as HCV-negative cells. However, in case of HCV-positive 85kDa transfected cells, no reduction was observed (Figure 19). The reason behind this reduction is the withdrawal of Nrf1 fragments from the nucleus due to the interaction with sMaf-NES proteins.

To restore the decreased promotor activity, caused by withdrawal of sMaf from the nucleus, Nrf1 fragments were coexpressed with sMaf proteins that contain a nuclear localization signal (NLS). Coexpression of Nrf1 fragments with sMaf-NLS proteins led to a rescue of the reporter gene activation in all settings, both in HCV-negative and HCV-positive cells. This means that the induced activation of the reporter gene could be observed once again after this coexpression, effectively restoring the ARE-dependent gene expression (Figure 19).

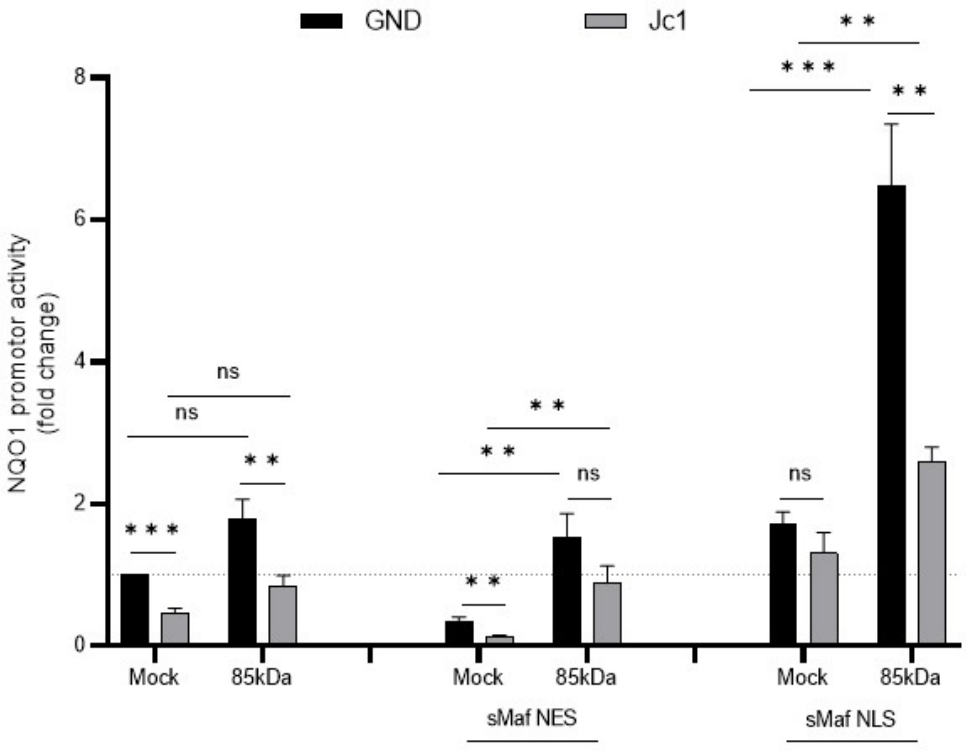

Figure 19. Overexpression of Nrf1 fragments fails to restore NQO1 expression. Impaired activation of Nrf1/ARE-dependent gene expression by coexpression of an extranuclear sMaf-variant HCV-positive or negative cells were cotransfected with a reporter construct expressing the luc reporter gene under the control of the NQO1 promoter and expression vectors encoding for the sMaf fusion proteins sMaf-NES or sMaf-NLS. In addition, the Nrf1-85 kDa fragment was overexpressed. The luciferase activity for mock transfected cells was arbitrarily set as 1 as visualized by the dotted line.

Collectively, these findings suggest that the withdrawal of sMaf from the nucleus within HCV-positive cells impairs the Nrf1-mediated activation of ARE-dependent gene expression, by leading to a deficiency of sMaf within the nucleus. The fusion of sMaf with a nuclear export signal (sMaf-NES) functions as a precise tool to manipulate Nrf-dependent gene expression.

5.6 Impaired activation of LXR promoter in HCV positive cells

Cells have evolved methods to control gene expression in response to intracellular signals, in order to keep their normal physiological activities as well as their capacity to efficiently respond to infections. Excess cholesterol removal is an essential process for cells and can be detected by multiple sensors within the ER. Excess cholesterol triggers an immunological response that stimulates cholesterol transport out of cells in order to maintain cholesterol homeostasis. The liver X receptor (LXR)-, which plays a vital role in governing cholesterol export from cells, serves as one of the sensors involved in cholesterol removal. A luciferase-coupled LXR reporter construct has been applied to indirectly monitor cholesterol efflux and assess LXR activity.

The overall activation signal of the reporter was stronger in cells that were negative as compared to cells that were positive for HCV was observed. Overexpression of the 85kDa Nrf1 fragment resulted in slight, but not significant activation of the reporter, suggesting that this fragment might enhance LXR activity and cholesterol efflux. Nonetheless, in HCV-positive cells, the activation of the reporter gene remained at a level that was two-fold lower in comparison to the GND cells (Figure 20 A).

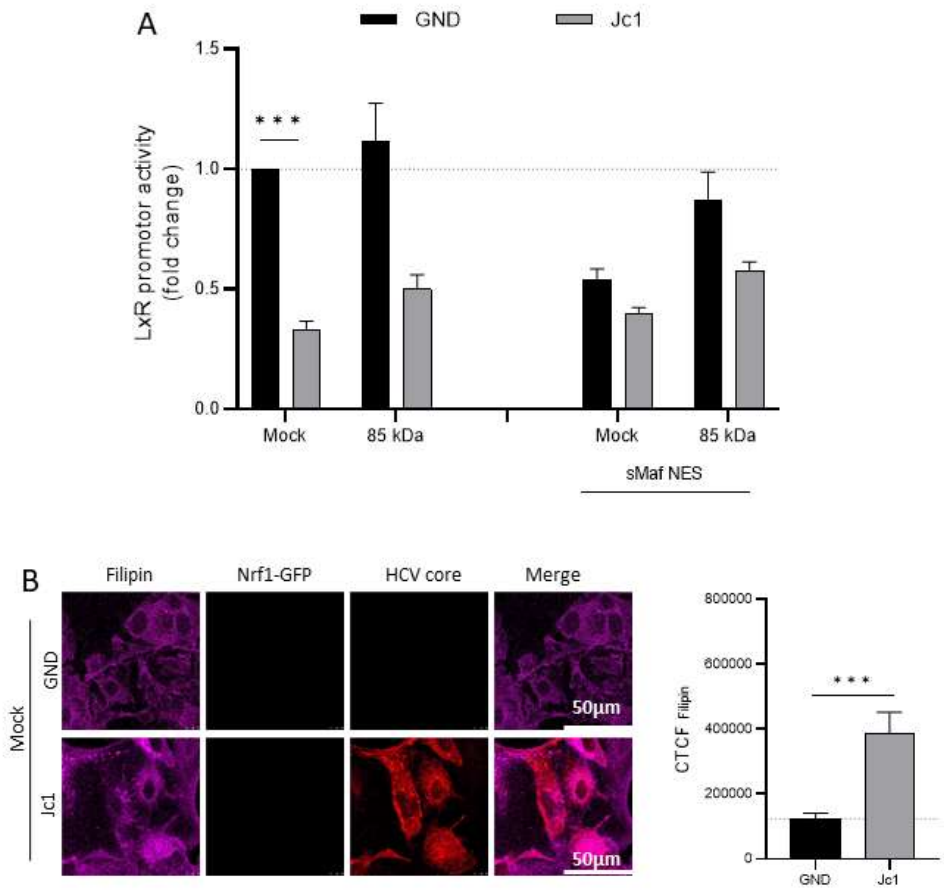
A
GND
Jc1
LxR promotor activity (fold change)
1.5
1.0
0.5
0.0
* * *
Mock
85 kDa
Mock
85 kDa
sMaf NES
B
Filipin
Nrf1-GFP
HCV core
Merge
Mock
GND
Jc1
50µm
50µm
CTCF Filipin
800000
600000
400000
200000
0
* * *
GND
Jc1

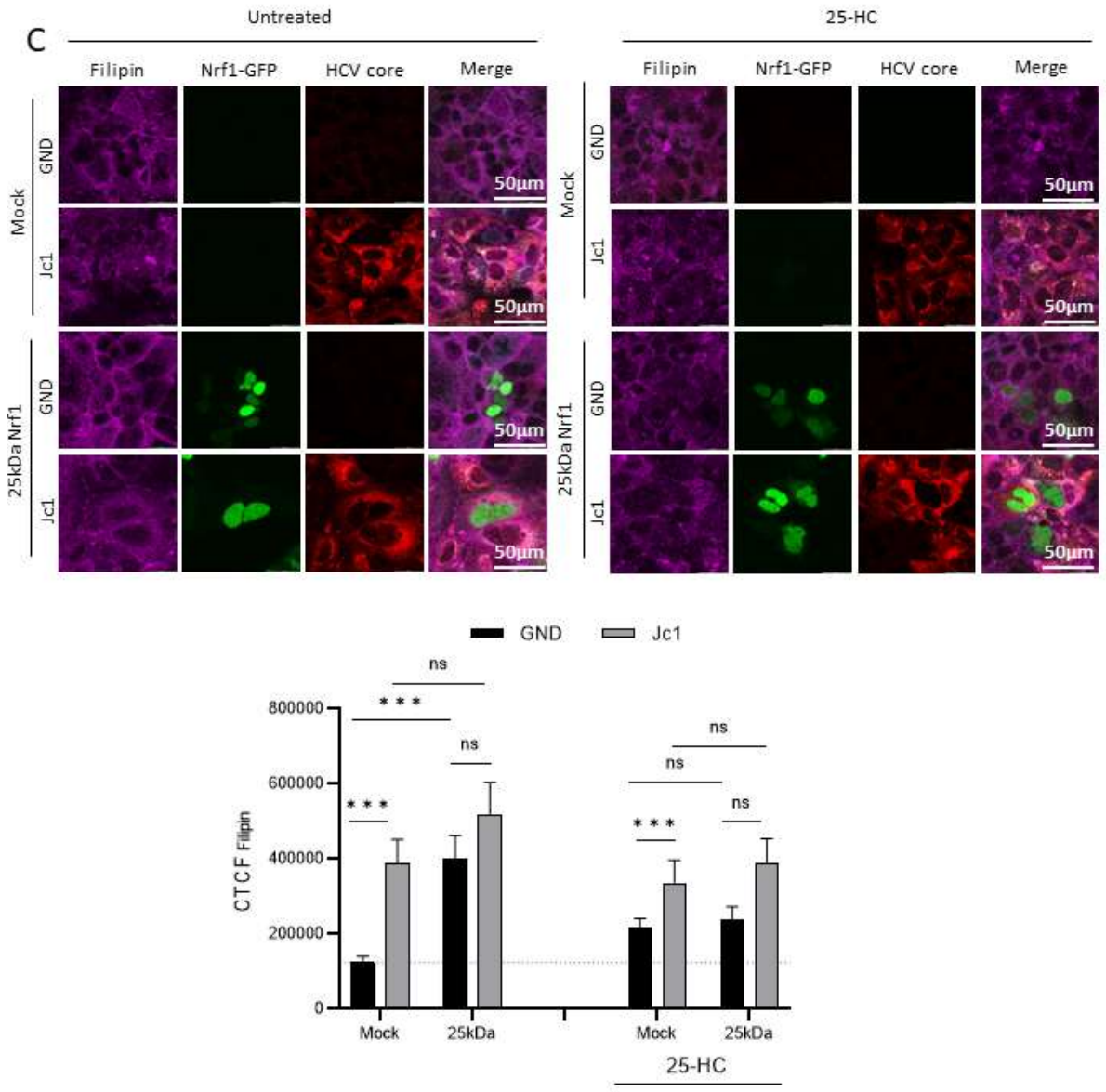

Figure 20. Nrf1 fragments modulate cellular cholesterol. (A) HCV-positive (Jc1) or negative cells (GND) were cotransfected with a reporter construct expressing the luc reporter gene under the control of the LxRα- promoter and expression vectors encoding for the sMaf fusion proteins sMaf-NES or sMaf-NLS. In addition, the Nrf1-85 kDa fragment was overexpressed. The luciferase activity for mock transfected cells was arbitrarily set as 1 as visualized by the dotted line. (B) CLSM images of HCV-positive (Jc1) and HCV negative (GND) cells. Cells were mock transfected. HCV core is visualized in red. For detection and quantification of cholesterol filipin (cyan) was used. Quantification of the filipin-specific signal intensity are expressed as CTCF. Values are referred to mock transfected cells that were arbitrarily set as 1. (C) CLSM images of HCV-positive (Jc1) and HCV negative (GND) cells. Cells were either mock transfected (upper panel) or with an expression vector encoding eGFP-Nrf1-25 kDa fusion protein (green). Cells were either control treated with 2% ethanol or treated with 25µM 25-hydroxycholesterol (25HC) for 24h. For detection and quantification of cholesterol filipin (magenta) was used. Quantification of the filipin-specific signal intensity are expressed as CTCF.

The coexpression of the sMaf-NES fusion protein in GND cells resulted in a significant reduction in LXR promoter activity (Figure 20 B). However, in Jc1 cells, whose promoter activity was already considerably lower compared with GND cells, the co-expression of the sMaf-NES fusion protein had no effect on promoter activity (Figure 20). Given the above result, it is

plausible to conclude that a loss of Nrf1 in the nucleus is an important factor contributing to the impaired activation of the LXR promoter in HCV-positive cells.

5.7 Impaired Nrf1-LXR-axis contributes to elevated cholesterol levels in HCV replicating cells

Considering the fact, that LXR is involved in the removal of cholesterol from cells, the next point was whether the reduced activation of LXR expression in HCV-positive cells correlates with an increased amount of intracellular cholesterol. The staining of intracellular cholesterol with filipin was performed to verify this claim. Later, confocal laser scanning microscopy (CLSM) was used to do a quantitative study of the filipin-specific fluorescent signal. The activation of the LXR promoter resulted in a slight reduction of intracellular cholesterol levels in HCV-positive cells, which was consistent with the data from the reporter gene experiments. In contrast, there was no additional decrease in the GND cells, which already had reduced cholesterol levels (Figure 20 B).

To further investigate the influence of impaired Nrf1 functionality on intracellular cholesterol levels, the Nrf1 activity was disrupted by coexpression of 25 kDa fragment of Nrf1, which retains the ARE binding site but lacks the transactivator domain. Therefore, the Nrf1-25 kDa variant acts as a dominant negative mutant and does not fulfill its transcriptional activator function. Interestingly, in HCV-negative cells, coexpression of Nrf1-25 kDa led to a significant increase in intracellular cholesterol content compared to the mock control. However, in HCV-positive cells, there was only a minor, statistically insignificant rise in the already increased cholesterol levels observed (Figure 20 C). Furthermore, cells treated with 25-HC (25-hydroxycholesterol) had increased intracellular cholesterol levels in HCV-negative cells. Overexpression of Nrf1-25 kDa resulted in an increase of elevated cholesterol levels in both HCV-negative and HCV-positive cells compared to mock-transfected cells (Figure 20 C). The impaired Nrf1-dependent activation of the LXR promoter in HCV-positive cells may be linked to compromised cholesterol export, what in the end leads to elevated intracellular cholesterol level. In HCV-positive cells, the coexpression of the Nrf1 85 kDa fragment partially reduces the intracellular cholesterol level because it results in a partial restoration of LXR activation, although limited due to the lack of nuclear sMaf.

These results indicate that the interaction of the liver X receptor (LXR), Nrf1 fragments, and sMaf proteins plays an important part in the removal of cholesterol from cells.

5.8 Inhibition of Nrf1 modulates the host-kinome related to inflammation, innate immunity and lipid metabolism

The interaction between HCV and Nrf1 significantly influences the activation of Nrf1-ARE-dependent gene expression. Kinome analysis was performed on both HCV-positive and HCV-negative cells overexpressing the inhibitory 25 kDa version of Nrf1 to acquire a better understanding of the resulting impact. Afterwards, kinases that exhibited significant deregulation were examined for their involvement in innate immune response, inflammatory response and lipid metabolism using a gene ontology search (Figure 21 A-F).

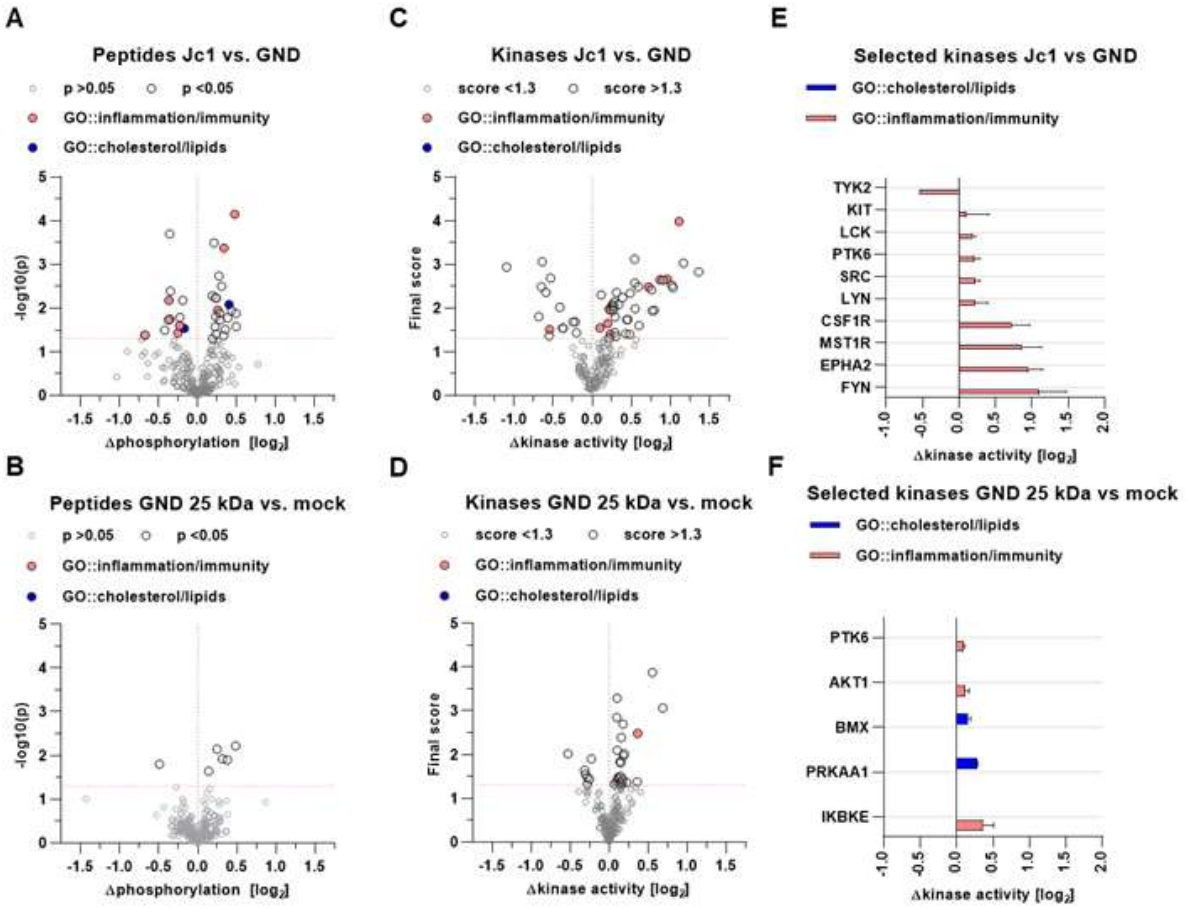

Figure 21. Inhibitory fragments of Nrf1 modulate the host-kinome related to inflammation, innate immunity and lipid metabolism Kinome profiling of HCV-producing cells (Jc1) and HCV-negative cells (GND) overexpressing the 25 kDa fragment of Nrf1. (A/B) Volcano plots of differential peptide phosphorylation in cell lysates of mock-transfected Jc1 versus GND (control) cells or GND cells overexpressing the inhibitory 25 kDa Nrf1 versus mock-transfected GND (control) cells; each dot represents a distinct 13-mer peptide derived from host-proteins; values on x-axis displayed in log2-space; values on y-axis reflect significance; significance cutoff set to p<0.05 as indicated by dashed, red line. (C/D) Volcano plots of predicted, differential kinase activity based on the phosphorylation pattern in A-B; values on x-axis displayed in log2-space; each dot represents a distinct kinase; values on y-axis reflect the final score of predicted kinases; significance cutoff set to score<1.3 as indicated by dashed, red line. (E/F) Detailed depiction of kinases and their activity marked in C-D; values depicted as mean -/+SD. Grey and black coloring represent peptides or kinases below or above threshold, respectively; red or blue coloring represent peptides or kinases being part of the gene ontology term inflammatory response (GO:0006954) and innate immune response (GO:0045087) or cholesterol biosynthetic process (GO:0006695) and lipid biosynthetic process (GO:0008610), respectively.

The kinome analysis identified novel modifications in the host kinase profile during HCV infection (Figure 21 A/C). Src-family kinases (SFKs) and receptor tyrosine kinases (RTKs) have been found to be integrally associated with the regulation of inflammatory and innate immune response among the affected kinases (Figure 21 E). Among these kinases is Protein Tyrosine Kinase 6 (PTK6), which is recognized not only for its role in inflammatory processes but also for its partial function in modulating the Akt/AMPK axis and so exerting control over cellular metabolism.

An analysis of GND cells overexpressing the Nrf1-25 kDa fragment in comparison to mock-transfected GND cells was conducted to determine whether the inhibition of Nrf1-dependent effects in HCV-positive cells was the causative factor behind the deregulation of kinases favoring inflammatory processes and influencing lipid metabolism. While the overall impact of

overexpressing the Nrf1-25 kDa fragment in HCV-negative cells was less pronounced, intriguingly, there were notable overlaps with the effects observed in HCV-infected cells (Figure 22 B/D). These shared effects encompassed the deregulation of kinases associated with host defense mechanisms and lipid metabolism (Figure 22 F).

Firstly, there was a considerable activation of inhibitor of nuclear factor kappa B kinase subunit epsilon (IKBKE), emphasizing its function in the control of inflammatory processes. Secondly, the common regulation of PTK6, when combined with the activation of the AMPK alpha subunit (PRKAA1), was found to be consistent with HCV-producing cells, suggesting an importance in metabolic processes. This data suggests that, while reducing Nrf1-dependent gene expression contributes to the proinflammatory kinase profile, it is not the only mechanism involved, and that a range of other variables contribute to the kinome profile of HCV-positive cells.

5.9 Modulation of Nrf1 activity directly affects LD size and number

HCV infection directly impacts the activation of Nrf1-ARE-dependent gene expression, which includes the genes involved in the regulation of lipid metabolism. Furthermore, the kinome data showed that important regulators like as AMPK and IKBKE are involved in the activation of these kinases. Therefore, the next step was to investigate the effect of Nrf1 on lipid droplets (LDs), which are central in the HCV life cycle.

Examining LDs in both HCV-positive and HCV-negative cells, the study focused on the amount and size of LDs in light of the interaction between the HCV and Nrf1 as well as Nrf1's function in controlling lipid metabolism (Figure 22 A). Interestingly, there was a decrease in LDs in HCV-positive cells compared to HCV-negative cells (Figure 22 B). Nonetheless, the size of LDs within HCV-positive cells significantly increased in parallel with the reduction in LD quantity. The following measures were used to define this increase: LD diameter, perimeter and ferret (Figure 22 C-E). Additionally, the overexpression of the Nrf1-85 kDa fragment led to significant reductions in the analyzed size parameters for HCV-negative cells, including a 0.24-fold reduction in diameter, a 0.44-fold reduction in ferret and a 0.37-fold reduction in perimeter. In contrast, the impact of Nrf1-85 kDa overexpression was less pronounced in HCV-positive cells, resulting in a 0.45-fold reduction in diameter, a 0.68-fold reduction in ferret and a 0.6-fold reduction in perimeter.

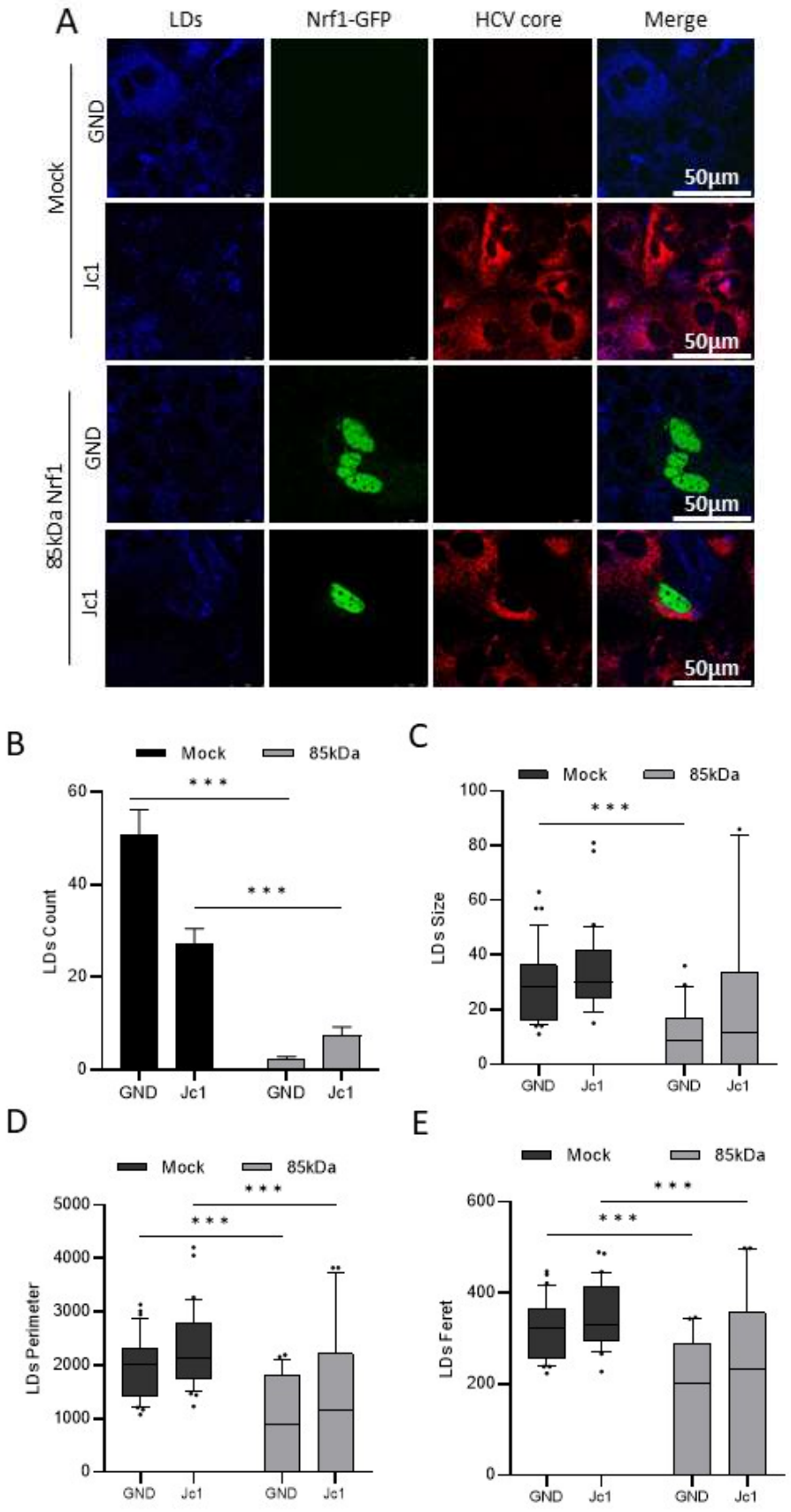

Figure 22. LDs analysis upon Nrf1 overexpression. (A) Representative CLSM images of LDs (blue), Nrf1 (green) and HCV core (red) of HCV-negative (GND) and HCV-positive (Jc1) cells. Change in LDs count in (B). Change in LDs size in (C). Change in LDs Perimeter in (D). Change in LDs Feret in (E).

The kinome analysis showed the networks of signaling pathways influenced by Nrf1. Therefore, Nrf1 was revealed as a regulator in fundamental cellular processes. Moreover, the discovery of LDs as the cellular compartments affected by Nrf1, provides valuable insights into the dynamics of Nrf1 and LDs indirect interaction, shedding further light on how Nrf1 and HCV influence one another. Additionally, HCV and lipid metabolism crosstalk is emphasized, as observed per shifts in LD quantity but in LD size, highlighting the impact of the HCV-Nrf1 crosstalk on the regulation of lipid homeostasis. The impact of Nrf1 deregulation extend to its effect on LXR activity, consequently affecting the cholesterol removal program. In high cholesterol challenge, cholesterol binding to Nrf1 in ER leads to de-repression of a cholesterol removal program, activates the LXR and leads to removal of excess cholesterol. In HCV-positive cells, Nrf1 cholesterol sensing is disrupted, what causes increased size of LDs. By disrupting the regulatory balance involving Nrf1 and LXR, the mechanisms controlling cholesterol metabolism may be modified, potentially leading to dysregulation in the cellular processes responsible for cholesterol export.

6 Discussion

Transcription factor Nrf1 helps in maintaining cellular homeostasis by responding to oxidative stress and regulating cholesterol sensing. However, the HCV infection disrupts homeostasis by induction of oxidative stress and causing an elevation in intracellular cholesterol levels. The preliminary discovery of this study was that an infection with HCV leads to a decrease in Nrf1 protein levels in Huh 7.5 cells. Similar observation was done in liver sections of patients suffering from HCC. Likewise, in livers of Iranian transplant patients, the Nrf1 protein levels were significantly decreased, while the level of mRNA transcripts was increased. Patients were infected with both hepatitis B and C virus infections and diagnosed with hepatocellular carcinoma (HCC). As an outcome of the study, Nrf1 protein was possibly identified as a factor in the progression of chronic liver disease. Reduction in Nrf1 protein level indicated Nrf1's possible involvement in the advancement of chronic liver disease and hepatocellular carcinoma (Abdolyousefi et al. 2022). Upon further investigation it was observed that HCV infection had no evident impact on the stability or degradation rate of Nrf1. Even under the HCV-induced stress, Nrf1 demonstrated no significant alterations in its half-life when compared to uninfected cells. Observed decrease in Nrf1 protein levels after HCV infection could not be attributed to a shortened half-life, what was the original hypothesis. Instead, it appeared to be linked to impaired translation. These mechanisms were previously described in infections caused by ZIKV or DENV (Singh et al. 2022). Evidently, Flaviviruses such as HCV are known to cause considerable effects on translation processes, with this impairment linked to Jak-Stat signaling – a pathway that has also been studied in relation to HCV infection (Nan et al. 2017; Himmelsbach et al. 2013). In conclusion, despite the HCV infection, Nrf1 maintains its stability, with no changes to its half-life. A decrease in Nrf1 protein level resulting from HCV infection could possibly be associated with inhibition of translation, which has been reported in other Flavivirus infections.

Due to the detected decreased amount of Nrf1 in HCV-positive cells, it was thought that a Nrf1 silencing may promote HCV replication. An analysis of Nrf1 KD's effect on the HCV life cycle revealed that, Nrf1 KD had a positive effect on the virus's life cycle. Although the increase in Nrf1 protein level was observed, the data analysis showed that the difference was not statistically significant. Certain limitations were associated with cell transfection and total lysate analysis. Incomplete silencing might not result in a strong enough signal to produce repeatable, statistically significant data, and in this particular case, the low number of cells where the knockdown occurred affected the observed results. A more accurate evaluation of Nrf1 KD's effects on the HCV life cycle was made possible by the single-cell analysis using CLSM. Statistically significant increase in viral structural (HCV core) and non-structural (NS3) proteins in single cells subjected to Nrf1 KD was observed, which suggested association between Nrf1 suppression and HCV. In conclusion, the significant increase in viral proteins at the single-cell level suggests that Nrf1 KD has an effect on the HCV life cycle.

Activation of the Nrf2-ARE pathway in early-stage infection of herpes simplex virus type 1 (HSV-1) point to shared mechanisms in antiviral responses due to similarities in the defensive responses triggered by Nrf1 (Zhang et al. 2022). Deregulation of Nrf2-ARE pathway has been observed in many viral infections such as dengue virus (Zevini et al. 2020), encephalomyocarditis virus (EMCV), vesicular stomatitis virus (VSV) (Wang et al. 2023) and hepatitis B virus (HBV) (Peiffer et al. 2015). One of those mechanisms is PI3K/Akt signaling pathway, known for its role in protecting against oxidative stress through various cell survival mechanisms, including the Nrf2-ARE-mediated antioxidant response. The pathway, is activated upon HCV infection (Shi et al. 2016; Liu et al. 2012). The PI3K/Akt is known to be used by SARS-CoV-2 for its survival within the host (Lekshmi et al 2023). Additionally, Nrf1 and Nrf2 share a common feature - the DNA binding basic region-leucine zipper domain. This

domain is crucial for their activity and forming heterodimers with one of small Maf proteins. Resulting heterodimer binds to the Maf recognition sequence, found in the promoters of target genes involved in the antioxidant response element (ARE). As a result, the expression of these target genes is triggered in response to oxidative stress (Ohtsuji et al. 2008). This suggests that Nrf1's involvement in similar pathways may contribute to its impact on HCV replication and infection. Moreover, the impaired accumulation and release of viral particles in the presence of higher Nrf1 levels further supports the theory of Nrf1-HCV crosstalk. Observed increase in viral genomes in this context is likely a result of the presence of unpackaged genomes and defective viral particles, which lack protective capsids or envelopes. Those undergo an autonomous replication within host cells, which leads to an augmented viral genome count. Consequently, these processes may disrupt intracellular cholesterol particle trafficking, affecting lipid raft formation and cellular processes reliant on cholesterol (Vignuzzi et al. 2019; Karamichali et al. 2018). The study's conclusions highlight the major impact of Nrf1 overexpression on multiple stages of the HCV life cycle. This suggests a possible function for this protein in controlling the dynamics of HCV infection. The complex interactions between Nrf1, viral replication and host-virus interactions require further investigation and could present promising targets for therapeutic interventions against HCV and related infections.

In addition to the reduced Nrf1 protein level observed in HCV-replicating cells, impaired Nrf1-dependent activation of ARE sites in these cells was observed. Both Nrf1 and Nrf2 have the capability to form heterodimers with sMaf proteins as mentioned before. In the case of Nrf2, it has been noted that the relocation of sMaf to the replicon complex prevents Nrf2 from entering the nucleus, as Nrf2 binds to sMaf outside of the nucleus. Interactions observed between sMaf proteins and Nrf1 fragments present an artificial system that can be used to study the Nrf1 and HCV crosstalk. Delocalization of sMaf proteins with nuclear export or nuclear localization signals, creates a controllable experimental model. This model can be used in vitro to investigate the dynamics and functional consequences of Nrf1 localization during HCV infection. Used methodology enabled the determination and artificial regulation of Nrf1 activity, leading to inducible expression of the ARE-driven genes through a dynamic nucleocytoplasmic shuttling pathway. Collected data suggest that overexpressing Nrf1 fragments alone could not fully restore the decreased expression of the cytoprotective gene NQO1, which highlights the role of sMafs in the nucleus. Presented artificial system is a valuable tool to research aspects of the mechanisms in which the sMaf, Nrf1 and HCV are involved. Furthermore, it presents opportunities for research of potential therapeutic strategies that target the Nrf1 and sMaf associated pathways for the treatment of HCV-associated diseases.

As HCV is dependent on accumulation of intracellular cholesterol, the question raised was: how Nrf1 and HCV interact in the cholesterol context? Liver X receptor (LXR)-α is one of the sensors involved in cholesterol removal in the cells. Moreover, the data showed a tendency that HCV infection leads to the suppression of the activatory effect of the 85kDa Nrf1 fragment, as observed by a reduction in LXR promoter activity. This observation further supports the theory that HCV can effectively interfere with key regulators of cholesterol metabolism, impacting the cellular response to changes in lipid levels. To visualize the cholesterol and oxysterols accumulation induced by HCV infection, indirect immunofluorescence via Filipin stain was employed. Observed decrease in LXR promoter activity in the presence of cholesterol accumulation suggests that HCV-induced changes in cholesterol metabolism might directly influence LXR-mediated transcriptional regulation. Such a potent interference with the LXR pathway underscores HCV's ability to tightly regulate cholesterol metabolism, overriding cellular attempts to modulate cholesterol levels (Jenelle et al. 2022; Garcia et al. 2012). Moreover, data revealed a trend indicating that HCV infection leads to the suppression of the activatory effect of the 85kDa Nrf1 fragment, as evidenced by a reduction in LXR promoter activity. This serves as evidence that HCV can effectively interfere with regulators of cholesterol

metabolism, impacting how cells respond to changes in lipid levels. The effect of HCV on cholesterol regulation becomes clear through its influence on Nrf1 fragments and subsequent effects on LXR-mediated transcriptional regulation. Additional experiment aimed to examine the intracellular effects of HCV infection on cholesterol metabolism and its potential influence on LXR-mediated transcriptional regulation. To visualize the accumulation of cholesterol and oxysterols induced by HCV infection, an indirect immunofluorescence technique using the Filipin stain was employed. Results obtained from this staining approach presented cholesterol accumulation in HCV-infected cells. The signals observed with Filipin stain provided visual confirmation of the increased levels of cholesterol and oxysterols within the infected cells, as observed before (Viscovo et al. 2012; Elgner et al. 2016). Importantly, the correlation between this cholesterol accumulation and the reduction in LXR promoter activity was particularly noteworthy. Recently, Nrf1 and Nrf2 were described to mediate cells response by complementary gene regulation against hepatic cholesterol overload (Akl et al. 2023). Collected results point to a potential mechanism by which HCV manipulation of cholesterol levels might disrupt the normal functioning of LXR, a key player in cellular cholesterol homeostasis.

In line with the HCV life cycle's dependence on lipid droplets and the increased intracellular lipid content, it has been observed that the activation of the LXRα promoter is impaired in HCV-positive cells. Furthermore, in HCV-negative cells, the activation of the LXRα promoter can be impaired by the expression of sMaf-NES expression vectors, highlighting that the withdrawal of sMaf from the nucleus has the potential to mimic effects on the promotor similar as in HCV-positive cells. Compromised Nrf1-LXRα axis in HCV-positive cells manifests as elevated intracellular cholesterol levels, a condition that can be partially mitigated by the coexpression of the Nrf1-85 kDa fragment. The disruption of the Nrf1-LXRα balance in HCV-positive cells results in an accumulation of intracellular cholesterol due to impaired cholesterol removal. Cholesterol-rich membrane domains are important for many aspects of the HCV life cycle, including the release and infectivity of progeny virus, virus entry and replication; escpecially influencing the formation of the membranous web (Hofmann et al. 2018; Wang et al. 2017; Paul et al. 2015). Intracellular accumulation of lipids, in the form of LDs, is a prerequisite for HCV replication. LDs serve as key sites for virus morphogenesis and constitute a central component of the membranous web that envelops LDs (Bley et al. 2020)

This scenario is similar to the HCV-Nrf2 crosstalk, where the impaired induction of cytoprotective Nrf2/ARE-dependent genes results in elevated levels of reactive oxygen species. Elevated ROS levels are critical for inducing autophagy, which takes part in the multivesicular body (MVB)-dependent release of HCV. The impaired cholesterol removal leads to a decreased Nrf1-dependent activation of LXRα. Lower activation of LXRa prevents the induction of an effective cholesterol removal program, which results in elevated intracellular cholesterol levels. High cholesterol levels can have a positive impact on HCV replication and contribute to HCV-associated conditions like steatosis (Elgretli et al. 2023). In addition to these direct effects of Nrf1 on lipid metabolism and its impact on HCV, there may also be numerous indirect factors at play. The kinome assays revealed that overexpression of the Nrf1-25 kDa fragment triggers an activation of AMP-activated kinase (AMPK). In this study it was observed that, 25kDa Nrf1 overexpression leads to the phosphorylation and subsequent activation of PRKAA1, a crucial subunit of AMP-activated protein kinase. Subsequent activation of AMPK has an effect on cellular lipid metabolism. Activated AMPK inhibitis fatty acid synthesis, by phosphorylating acetyl-CoA carboxylase (ACC) 1 at Ser^{79} and ACC2 at Ser^{212} (Galic et al. 2017). Mentioned phosphorylation events represent a rate-limiting step in lipogenesis, the process of fatty acid synthesis. AMPK helps to regulate lipid levels and prevents excess fat accumulation, by inhibiting fatty acid synthesis.

Kinome analysis and LDs staining data point to the possibility that Nrf1 overexpression functions as a cell regulator, preventing lipogenesis and promoting lipolysis. Upon Nrf1 overexpression, lipogenesis is inhibited, what suggests a possible decrease in the synthesis of new fatty acids and triglycerides. This might result in a reduction in the build-up of lipids in LDs (including cholesterol). The reduced availability of newly synthesized lipids within LDs might limit the resources available for the HCV life cycle, ultimately impacting viral replication, assembly and maturation. Combined effects of Nrf1 overexpression may lead to a decrease in the overall pool of LDs and the availability of lipids for the HCV life cycle.

When combined, these findings support Nrf1's potential role as an antiviral factor because of its connection to the oxidative stress response and cholesterol elimination pathway. The study demonstrates that the HCV life cycle is affected through regulation of Nrf1-sMaf interaction and the disruption of Nrf1-dependent transcriptional activation by HCV. As a consequence, the regulation of ARE-dependent gene expression, control of intracellular cholesterol levels and the formation of lipid droplets might be affected. It is essential to determine if restoring Nrf1 activity might be an appropriate target for therapy. Such an approach might initiate a cholesterol removal program, affecting HCV replication and minimizing HCV-associated pathogenesis. Restoration of Nrf1 activity might initiate a cholesterol removal program making it a suitable therapeutic target, due to the potential impact on HCV replication and reduced HCV-associated pathogenesis. Further studies in addressing the question about the Nrf1-HCV crosstalk, could be of interest to gain a better understanding of how Nrf1 precisely modulates the oxidative stress response and cholesterol removal program in the context of viral infections.

7 Summary

Hepatitis C virus (HCV) infection may lead to chronic hepatitis. Currently, there are more than 57,8 million individuals globally who experience persistent infection, enduring the consequences of chronic hepatitis, which can often progress to liver fibrosis, cirrhosis and hepatocellular carcinoma (HCC). One mechanism to protect against oxidative stress is the Nrf2/Keap1 pathway. Nrf2/ARE signalling is impaired in HCV replicating cells, due to withdrawal of sMaf proteins from nucleus and binding to NS3 on the cytoplasmic site of the ER, as the integral part of replicon complex. The NS3-bound sMaf proteins bind to Nrf2, which prevents Nrf2 from entering the nucleus to trigger the expression of the genes responsible for protection against oxidative stress. Another factor involved in redox homeostasis is the ubiquitously expressed transcription factor Nrf1 of the Cap´N´Collar family. Nrf1 is located in the ER and upon stimulus, the inactive 120 kDa glycoprotein is selectively processed in the ER to gain distinct multiple isoforms (between ~25-kDa and ~140-kDa). Besides, Nrf1 has been recently described as a cholesterol sensor that protects the liver from excess cholesterol.

In this thesis, the impact of HCV infection on Nrf1 expression, localization, antioxidant response and cholesterol sensing ability were studied. Additionally, the relevance of the Nrf1-HCV crosstalk for the viral life cycle and virus-associated pathogenesis was examined. The data indicated that, HCV infection reduced Nrf1 protein levels while increasing Nrf1 transcript expression in both cell culture models and liver sections of patients with chronic HCV infection. However, the HCV-induced decrease in Nrf1 protein levels was not attributed to a shortened half-life. Nrf1 knockdown experiments showed an impact on HCV protein levels and viral titers. Overexpression of Nrf1 fragments, specifically the 25kDa (dominant-negative inhibitor of longer NRF1 isoforms and NRF2) and 85kDa (cleaved and transcriptionally active isoform of Nrf1) isoforms, led to negative effects on the HCV life cycle, including replication, accumulation and release of viral particles. Additionally, the interplay between Nrf1 fragments and sMaf proteins influenced Nrf1 fragments localization. Overexpressing Nrf1 fragments could not rescue the decreased expression of the cytoprotective gene NQO1, suggesting the complexity of Nrf1's regulation in HCV infection.

HCV infection impacts Nrf1 expression, localization and activity, disrupting host-virus interactions essential for efficient replication. The observed decrease in viral replication and impaired release of viral particles suggest Nrf1's potential regulatory role in modulating HCV infection. Additionally, the crosstalk between HCV and Nrf1 has a direct impact on the activation of Nrf1-ARE dependent gene expression including genes related to controlling of the lipid metabolism. HCV infection affects LXR promoter activity and Nrf1 fragments' overexpression has an impact on cholesterol regulation. The reduced activation of the LXR expression in HCV positive cells due to an impaired Nrf1-dependent activation of the LXR-promoter may be reflected by an impaired cholesterol export leading to an elevated intracellular cholesterol level. Inhibited activity of Nrf1 in HCV-positive cells influences the lipid content and therefore the number and size of lipid droplets. Targeting Nrf1 or its associated pathways may offer promising therapeutic strategies to disrupt the HCV life cycle and inhibit viral replication. The use of cell culture models is one of the study's limitations, which emphasizes the necessity of validation in in vivo systems or clinical samples.

Taken together, these data provide the relevance of Nrf1's role as an antiviral factor in response to HCV infection in addition to a well-known crucial role in oxidative stress and cholesterol removal program. This study described for the first-time extensive work on the various mechanisms and explores the fragments of Nrf1 specific fragments in affecting HCV replication and host cells. Further studies in addressing the question about the about the Nrf1-HCV crosstalk, could be of interest to gain a better understanding of how Nrf1 modulates the oxidative stress response and cholesterol removal program in the context of viral infections.

8 Zusamenfassung

Die Infektion mit dem Hepatitis-C-Virus (HCV) führt zu chronischer Hepatitis. Derzeit sind weltweit mehr als 57,8 Millionen Menschen von einer persistierenden Infektion betroffen und leiden unter den Folgen einer chronischen Hepatitis, die häufig zu Leberfibrose, Zirrhose und Leberzellkarzinom (HCC) führen kann. Ein Mechanismus zum Schutz vor oxidativem Stress ist der Nrf2/Keap1-Signalweg. Der Nrf2/ARE-Signalweg ist in sich replizierenden HCV-Zellen beeinträchtigt, was darauf zurückzuführen ist, dass sich sMaf-Proteine aus dem Zellkern zurückziehen und an NS3 auf der zytoplasmatischen Seite des ER binden, das integraler Bestandteil des Replikonkomplexes ist. Die an NS3 gebundenen sMaf-Proteine binden an Nrf2, was Nrf2 daran hindert, in den Zellkern zu gelangen, um die Expression von Genen auszulösen, die für den Schutz vor oxidativem Stress verantwortlich sind. Ein weiterer an der Redox-Homöostase beteiligter Faktor ist der ubiquitär exprimierte Transkriptionsfaktor Nrf1 der Cap'N'Collar-Familie. Nrf1 ist im ER lokalisiert, und auf einen Stimulus hin wird das inaktive 120-kDa-Glykoprotein im ER selektiv prozessiert, um verschiedene multiple Isoformen (zwischen ~25-kDa und ~140-kDa) zu bilden. Außerdem wurde Nrf1 kürzlich als Cholesterinsensor beschrieben, der die Leber vor überschüssigem Cholesterin schützt.

In dieser Arbeit wurden die Auswirkungen einer HCV-Infektion auf die Nrf1-Expression, die Lokalisierung, die antioxidative Reaktion und die Fähigkeit, Cholesterin zu erkennen, untersucht. Außerdem wurde die Bedeutung des Nrf1-HCV-Crosstalk für den viralen Lebenszyklus und die virusassoziierte Pathogenese untersucht. Die Daten zeigten, dass die HCV-Infektion die Nrf1-Proteinspiegel reduzierte, während die Nrf1-Transkript-Expression sowohl in Zellkulturmodellen als auch in Leberschnitten von Patienten mit chronischer HCV-Infektion anstieg. Der HCV-induzierte Rückgang des Nrf1-Proteinspiegels wurde jedoch nicht auf eine verkürzte Halbwertszeit zurückgeführt. Nrf1-Knockdown-Experimente zeigten eine Auswirkung auf HCV-Proteinspiegel und Virustiter. Die Überexpression von Nrf1-Fragmenten, insbesondere der 25kDa- (dominant-negativer Inhibitor längerer NRF1-Isoformen und NRF2) und 85kDa-Isoformen (gespaltene und transkriptionell aktive Isoform von Nrf1), führte zu negativen Auswirkungen auf den HCV-Lebenszyklus, einschließlich Replikation, Akkumulation und Freisetzung viraler Partikel. Außerdem beeinflusste das Zusammenspiel zwischen Nrf1-Fragmenten und sMaf-Proteinen die Lokalisierung der Nrf1-Fragmente. Die Überexpression von Nrf1-Fragmenten konnte die verminderte Expression des zytoprotektiven Gens NQO1 nicht retten, was auf die Komplexität der Nrf1-Regulierung bei HCV-Infektionen hindeutet.

Eine HCV-Infektion beeinflusst die Nrf1-Expression, -Lokalisierung und -Aktivität und stört die für eine effiziente Replikation wichtigen Wirt-Virus-Interaktionen. Der beobachtete Rückgang der viralen Replikation und die beeinträchtigte Freisetzung von Viruspartikeln deuten auf eine mögliche regulatorische Rolle von Nrf1 bei der Modulation der HCV-Infektion hin. Darüber hinaus hat die Wechselwirkung zwischen HCV und Nrf1 einen direkten Einfluss auf die Aktivierung der Nrf1-ARE-abhängigen Genexpression, einschließlich der Gene, die mit der Kontrolle des Fettstoffwechsels zusammenhängen. Die HCV-Infektion beeinträchtigt die Aktivität des LXR-Promotors, und die Überexpression von Nrf1-Fragmenten wirkt sich auf die Cholesterinregulation aus. Die verminderte Aktivierung der LXR-Expression in HCV-positiven Zellen aufgrund einer gestörten Nrf1-abhängigen Aktivierung des LXR-Promotors kann sich in einem gestörten Cholesterinexport niederschlagen, der zu einem erhöhten intrazellulären Cholesterinspiegel führt. Die gehemmte Aktivität von Nrf1 in HCV-positiven Zellen beeinflusst den Lipidgehalt und damit die Anzahl und Größe der Lipidtröpfchen. Die gezielte Beeinflussung von Nrf1 oder der damit verbundenen Signalwege könnte vielversprechende therapeutische Strategien zur Unterbrechung des HCV-Lebenszyklus und zur Hemmung der viralen Replikation bieten. Die Einschränkungen der Studie, wie die Verwendung von Zellkulturmodellen, unterstreichen jedoch die Notwendigkeit einer Validierung in In-vivo-Systemen oder klinischen Proben.

Zusammenfassend lässt sich sagen, dass diese Studie wertvolle Einblicke in die potenzielle Rolle von Nrf1 als antiviraler Faktor bei der Reaktion auf HCV-Infektionen liefert. Die Interaktion zwischen Nrf1 und HCV wirkt sich auf die virale Replikation und Freisetzung aus, was das therapeutische Potenzial von Nrf1 bei der Bekämpfung von Virusinfektionen unterstreicht. Zukünftige Forschungen werden entscheidend sein, um die genauen Mechanismen aufzudecken, durch die Nrf1 seine antiviralen Wirkungen entfaltet, und so den Weg für innovative Interventionen zur Verbesserung der Abwehrmechanismen des Wirts gegen virale Krankheitserreger zu öffnen.

9 References

Abdolyousefi EN, Motalleb G, Yaghobi R. Association Between ACOX1 and NRF1 Gene Expression and Hepatitis B and C Virus Infections and Hepatocellular Carcinoma in Liver Transplant Patients (Shiraz, Iran). *Exp Clin Transplant*. 2022;20(1):52-58. doi:10.6002/ect.2021.0175

Adams CM, Reitz J, De Brabander JK, et al. Cholesterol and 25-hydroxycholesterol inhibit activation of SREBPs by different mechanisms, both involving SCAP and Insigs. *J Biol Chem*. 2004;279(50):52772-52780. doi:10.1074/jbc.M410302200

Afonso MS, Machado RM, Lavrador MS, Quintao ECR, Moore KJ, Lottenberg AM. Molecular Pathways Underlying Cholesterol Homeostasis. *Nutrients*. 2018; 10(6):760. https://doi.org/10.3390/nu10060760

Akl MG, Li L, Baccetto R, et al. Complementary gene regulation by NRF1 and NRF2 protects against hepatic cholesterol overload [published online ahead of print, 2023 Apr 14] [published correction appears in Cell Rep. 2023 Jul 15;42(7):112872]. *Cell Rep*. 2023;42(4):112399. doi:10.1016/j.celrep.2023.112399

Alazard-Dany N, Denolly S, Boson B, Cosset FL. Overview of HCV Life Cycle with a Special Focus on Current and Possible Future Antiviral Targets. *Viruses*. 2019;11(1):30. Published 2019 Jan 6. doi:10.3390/v11010030

Albecka A, Belouzard S, Op de Beeck A, et al. Role of low-density lipoprotein receptor in the hepatitis C virus life cycle. *Hepatology*. 2012;55(4):998-1007. doi:10.1002/hep.25501

Alexopoulou A, Karayiannis P. Interferon-based combination treatment for chronic hepatitis C in the era of direct acting antivirals. *Ann Gastroenterol*. 2015;28(1):55-65.

Allaire M, Gilgenkrantz H. The impact of steatosis on liver regeneration. Horm Mol Biol Clin Investig. 2018;41(1):/j/hmbci.2020.41.issue-1/hmbci-2018-0050/hmbci-2018-0050.xml. Published 2018 Nov 21. doi:10.1515/hmbci-2018-0050

Alter, M. J. (1997): Epidemiology of hepatitis C. In *Hepatology (Baltimore, Md.)* 26 (3 Suppl 1), 62S-65S. DOI: 10.1002/hep.510260711.

Altmann SW, Davis HR Jr, Zhu LJ, et al. Niemann-Pick C1 Like 1 protein is critical for intestinal cholesterol absorption. *Science*. 2004;303(5661):1201-1204. doi:10.1126/science.1093131

Appel N, Zayas M, Miller S, et al. Essential role of domain III of nonstructural protein 5A for hepatitis C virus infectious particle assembly. *PLoS Pathog*. 2008;4(3):e1000035. Published 2008 Mar 28. doi:10.1371/journal.ppat.1000035

Asabe SI, Tanji Y, Satoh S, Kaneko T, Kimura K, Shimotohno K. The N-terminal region of hepatitis C virus-encoded NS5A is important for NS4A-dependent phosphorylation. *J Virol*. 1997;71(1):790-796. doi:10.1128/JVI.71.1.790-796.1997

Ashfaq UA, Javed T, Rehman S, Nawaz Z, Riazuddin S. An overview of HCV molecular biology, replication and immune responses. *Virol J*. 2011;8:161. Published 2011 Apr 11. doi:10.1186/1743-422X-8-161

Avula K, Singh B, Kumar PV, Syed GH. Role of Lipid Transfer Proteins (LTPs) in the Viral Life Cycle. *Front Microbiol*. 2021;12:673509. Published 2021 Jun 23. doi:10.3389/fmicb.2021.673509

Baird L, Tsujita T, Kobayashi EH, et al. A Homeostatic Shift Facilitates Endoplasmic Reticulum Proteostasis through Transcriptional Integration of Proteostatic Stress Response Pathways. *Mol Cell Biol*. 2017;37(4):e00439-16. Published 2017 Feb 1. doi:10.1128/MCB.00439-16

Barba G, Harper F, Harada T, et al. Hepatitis C virus core protein shows a cytoplasmic localization and associates to cellular lipid storage droplets. *Proc Natl Acad Sci U S A*. 1997;94(4):1200-1205. doi:10.1073/pnas.94.4.1200

Barba G, Harper F, Harada T, et al. Hepatitis C virus core protein shows a cytoplasmic localization and associates to cellular lipid storage droplets. *Proc Natl Acad Sci U S A*. 1997;94(4):1200-1205. doi:10.1073/pnas.94.4.1200

Bartenschlager R, Frese M, Pietschmann T. Novel insights into hepatitis C virus replication and persistence. *Adv Virus Res*. 2004;63:71-180. doi:10.1016/S0065-3527(04)63002-8

Bartenschlager R, Lohmann V, Penin F. The molecular and structural basis of advanced antiviral therapy for hepatitis C virus infection. *Nat Rev Microbiol*. 2013;11(7):482-496. doi:10.1038/nrmicro3046

Bartenschlager R, Lohmann V, Penin F. The molecular and structural basis of advanced antiviral therapy for hepatitis C virus infection. *Nat Rev Microbiol*. 2013;11(7):482-496. doi:10.1038/nrmicro3046

Bartenschlager R, Penin F, Lohmann V andré P. Assembly of infectious hepatitis C virus particles. *Trends Microbiol*. 2011;19(2):95-103. doi:10.1016/j.tim.2010.11.005

Bartenschlager R, Penin F, Lohmann V andré P. Assembly of infectious hepatitis C virus particles. *Trends Microbiol*. 2011;19(2):95-103. doi:10.1016/j.tim.2010.11.005

Bartosch B, Dubuisson J, Cosset FL. Infectious hepatitis C virus pseudo-particles containing functional E1-E2 envelope protein complexes. *J Exp Med*. 2003;197(5):633-642. doi:10.1084/jem.20021756

Bartosch B, Dubuisson J, Cosset FL. Infectious hepatitis C virus pseudo-particles containing functional E1-E2 envelope protein complexes. *J Exp Med*. 2003;197(5):633-642. doi:10.1084/jem.20021756

Bayer K, Banning C, Bruss V, Wiltzer-Bach L, Schindler M. Hepatitis C Virus Is Released via a Noncanonical Secretory Route. *J Virol*. 2016;90(23):10558-10573. Published 2016 Nov 14. doi:10.1128/JVI.01615-16

Bender D, Hildt E. Effect of Hepatitis Viruses on the Nrf2/Keap1-Signaling Pathway and Its Impact on Viral Replication and Pathogenesis. *Int J Mol Sci*. 2019;20(18):4659. Published 2019 Sep 19. doi:10.3390/ijms20184659

Benedicto I, Molina-Jiménez F, Bartosch B, et al. The tight junction-associated protein occludin is required for a postbinding step in hepatitis C virus entry and infection. *J Virol*. 2009;83(16):8012-8020. doi:10.1128/JVI.00038-09

Bhattacharjee C, Singh M, Das D, Chaudhuri S, Mukhopadhyay A. Current therapeutics against HCV. *Virusdisease*. 2021;32(2):228-243. doi:10.1007/s13337-021-00697-0

Blanchard E, Roingeard P. The Hepatitis C Virus-Induced Membranous Web in Liver Tissue. *Cells*. 2018;7(11):191. Published 2018 Nov 1. doi:10.3390/cells7110191

Blight KJ, Kolykhalov AA, Rice CM. Efficient initiation of HCV RNA replication in cell culture. *Science*. 2000;290(5498):1972-1974. doi:10.1126/science.290.5498.1972

Blight KJ, Kolykhalov AA, Rice CM. Efficient initiation of HCV RNA replication in cell culture. *Science*. 2000;290(5498):1972-1974. doi:10.1126/science.290.5498.1972

Blight KJ, McKeating JA, Rice CM. Highly permissive cell lines for subgenomic and genomic hepatitis C virus RNA replication. *J Virol*. 2002;76(24):13001-13014. doi:10.1128/jvi.76.24.13001-13014.2002

Borowski P, Oehlmann K, Heiland M, Laufs R. Nonstructural protein 3 of hepatitis C virus blocks the distribution of the free catalytic subunit of cyclic AMP-dependent protein kinase. *J Virol*. 1997;71(4):2838-2843. doi:10.1128/JVI.71.4.2838-2843.1997

Boulant S, Montserret R, Hope RG, et al. Structural determinants that target the hepatitis C virus core protein to lipid droplets. *J Biol Chem*. 2006;281(31):22236-22247. doi:10.1074/jbc.M601031200

Bourlière M, Gordon SC, Flamm SL, et al. Sofosbuvir, Velpatasvir and Voxilaprevir for Previously Treated HCV Infection. *N Engl J Med*. 2017;376(22):2134-2146. doi:10.1056/NEJMoa1613512

Bradford MM. A rapid and sensitive method for the quantitation of microgram quantities of protein utilizing the principle of protein-dye binding. *Anal Biochem*. 1976;72:248-254. doi:10.1006/abio.1976.9999

Brass V, Bieck E, Montserret R, et al. An amino-terminal amphipathic alpha-helix mediates membrane association of the hepatitis C virus nonstructural protein 5A. *J Biol Chem*. 2002;277(10):8130-8139. doi:10.1074/jbc.M111289200

Brault C, Levy PL, Bartosch B. Hepatitis C virus-induced mitochondrial dysfunctions. *Viruses*. 2013;5(3):954-980. Published 2013 Mar 21. doi:10.3390/v5030954

Breslow DK, Weissman JS. Membranes in balance: mechanisms of sphingolipid homeostasis. *Mol Cell*. 2010;40(2):267-279. doi:10.1016/j.molcel.2010.10.005

Brookes PS, Yoon Y, Robotham JL anders MW, Sheu SS. Calcium, ATP and ROS: a mitochondrial love-hate triangle. *Am J Physiol Cell Physiol*. 2004;287(4):C817-C833. doi:10.1152/ajpcell.00139.2004

Brown MS, Radhakrishnan A, Goldstein JL. Retrospective on Cholesterol Homeostasis: The Central Role of Scap. *Annu Rev Biochem*. 2018;87:783-807. doi:10.1146/annurev-biochem-062917-011852

Budkowska A. Heterogeneity of Hepatitis C Virus Particles and Their Evolution During Infection. *Cell Mol Gastroenterol Hepatol*. 2017;4(3):443-444. Published 2017 Sep 18. doi:10.1016/j.jcmgh.2017.09.001

Bürckstümmer T, Kriegs M, Lupberger J, Pauli EK, Schmittel S, Hildt E. Raf-1 kinase associates with Hepatitis C virus NS5A and regulates viral replication. *FEBS Lett*. 2006;580(2):575-580. doi:10.1016/j.febslet.2005.12.071

Carcamo WC, Nguyen CQ. Advancement in the development of models for hepatitis C research. *J Biomed Biotechnol*. 2012;2012:346761. doi:10.1155/2012/346761

Casares D, Escribá PV, Rosselló CA. Membrane Lipid Composition: Effect on Membrane and Organelle Structure, Function and Compartmentalization and Therapeutic Avenues. *Int J Mol Sci*. 2019;20(9):2167. Published 2019 May 1. doi:10.3390/ijms20092167

Centers for Disease Control and Prevention (CDC). Hepatitis C virus infection among adolescents and young adults:Massachusetts, 2002-2009. *MMWR Morb Mortal Wkly Rep*. 2011;60(17):537-541.

Chaudhari R, Fouda S, Sainu A, Pappachan JM. Metabolic complications of hepatitis C virus infection. *World J Gastroenterol*. 2021;27(13):1267-1282. doi:10.3748/wjg.v27.i13.1267

Chaudhary R, Garg J, Shah N, Sumner A. PCSK9 inhibitors: A new era of lipid lowering therapy. *World J Cardiol*. 2017;9(2):76-91. doi:10.4330/wjc.v9.i2.76

Chen CH, Yu ML. Evolution of interferon-based therapy for chronic hepatitis C. *Hepat Res Treat*. 2010;2010:140953. doi:10.1155/2010/140953

Chen J, Liu X, Lü F, et al. Transcription factor Nrf1 is negatively regulated by its O-GlcNAcylation status. *FEBS Lett*. 2015;589(18):2347-2358. doi:10.1016/j.febslet.2015.07.030

Chiang CH, Lai YL, Huang YN, et al. Sequential Phosphorylation of the Hepatitis C Virus NS5A Protein Depends on NS3-Mediated Autocleavage between NS3 and NS4A. *J Virol*. 2020;94(19):e00420-20. Published 2020 Sep 15. doi:10.1128/JVI.00420-20

Choudhary V, Ojha N, Golden A, Prinz WA. A conserved family of proteins facilitates nascent lipid droplet budding from the ER. *J Cell Biol*. 2015;211(2):261-271. doi:10.1083/jcb.201505067

Clément S, Pascarella S, Negro F. Hepatitis C virus infection: molecular pathways to steatosis, insulin resistance and oxidative stress. *Viruses*. 2009;1(2):126-143. doi:10.3390/v1020126

Cohen S. Lipid Droplets as Organelles. *Int Rev Cell Mol Biol*. 2018;337:83-110. doi:10.1016/bs.ircmb.2017.12.007

Cook EC, Nelson JK, Sorrentino V, et al. Identification of the ER-resident E3 ubiquitin ligase RNF145 as a novel LXR-regulated gene. *PLoS One*. 2017;12(2):e0172721. Published 2017 Feb 23. doi:10.1371/journal.pone.0172721

Cui F, Blach S, Manzengo Mingiedi C, et al. Global reporting of progress towards elimination of hepatitis B and hepatitis C. *Lancet Gastroenterol Hepatol*. 2023;8(4):332-342. doi:10.1016/S2468-1253(22)00386-7

Cui M, Atmanli A, Morales MG, et al. Nrf1 promotes heart regeneration and repair by regulating proteostasis and redox balance. *Nat Commun*. 2021;12(1):5270. Published 2021 Sep 6. doi:10.1038/s41467-021-25653-w

Cun W, Jiang J, Luo G. The C-terminal alpha-helix domain of apolipoprotein E is required for interaction with nonstructural protein 5A and assembly of hepatitis C virus. J Virol. 2010;84(21):11532-11541. doi:10.1128/JVI.01021-10

Day AP, Bellavia S, Jones OT, Stansbie D. Effect of simvastatin therapy on cell membrane cholesterol content and membrane function as assessed by polymorphonuclear cell NADPH oxidase activity. *Ann Clin Biochem*. 1997;34 (Pt 3):269-275. doi:10.1177/000456329703400308

Deleersnyder V, Pillez A, Wychowski C, et al. Formation of native hepatitis C virus glycoprotein complexes. *J Virol*. 1997;71(1):697-704. doi:10.1128/JVI.71.1.697-704.1997

Delsing DJ, Offerman EH, van Duyvenvoorde W, et al. Acyl-CoA:cholesterol acyltransferase inhibitor avasimibe reduces atherosclerosis in addition to its cholesterol-lowering effect in ApoE*3-Leiden mice. *Circulation*. 2001;103(13):1778-1786. doi:10.1161/01.cir.103.13.1778

Dimitrova M, Imbert I, Kieny MP, Schuster C. Protein-protein interactions between hepatitis C virus nonstructural proteins. *J Virol*. 2003;77(9):5401-5414. doi:10.1128/jvi.77.9.5401-5414.2003

Douam F, Dao Thi VL, Maurin G, et al. Critical interaction between E1 and E2 glycoproteins determines binding and fusion properties of hepatitis C virus during cell entry. *Hepatology*. 2014;59(3):776-788. doi:10.1002/hep.26733

Duan Y, Gong K, Xu S, Zhang F, Meng X, Han J. Regulation of cholesterol homeostasis in health and diseases: from mechanisms to targeted therapeutics. *Signal Transduct Target Ther*. 2022;7(1):265. Published 2022 Aug 2. doi:10.1038/s41392-022-01125-5

Dubuisson J, Cosset FL. Virology and cell biology of the hepatitis C virus life cycle: an update. *J Hepatol*. 2014;61(1 Suppl):S3-S13. doi:10.1016/j.jhep.2014.06.031

Dubuisson J. Hepatitis C virus proteins. *World J Gastroenterol*. 2007;13(17):2406-2415. doi:10.3748/wjg.v13.i17.2406

Duverlie G, Wychowski C. Cell culture systems for the hepatitis C virus. *World J Gastroenterol*. 2007;13(17):2442-2445. doi:10.3748/wjg.v13.i17.2442

Egger D, Wölk B, Gosert R, et al. Expression of hepatitis C virus proteins induces distinct membrane alterations including a candidate viral replication complex. *J Virol*. 2002;76(12):5974-5984. doi:10.1128/jvi.76.12.5974-5984.2002

Elgner F, Donnerhak C, Ren H, et al. Characterization of α-taxilin as a novel factor controlling the release of hepatitis C virus. *Biochem J*. 2016;473(2):145-155. doi:10.1042/BJ20150717

Elgner F, Ren H, Medvedev R, et al. The Intracellular Cholesterol Transport Inhibitor U18666A Inhibits the Exosome-Dependent Release of Mature Hepatitis C Virus. *J Virol*. 2016;90(24):11181-11196. Published 2016 Nov 28. doi:10.1128/JVI.01053-16

Elgretli W, Chen T, Kronfli N, Sebastiani G. Hepatitis C Virus-Lipid Interplay: Pathogenesis and Clinical Impact. *Biomedicines*. 2023;11(2):271. Published 2023 Jan 19. doi:10.3390/biomedicines11020271

Elgretli W, Chen T, Kronfli N, Sebastiani G. Hepatitis C Virus-Lipid Interplay: Pathogenesis and Clinical Impact. *Biomedicines*. 2023;11(2):271. Published 2023 Jan 19. doi:10.3390/biomedicines11020271

Feinstone SM, Kapikian AZ, Purcell RH, Alter HJ, Holland PV. Transfusion-associated hepatitis not due to viral hepatitis type A or B. *N Engl J Med*. 1975;292(15):767-770. doi:10.1056/NEJM197504102921502

Felmlee DJ, Hafirassou ML, Lefevre M, Baumert TF, Schuster C. Hepatitis C virus, cholesterol and lipoproteins--impact for the viral life cycle and pathogenesis of liver disease. *Viruses*. 2013;5(5):1292-1324. Published 2013 May 23. doi:10.3390/v5051292

Friche E, Jensen PB, Nissen NI. Comparison of cyclosporin A and SDZ PSC833 as multidrug-resistance modulators in a daunorubicin-resistant Ehrlich ascites tumor. *Cancer Chemother Pharmacol*. 1992;30(3):235-237. doi:10.1007/BF00686321

Fujita N, Sugimoto R, Ma N, et al. Comparison of hepatic oxidative DNA damage in patients with chronic hepatitis B and C. *J Viral Hepat*. 2008;15(7):498-507. doi:10.1111/j.1365-2893.2008.00972.x

Gale MJ Jr, Korth MJ, Tang NM, et al. Evidence that hepatitis C virus resistance to interferon is mediated through repression of the PKR protein kinase by the nonstructural 5A protein. *Virology*. 1997;230(2):217-227. doi:10.1006/viro.1997.8493

Galic S, Loh K, Murray-Segal L, Steinberg GR andrews ZB, Kemp BE. AMPK signaling to acetyl-CoA carboxylase is required for fasting- and cold-induced appetite but not thermogenesis. *Elife*. 2018;7:e32656. Published 2018 Feb 13. doi:10.7554/eLife.32656

Gallinari P, Brennan D, Nardi C, et al. Multiple enzymatic activities associated with recombinant NS3 protein of hepatitis C virus. *J Virol*. 1998;72(8):6758-6769. doi:10.1128/JVI.72.8.6758-6769.1998

García-Mediavilla MV, Pisonero-Vaquero S, Lima-Cabello E, et al. Liver X receptor α-mediated regulation of lipogenesis by core and NS5A proteins contributes to HCV-induced liver steatosis and HCV replication. *Lab Invest*. 2012;92(8):1191-1202. doi:10.1038/labinvest.2012.88

Gastaldi G, Goossens N, Clément S, Negro F. Current level of evidence on causal association between hepatitis C virus and type 2 diabetes: A review. *J Adv Res*. 2017;8(2):149-159. doi:10.1016/j.jare.2016.11.003

Gastaminza P, Cheng G, Wieland S, Zhong J, Liao W, Chisari FV. Cellular determinants of hepatitis C virus assembly, maturation, degradation and secretion. *J Virol*. 2008;82(5):2120-2129. doi:10.1128/JVI.02053-07

Gastaminza P, Dryden KA, Boyd B, et al. Ultrastructural and biophysical characterization of hepatitis C virus particles produced in cell culture. *J Virol*. 2010;84(21):10999-11009. doi:10.1128/JVI.00526-10

Gastaminza P, Kapadia SB, Chisari FV. Differential biophysical properties of infectious intracellular and secreted hepatitis C virus particles. *J Virol*. 2006;80(22):11074-11081. doi:10.1128/JVI.01150-06

Goldstein JL, Brown MS. The LDL receptor. *Arterioscler Thromb Vasc Biol*. 2009;29(4):431-438. doi:10.1161/ATVBAHA.108.179564

Goonawardane N, Gebhardt A, Bartlett C, Pichlmair A, Harris M. Phosphorylation of Serine 225 in Hepatitis C Virus NS5A Regulates Protein-Protein Interactions. *J Virol*. 2017;91(17):e00805-17. Published 2017 Aug 10. doi:10.1128/JVI.00805-17

Graham CS, Baden LR, Yu E, et al. Influence of human immunodeficiency virus infection on the course of hepatitis C virus infection: a meta-analysis. *Clin Infect Dis*. 2001;33(4):562-569. doi:10.1086/321909

Grakoui A, McCourt DW, Wychowski C, Feinstone SM, Rice CM. A second hepatitis C virus-encoded proteinase. *Proc Natl Acad Sci U S A*. 1993;90(22):10583-10587. doi:10.1073/pnas.90.22.10583

Griffin SD, Beales LP, Clarke DS, et al. The p7 protein of hepatitis C virus forms an ion channel that is blocked by the antiviral drug, Amantadine. *FEBS Lett*. 2003;535(1-3):34-38. doi:10.1016/s0014-5793(02)03851-6

Hammad M, Raftari M, Cesário R, Salma R, Godoy P, Emami SN, Haghdoost S. Roles of Oxidative Stress and Nrf2 Signaling in Pathogenic and Non-Pathogenic Cells: A Possible General Mechanism of Resistance to Therapy. *Antioxidants*. 2023; 12(7):1371. https://doi.org/10.3390/antiox12071371

Harder B, Jiang T, Wu T, et al. Molecular mechanisms of Nrf2 regulation and how these influence chemical modulation for disease intervention. *Biochem Soc Trans*. 2015;43(4):680-686. doi:10.1042/BST20150020

Hayes M, Choudhary V, Ojha N, et al. Fat storage-inducing transmembrane (FIT or FITM) proteins are related to lipid phosphatase/phosphotransferase enzymes. *Microb Cell*. 2017;5(2):88-103. Published 2017 Dec 28. doi:10.15698/mic2018.02.614

Herker E, Harris C, Hernandez C, et al. Efficient hepatitis C virus particle formation requires diacylglycerol acyltransferase-1. *Nat Med*. 2010;16(11):1295-1298. doi:10.1038/nm.2238

Himmelsbach K, Hildt E. The kinase inhibitor Sorafenib impairs the antiviral effect of interferon α on hepatitis C virus replication. Eur J Cell Biol. 2013 Jan;92(1):12-20. doi: 10.1016/j.ejcb.2012.09.001. Epub 2012 Oct 27. PMID: 23107224.

Himmelsbach K, Sauter D, Baumert TF, Ludwig L, Blum HE, Hildt E. New aspects of an anti-tumour drug: sorafenib efficiently inhibits HCV replication. Gut. 2009;58(12):1644-1653. doi:10.1136/gut.2009.182212

Hirotsu Y, Hataya N, Katsuoka F, Yamamoto M. NF-E2-related factor 1 (Nrf1) serves as a novel regulator of hepatic lipid metabolism through regulation of the Lipin1 and PGC-1β genes. *Mol Cell Biol*. 2012;32(14):2760-2770. doi:10.1128/MCB.06706-11

Hirschfield GM, Chazouillères O, Drenth JP, et al. Effect of NGM282, an FGF19 analogue, in primary sclerosing cholangitis: A multicenter, randomized, double-blind, placebo-controlled phase II trial. *J Hepatol*. 2019;70(3):483-493. doi:10.1016/j.jhep.2018.10.035

Hla T, Dannenberg AJ. Sphingolipid signaling in metabolic disorders. *Cell Metab*. 2012;16(4):420-434. doi:10.1016/j.cmet.2012.06.017

Hofmann S, Krajewski M, Scherer C, et al. Complex lipid metabolic remodeling is required for efficient hepatitis C virus replication. *Biochim Biophys Acta Mol Cell Biol Lipids*. 2018;1863(9):1041-1056. doi:10.1016/j.bbalip.2018.06.002

Hong C, Duit S, Jalonen P, et al. The E3 ubiquitin ligase IDOL induces the degradation of the low density lipoprotein receptor family members VLDLR and ApoER2. *J Biol Chem*. 2010;285(26):19720-19726. doi:10.1074/jbc.M110.123729

Hope RG, Murphy DJ, McLauchlan J. The domains required to direct core proteins of hepatitis C virus and GB virus-B to lipid droplets share common features with plant oleosin proteins. *J Biol Chem*. 2002;277(6):4261-4270. doi:10.1074/jbc.M108798200

Horinouchi Y, Murashima Y, Yamada Y, et al. Pemafibrate inhibited renal dysfunction and fibrosis in a mouse model of adenine-induced chronic kidney disease. *Life Sci*. 2023;321:121590. doi:10.1016/j.lfs.2023.121590

Horn A, Jaiswal JK. Structural and signaling role of lipids in plasma membrane repair. *Curr Top Membr*. 2019;84:67-98. doi:10.1016/bs.ctm.2019.07.001

Hügle T, Fehrmann F, Bieck E, et al. The hepatitis C virus nonstructural protein 4B is an integral endoplasmic reticulum membrane protein. *Virology*. 2001;284(1):70-81. doi:10.1006/viro.2001.0873

Isken O, Langerwisch U, Jirasko V, et al. A conserved NS3 surface patch orchestrates NS2 protease stimulation, NS5A hyperphosphorylation and HCV genome replication [published correction appears in PLoS Pathog. 2016 Jan;12(1):e1005394]. *PLoS Pathog*. 2015;11(3):e1004736. Published 2015 Mar 16. doi:10.1371/journal.ppat.1004736

Ivanov AV, Bartosch B, Smirnova OA, Isaguliants MG, Kochetkov SN. HCV and oxidative stress in the liver. Viruses. 2013;5(2):439-469. Published 2013 Jan 28. doi:10.3390/v5020439

Ivanov AV, Bartosch B, Smirnova OA, Isaguliants MG, Kochetkov SN. HCV and oxidative stress in the liver. *Viruses*. 2013;5(2):439-469. Published 2013 Jan 28. doi:10.3390/v5020439

Janiak, Maciej; Caraballo Cortes, Kamila; Demkow, Urszula; Radkowski, Marek (2018): Spontaneous Elimination of Hepatitis C Virus Infection. In *Advances in experimental medicine and biology* 1039, pp. 45–54. DOI: 10.1007/5584_2017_76.

Jennelle LT, Magoro T, Angelucci AR, Dandekar A, Hahn YS. Hepatitis C Virus Alters Macrophage Cholesterol Metabolism Through Interaction with Scavenger Receptors. *Viral Immunol*. 2022;35(3):223-235. doi:10.1089/vim.2021.0101

Jiang B, Himmelsbach K, Ren H, Boller K, Hildt E. Subviral Hepatitis B Virus Filaments, like Infectious Viral Particles, Are Released via Multivesicular Bodies. *J Virol*. 2015;90(7):3330-3341. Published 2015 Dec 30. doi:10.1128/JVI.03109-15

Jin C, Kumar P, Gracia-Sancho J, Dufour JF. Calcium transfer between endoplasmic reticulum and mitochondria in liver diseases. *FEBS Lett*. 2021;595(10):1411-1421. doi:10.1002/1873-3468.14078

Jindal A, Jagdish RK, Kumar A. Hepatic Regeneration in Cirrhosis. J Clin Exp Hepatol. 2022;12(2):603-616. doi:10.1016/j.jceh.2021.08.029

Johri MK, Lashkari HV, Gupta D, Vedagiri D, Harshan KH. mTORC1 restricts hepatitis C virus RNA replication through ULK1-mediated suppression of miR-122 and facilitates post-replication events. *J Gen Virol*. 2020;101(1):86-95. doi:10.1099/jgv.0.001356

Jopling C. Liver-specific microRNA-122: Biogenesis and function. *RNA Biol*. 2012;9(2):137-142. doi:10.4161/rna.18827

Karamichali E, Chihab H, Kakkanas A, Marchio A, Karamitros T, Pogka V, Varaklioti A, Kalliaropoulos A, Martinez-Gonzales B, Foka P, Koskinas I, Mentis A, Benjelloun S, Pineau P, Georgopoulou U. HCV Defective Genomes Promote Persistent Infection by Modulating the Viral Life Cycle. Front Microbiol. 2018 Dec 3;9:2942. doi: 10.3389/fmicb.2018.02942. PMID: 30559733; PMCID: PMC6287115.

Karathanasis SK, Freeman LA, Gordon SM, Remaley AT. The Changing Face of HDL and the Best Way to Measure It. *Clin Chem*. 2017;63(1):196-210. doi:10.1373/clinchem.2016.257725

Kato N, Nakazawa T, Mizutani T, Shimotohno K. Susceptibility of human T-lymphotropic virus type I infected cell line MT-2 to hepatitis C virus infection. *Biochem Biophys Res Commun*. 1995;206(3):863-869. doi:10.1006/bbrc.1995.1123

Ke PY, Chen SS. Activation of the unfolded protein response and autophagy after hepatitis C virus infection suppresses innate antiviral immunity in vitro. *J Clin Invest*. 2011;121(1):37-56. doi:10.1172/JCI41474

Kim CW, Chang KM. Hepatitis C virus: virology and life cycle. *Clin Mol Hepatol*. 2013;19(1):17-25. doi:10.3350/cmh.2013.19.1.17

Kim HM, Han JW, Chan JY. Nuclear Factor Erythroid-2 Like 1 (NFE2L1): Structure, function and regulation. *Gene*. 2016;584(1):17-25. doi:10.1016/j.gene.2016.03.002

Kim JL, Morgenstern KA, Lin C, et al. Crystal structure of the hepatitis C virus NS3 protease domain complexed with a synthetic NS4A cofactor peptide [published correction appears in Cell 1997 Apr 4;89(1):159]. *Cell*. 1996;87(2):343-355. doi:10.1016/s0092-8674(00)81351-3

Kim KH, Hong SP, Kim K, Park MJ, Kim KJ, Cheong J. HCV core protein induces hepatic lipid accumulation by activating SREBP1 and PPARgamma. *Biochem Biophys Res Commun*. 2007;355(4):883-888. doi:10.1016/j.bbrc.2007.02.044

Kim SJ, Syed GH, Khan M, et al. Hepatitis C virus triggers mitochondrial fission and attenuates apoptosis to promote viral persistence. *Proc Natl Acad Sci U S A*. 2014;111(17):6413-6418. doi:10.1073/pnas.1321114111

Kong F, Pan Y, Chi X, et al. Factors associated with spontaneous clearance of hepatitis C virus in Chinese population. *Biomed Res Int*. 2014;2014:527030. doi:10.1155/2014/527030

Korenaga M, Wang T, Li Y, et al. Hepatitis C virus core protein inhibits mitochondrial electron transport and increases reactive oxygen species (ROS) production. *J Biol Chem*. 2005;280(45):37481-37488. doi:10.1074/jbc.M506412200

Koutsoudakis G, Kaul A, Steinmann E, et al. Characterization of the early steps of hepatitis C virus infection by using luciferase reporter viruses. *J Virol*. 2006;80(11):5308-5320. doi:10.1128/JVI.02460-05

Kukla M, Mazur W, Bułdak RJ, Zwirska-Korczala K. Potential role of leptin, adiponectin and three novel adipokines--visfatin, chemerin and vaspin--in chronic hepatitis. *Mol Med*. 2011;17(11-12):1397-1410. doi:10.2119/molmed.2010.00105

Kumashiro N, Tamura Y, Uchida T, et al. Impact of oxidative stress and peroxisome proliferator-activated receptor gamma coactivator-1alpha in hepatic insulin resistance. *Diabetes*. 2008;57(8):2083-2091. doi:10.2337/db08-0144

Kunden RD, Khan JQ, Ghezelbash S, Wilson JA. The Role of the Liver-Specific microRNA, miRNA-122 in the HCV Replication Cycle. *Int J Mol Sci*. 2020;21(16):5677. Published 2020 Aug 7. doi:10.3390/ijms21165677

Laemmli UK. Cleavage of structural proteins during the assembly of the head of bacteriophage T4. *Nature*. 1970;227(5259):680-685. doi:10.1038/227680a0

Lanford RE, Sureau C, Jacob JR, White R, Fuerst TR. Demonstration of in vitro infection of chimpanzee hepatocytes with hepatitis C virus using strand-specific RT/PCR. *Virology*. 1994;202(2):606-614. doi:10.1006/viro.1994.1381

Lee HR, Lee GY, You DG, Kim HK, Yoo YD. Hepatitis C Virus p7 Induces Membrane Permeabilization by Interacting with Phosphatidylserine. *Int J Mol Sci*. 2020;21(3):897. Published 2020 Jan 30. doi:10.3390/ijms21030897

Lee HW, Lee H, Kim BK, Chang Y, Jang JY, Kim DY. Cost-effectiveness of chronic hepatitis C screening and treatment. *Clin Mol Hepatol*. 2022;28(2):164-173. doi:10.3350/cmh.2021.0193

Lee JY, Cortese M, Haselmann U, et al. Spatiotemporal Coupling of the Hepatitis C Virus Replication Cycle by Creating a Lipid Droplet- Proximal Membranous Replication Compartment. *Cell Rep*. 2019;27(12):3602-3617.e5. doi:10.1016/j.celrep.2019.05.063

Li X, Wu K, Zeng S, et al. Viral Infection Modulates Mitochondrial Function. *Int J Mol Sci*. 2021;22(8):4260. Published 2021 Apr 20. doi:10.3390/ijms22084260

Lin J, Handschin C, Spiegelman BM. Metabolic control through the PGC-1 family of transcription coactivators. *Cell Metab*. 2005;1(6):361-370. doi:10.1016/j.cmet.2005.05.004

Lindenbach BD, Meuleman P, Ploss A, et al. Cell culture-grown hepatitis C virus is infectious in vivo and can be recultured in vitro. *Proc Natl Acad Sci U S A*. 2006;103(10):3805-3809. doi:10.1073/pnas.0511218103

Lindenbach BD, Meuleman P, Ploss A, et al. Cell culture-grown hepatitis C virus is infectious in vivo and can be recultured in vitro. *Proc Natl Acad Sci U S A*. 2006;103(10):3805-3809. doi:10.1073/pnas.0511218103

Lindenbach BD, Rice CM. Unravelling hepatitis C virus replication from genome to function. *Nature*. 2005;436(7053):933-938. doi:10.1038/nature04077

Lingala S, Ghany MG. Natural History of Hepatitis C. Gastroenterol Clin North Am. 2015 Dec;44(4):717-34. doi: 10.1016/j.gtc.2015.07.003. Epub 2015 Aug 25. PMID: 26600216; PMCID: PMC5939344.

Lohmann V, Körner F, Koch J, Herian U, Theilmann L, Bartenschlager R. Replication of subgenomic hepatitis C virus RNAs in a hepatoma cell line. *Science*. 1999;285(5424):110-113. doi:10.1126/science.285.5424.110

Loo YM, Owen DM, Li K, et al. Viral and therapeutic control of IFN-beta promoter stimulator 1 during hepatitis C virus infection. *Proc Natl Acad Sci U S A*. 2006;103(15):6001-6006. doi:10.1073/pnas.0601523103

Loomba R, Rivera MM, McBurney R, Park Y, Haynes-Williams V, Rehermann B, Alter HJ, Herrine SK, Liang TJ, Hoofnagle JH, Heller T. The natural history of acute hepatitis C: clinical presentation, laboratory findings and treatment outcomes. Aliment Pharmacol Ther. 2011 Mar;33(5):559-65. doi: 10.1111/j.1365-2036.2010.04549.x. Epub 2010 Dec 29. PMID: 21198704; PMCID: PMC5577910.

Lorenz IC, Marcotrigiano J, Dentzer TG, Rice CM. Structure of the catalytic domain of the hepatitis C virus NS2-3 protease. *Nature*. 2006;442(7104):831-835. doi:10.1038/nature04975

Lorenz IC. The Hepatitis C Virus Nonstructural Protein 2 (NS2): An Up-and-Coming Antiviral Drug Target. *Viruses*. 2010;2(8):1635-1646. doi:10.3390/v2081635

Luo J, Yang H, Song BL. Mechanisms and regulation of cholesterol homeostasis. *Nat Rev Mol Cell Biol*. 2020;21(4):225-245. doi:10.1038/s41580-019-0190-7

Marshall AD, Pawlotsky JM, Lazarus JV, Aghemo A, Dore GJ, Grebely J. The removal of DAA restrictions in Europe - One step closer to eliminating HCV as a major public health threat. *J Hepatol*. 2018;69(5):1188-1196. doi:10.1016/j.jhep.2018.06.016

Martell M, Esteban JI, Quer J, et al. Hepatitis C virus (HCV) circulates as a population of different but closely related genomes: quasispecies nature of HCV genome distribution. *J Virol*. 1992;66(5):3225-3229. doi:10.1128/JVI.66.5.3225-3229.1992

Martin DN, Uprichard SL. Identification of transferrin receptor 1 as a hepatitis C virus entry factor. *Proc Natl Acad Sci U S A*. 2013;110(26):10777-10782. doi:10.1073/pnas.1301764110

Maxfield FR, van Meer G. Cholesterol, the central lipid of mammalian cells. *Curr Opin Cell Biol*. 2010;22(4):422-429. doi:10.1016/j.ceb.2010.05.004

McCullough AJ. Pathophysiology of nonalcoholic steatohepatitis. *J Clin Gastroenterol*. 2006;40 Suppl 1:S17-S29. doi:10.1097/01.mcg.0000168645.86658.22

McLauchlan J. Properties of the hepatitis C virus core protein: a structural protein that modulates cellular processes. *J Viral Hepat*. 2000;7(1):2-14. doi:10.1046/j.1365-2893.2000.00201.x

McLaughlin M, Esterly J. The evolving management of hepatitis C virus. US Pharmacist. 2015;40(4):HS2–HS6.

Mekahli D, Bultynck G, Parys JB, De Smedt H, Missiaen L. Endoplasmic-reticulum calcium depletion and disease. *Cold Spring Harb Perspect Biol*. 2011;3(6):a004317. Published 2011 Jun 1. doi:10.1101/cshperspect.a004317

Meng Z, Liu Q, Sun F, Qiao L. Hepatitis C virus nonstructural protein 5A perturbs lipid metabolism by modulating AMPK/SREBP-1c signaling. Lipids Health Dis. 2019;18(1):191. Published 2019 Nov 4. doi:10.1186/s12944-019-1136-y

Menzel N, Fischl W, Hueging K, et al. MAP-kinase regulated cytosolic phospholipase A2 activity is essential for production of infectious hepatitis C virus particles. *PLoS Pathog*. 2012;8(7):e1002829. doi:10.1371/journal.ppat.1002829

Mercer DF, Schiller DE, Elliott JF, et al. Hepatitis C virus replication in mice with chimeric human livers. *Nat Med*. 2001;7(8):927-933. doi:10.1038/90968

Merscher S, Pedigo CE, Mendez AJ. Metabolism, energetics and lipid biology in the podocyte - cellular cholesterol-mediated glomerular injury. *Front Endocrinol (Lausanne)*. 2014;5:169. Published 2014 Oct 14. doi:10.3389/fendo.2014.00169

Miyanari Y, Atsuzawa K, Usuda N, et al. The lipid droplet is an important organelle for hepatitis C virus production [published correction appears in Nat Cell Biol. 2007 Oct;9(10):1216]. *Nat Cell Biol*. 2007;9(9):1089-1097. doi:10.1038/ncb1631

Moradpour D, Penin F, Rice CM. Replication of hepatitis C virus. *Nat Rev Microbiol*. 2007;5(6):453-463. doi:10.1038/nrmicro1645

Morozov VA, Lagaye S. Hepatitis C virus: Morphogenesis, infection and therapy. *World J Hepatol*. 2018;10(2):186-212. doi:10.4254/wjh.v10.i2.186

Nagao K, Maeda M, Mañucat NB, Ueda K. Cyclosporine A and PSC833 inhibit ABCA1 function via direct binding. *Biochim Biophys Acta*. 2013;1831(2):398-406. doi:10.1016/j.bbalip.2012.11.002

Nan Y, Wu C and Zhang Y-J (2017) Interplay between Janus Kinase/Signal Transducer and Activator of Transcription Signaling Activated by Type I Interferons and Viral Antagonism. *Front. Immunol.* 8:1758. doi: 10.3389/fimmu.2017.01758

Nawaz, Allah; Zaidi, Syed Faisal; Usmanghani, Khan; Ahmad, Irshad (2015): Concise review on the insight of hepatitis C. In *Journal of Taibah University Medical Sciences* 10 (2), pp. 132–139. DOI: 10.1016/j.jtumed.2014.08.004

Neveu G, Barouch-Bentov R, Ziv-Av A, Gerber D, Jacob Y, Einav S. Identification and targeting of an interaction between a tyrosine motif within hepatitis C virus core protein and AP2M1 essential for viral assembly. *PLoS Pathog*. 2012;8(8):e1002845. doi:10.1371/journal.ppat.1002845

Nguyen TB, Olzmann JA. Lipid droplets and lipotoxicity during autophagy. *Autophagy*. 2017;13(11):2002-2003. doi:10.1080/15548627.2017.1359451

Nguyen TM, Sawyer JK, Kelley KL, Davis MA, Rudel LL. Cholesterol esterification by ACAT2 is essential for efficient intestinal cholesterol absorption: evidence from thoracic lymph duct cannulation. *J Lipid Res*. 2012;53(1):95-104. doi:10.1194/jlr.M018820

Oancea CN, Butaru AE, Streba CT, et al. Global hepatitis C elimination: history, evolution, revolutionary changes and barriers to overcome. Rom J Morphol Embryol. 2020;61(3):643-653. doi:10.47162/RJME.61.3.02

O'Connell MA, Hayes JD. The Keap1/Nrf2 pathway in health and disease: from the bench to the clinic. *Biochem Soc Trans*. 2015;43(4):687-689. doi:10.1042/BST20150069

Ohtsuji M, Katsuoka F, Kobayashi A, Aburatani H, Hayes JD, Yamamoto M. Nrf1 and Nrf2 play distinct roles in activation of antioxidant response element-dependent genes. *J Biol Chem*. 2008;283(48):33554-33562. doi:10.1074/jbc.M804597200

Olzmann JA, Carvalho P. Dynamics and functions of lipid droplets. *Nat Rev Mol Cell Biol*. 2019;20(3):137-155. doi:10.1038/s41580-018-0085-z

Panda S, Behera S, Alam MF, Syed GH. Endoplasmic reticulum & mitochondrial calcium homeostasis: The interplay with viruses. *Mitochondrion*. 2021;58:227-242. doi:10.1016/j.mito.2021.03.008

Paracha UZ, Fatima K, Alqahtani M, et al. Oxidative stress and hepatitis C virus. *Virol J*. 2013;10:251. Published 2013 Aug 7. doi:10.1186/1743-422X-10-251

Pascut D, Hoang M, Nguyen NNQ, Pratama MY, Tiribelli C. HCV Proteins Modulate the Host Cell miRNA Expression Contributing to Hepatitis C Pathogenesis and Hepatocellular Carcinoma Development. *Cancers (Basel)*. 2021;13(10):2485. Published 2021 May 19. doi:10.3390/cancers13102485

Paul D, Bartenschlager R. Flaviviridae Replication Organelles: Oh, What a Tangled Web We Weave. *Annu Rev Virol*. 2015;2(1):289-310. doi:10.1146/annurev-virology-100114-055007

Pawlotsky, Jean-Michel; Feld, Jordan J.; Zeuzem, Stefan; Hoofnagle, Jay H. (2015): From non-A, non-B hepatitis to hepatitis C virus cure. In *Journal of hepatology* 62 (1 Suppl), S87-99. DOI: 10.1016/j.jhep.2015.02.006.

Peiffer KH, Akhras S, Himmelsbach K, et al. Intracellular accumulation of subviral HBsAg particles and diminished Nrf2 activation in HBV genotype G expressing cells lead to an increased ROI level. *J Hepatol*. 2015;62(4):791-798. doi:10.1016/j.jhep.2014.11.028

Petruzziello A, Marigliano S, Loquercio G, Cozzolino A, Cacciapuoti C. Global epidemiology of hepatitis C virus infection: An up-date of the distribution and circulation of hepatitis C virus genotypes. *World J Gastroenterol*. 2016;22(34):7824-7840. doi:10.3748/wjg.v22.i34.7824

Piecha F, Gänßler JM, Ozga AK, et al. Treatment and re-treatment results of HCV patients in the DAA era. *PLoS One*. 2020;15(5):e0232773. Published 2020 May 5. doi:10.1371/journal.pone.0232773

Ploen D, Hafirassou ML, Himmelsbach K, et al. TIP47 is associated with the hepatitis C virus and its interaction with Rab9 is required for release of viral particles. *Eur J Cell Biol*. 2013;92(12):374-382. doi:10.1016/j.ejcb.2013.12.003

Ploss A, Evans MJ, Gaysinskaya VA, et al. Human occludin is a hepatitis C virus entry factor required for infection of mouse cells. *Nature*. 2009;457(7231):882-886. doi:10.1038/nature07684

Poirier S, Mayer G, Poupon V, et al. Dissection of the endogenous cellular pathways of PCSK9-induced low density lipoprotein receptor degradation: evidence for an intracellular route. *J Biol Chem*. 2009;284(42):28856-28864. doi:10.1074/jbc.M109.037085

Pokharel SM, Shil NK, Gc JB, et al. Integrin activation by the lipid molecule 25-hydroxycholesterol induces a proinflammatory response. *Nat Commun*. 2019;10(1):1482. Published 2019 Apr 1. doi:10.1038/s41467-019-09453-x

Polaris Observatory HCV Collaborators. Global prevalence and genotype distribution of hepatitis C virus infection in 2015: a modelling study. *Lancet Gastroenterol Hepatol*. 2017;2(3):161-176. doi:10.1016/S2468-1253(16)30181-9

Popescu CI, Callens N, Trinel D, et al. NS2 protein of hepatitis C virus interacts with structural and non-structural proteins towards virus assembly. *PLoS Pathog*. 2011;7(2):e1001278. Published 2011 Feb 10. doi:10.1371/journal.ppat.1001278

Post, S.M.; Duez, H.; Gervois, P.P.; Staels, B.; Kuipers, F.; Princen, H.M. Fibrates suppress bile acid synthesis via peroxisome proliferator-activated receptoralpha-mediated downregulation of cholesterol 7alpha-hydroxylase and sterol 27- hydroxylase expression. *Arterioscler. Thromb. Vasc. Biol.* **2001**, *21*, 1840–1845,doi:10.1161/hq1101.098228.

Poynard T, Bedossa P, Opolon P. Natural history of liver fibrosis progression in patients with chronic hepatitis C. The OBSVIRC, METAVIR, CLINIVIR and DOSVIRC groups. *Lancet*. 1997;349(9055):825-832. doi:10.1016/s0140-6736(96)07642-8

Qiu L, Yang Q, Zhao W, et al. Dysfunction of the energy sensor NFE2L1 triggers uncontrollable AMPK signaling and glucose metabolism reprogramming. *Cell Death Dis*. 2022;13(5):501. Published 2022 May 25. doi:10.1038/s41419-022-04917-3

Rayner KJ, Sheedy FJ, Esau CC, et al. Antagonism of miR-33 in mice promotes reverse cholesterol transport and regression of atherosclerosis. *J Clin Invest*. 2011;121(7):2921-2931. doi:10.1172/JCI57275

Rebbani K, Tsukiyama-Kohara K. HCV-Induced Oxidative Stress: Battlefield-Winning Strategy. *Oxid Med Cell Longev*. 2016;2016:7425628. doi:10.1155/2016/7425628

Riva L, Spriet C, Barois N, Popescu CI, Dubuisson J, Rouillé Y. Comparative Analysis of Hepatitis C Virus NS5A Dynamics and Localization in Assembly-Deficient Mutants. Pathogens. 2021;10(2):172. Published 2021 Feb 4. doi:10.3390/pathogens10020172

Röhrig F, Schulze A. The multifaceted roles of fatty acid synthesis in cancer. *Nat Rev Cancer*. 2016;16(11):732-749. doi:10.1038/nrc.2016.89

Romero-Brey I, Bartenschlager R. Membranous replication factories induced by plus-strand RNA viruses. *Viruses*. 2014;6(7):2826-2857. Published 2014 Jul 22. doi:10.3390/v6072826

Romero-Brey I, Merz A, Chiramel A, et al. Three-dimensional architecture and biogenesis of membrane structures associated with hepatitis C virus replication. *PLoS Pathog*. 2012;8(12):e1003056. doi:10.1371/journal.ppat.1003056

Ross-Thriepland D, Amako Y, Harris M. The C terminus of NS5A domain II is a key determinant of hepatitis C virus genome replication, but is not required for virion assembly and release. *J Gen Virol*. 2013;94(Pt 5):1009-1018. doi:10.1099/vir.0.050633-0

Roudot-Thoraval F. Epidemiology of hepatitis C virus infection. *Clin Res Hepatol Gastroenterol*. 2021;45(3):101596. doi:10.1016/j.clinre.2020.101596

Rungta S, Kumari S, Deep A, Verma K, Swaroop S. APRI and FIB-4 performance to assess liver fibrosis against predefined Fibroscan values in chronic hepatitis C virus infection. *J Family Med Prim Care*. 2021;10(11):4082-4088. doi:10.4103/jfmpc.jfmpc_666_21

Sabatine MS, Giugliano RP, Wiviott SD, et al. Efficacy and safety of evolocumab in reducing lipids and cardiovascular events. *N Engl J Med*. 2015;372(16):1500-1509. doi:10.1056/NEJMoa1500858

Saleh M, Rüschenbaum S, Welsch C, et al. Glycogen Synthase Kinase 3β Enhances Hepatitis C Virus Replication by Supporting miR-122. *Front Microbiol*. 2018;9:2949. Published 2018 Nov 27. doi:10.3389/fmicb.2018.02949

Salloum S, Wang H, Ferguson C, Parton RG, Tai AW. Rab18 binds to hepatitis C virus NS5A and promotes interaction between sites of viral replication and lipid droplets. *PLoS Pathog*. 2013;9(8):e1003513. doi:10.1371/journal.ppat.1003513

Scarselli E, Ansuini H, Cerino R, et al. The human scavenger receptor class B type I is a novel candidate receptor for the hepatitis C virus. *EMBO J*. 2002;21(19):5017-5025. doi:10.1093/emboj/cdf529

Schlabe S, Rockstroh JK. Advances in the treatment of HIV/HCV coinfection in adults. *Expert Opin Pharmacother*. 2018;19(1):49-64. doi:10.1080/14656566.2017.1419185

Sengoku T, Shiina M, Suzuki K, et al. Structural basis of transcription regulation by CNC family transcription factor, Nrf2. Nucleic Acids Res. 2022;50(21):12543-12557. doi:10.1093/nar/gkac1102

Serebrov V, Pyle AM. Periodic cycles of RNA unwinding and pausing by hepatitis C virus NS3 helicase. *Nature*. 2004;430(6998):476-480. doi:10.1038/nature02704

Shi Q, Chen J, Zou X, Tang X. Intracellular Cholesterol Synthesis and Transport. *Front Cell Dev Biol*. 2022;10:819281. Published 2022 Mar 21. doi:10.3389/fcell.2022.819281

Shi ST, Polyak SJ, Tu H, Taylor DR, Gretch DR, Lai MM. Hepatitis C virus NS5A colocalizes with the core protein on lipid droplets and interacts with apolipoproteins. Virology. 2002;292(2):198-210. doi:10.1006/viro.2001.1225

Shin SM, Yang JH, Ki SH. Role of the Nrf2-ARE pathway in liver diseases. *Oxid Med Cell Longev*. 2013;2013:763257. doi:10.1155/2013/763257

Shlomai A, Rechtman MM, Burdelova EO, et al. The metabolic regulator PGC-1α links hepatitis C virus infection to hepatic insulin resistance. *J Hepatol*. 2012;57(4):867-873. doi:10.1016/j.jhep.2012.06.021

Sidorkiewicz M. Hepatitis C Virus Uses Host Lipids to Its Own Advantage. *Metabolites*. 2021;11(5):273. Published 2021 Apr 27. doi:10.3390/metabo11050273

Silvestro S, Mazzon E. Nrf2 Activation: Involvement in Central Nervous System Traumatic Injuries. A Promising Therapeutic Target of Natural Compounds. Int J Mol Sci. 2022;24(1):199. Published 2022 Dec 22. doi:10.3390/ijms24010199

Singh K, Martinez MG, Lin J, Gregory J, Nguyen TU, Abdelaal R, Kang K, Brennand K, Grünweller A, Ouyang Z, Phatnani H, Kielian M, Wendel HG. Transcriptional and Translational Dynamics of Zika and Dengue Virus Infection. Viruses. 2022 Jun 28;14(7):1418. doi: 10.3390/v14071418. PMID: 35891396; PMCID: PMC9316442.

Sorrentino V, Nelson JK, Maspero E, et al. The LXR-IDOL axis defines a clathrin-, caveolae- and dynamin-independent endocytic route for LDLR internalization and lysosomal degradation. *J Lipid Res*. 2013;54(8):2174-2184. doi:10.1194/jlr.M037713

Steinmann E, Penin F, Kallis S, Patel AH, Bartenschlager R, Pietschmann T. Hepatitis C virus p7 protein is crucial for assembly and release of infectious virions. *PLoS Pathog*. 2007;3(7):e103. doi:10.1371/journal.ppat.0030103

Stöhr S, Costa R, Sandmann L, et al. Host cell mTORC1 is required for HCV RNA replication. *Gut*. 2016;65(12):2017-2028. doi:10.1136/gutjnl-2014-308971

Strating JR, van Kuppeveld FJ. Viral rewiring of cellular lipid metabolism to create membranous replication compartments. *Curr Opin Cell Biol*. 2017;47:24-33. doi:10.1016/j.ceb.2017.02.005

Strating JR, van Kuppeveld FJ. Viral rewiring of cellular lipid metabolism to create membranous replication compartments. *Curr Opin Cell Biol*. 2017;47:24-33. doi:10.1016/j.ceb.2017.02.005

Sullivan DG, Bruden D, Deubner H, et al. Hepatitis C virus dynamics during natural infection are associated with long-term histological outcome of chronic hepatitis C disease. *J Infect Dis*. 2007;196(2):239-248. doi:10.1086/518895

Sun LP, Li L, Goldstein JL, Brown MS. Insig required for sterol-mediated inhibition of Scap/SREBP binding to COPII proteins in vitro. *J Biol Chem*. 2005;280(28):26483-26490. doi:10.1074/jbc.M504041200

Suzuki R, Matsuda M, Watashi K, et al. Signal peptidase complex subunit 1 participates in the assembly of hepatitis C virus through an interaction with E2 and NS2. *PLoS Pathog*. 2013;9(8):e1003589. doi:10.1371/journal.ppat.1003589

Tanaka H, Ohtsuka I, Kogushi M, et al. Effect of the acyl-CoA:cholesterol acyltransferase inhibitor, E5324, on experimental atherosclerosis in rabbits. *Atherosclerosis*. 1994;107(2):187-201. doi:10.1016/0021-9150(94)90020-5

Tedbury P, Welbourn S, Pause A, King B, Griffin S, Harris M. The subcellular localization of the hepatitis C virus non-structural protein NS2 is regulated by an ion channel-independent function of the p7 protein. *J Gen Virol*. 2011;92(Pt 4):819-830. doi:10.1099/vir.0.027441-0

Terrault NA, Levy MT, Cheung KW, Jourdain G. Viral hepatitis and pregnancy. *Nat Rev Gastroenterol Hepatol*. 2021;18(2):117-130. doi:10.1038/s41575-020-00361-w

Thomas DL, Thio CL, Martin MP, et al. Genetic variation in IL28B and spontaneous clearance of hepatitis C virus. *Nature*. 2009;461(7265):798-801. doi:10.1038/nature08463

Tonelli C, Chio IIC, Tuveson DA. Transcriptional Regulation by Nrf2. *Antioxid Redox Signal*. 2018;29(17):1727-1745. doi:10.1089/ars.2017.7342

Tsukiyama-Kohara K, Kohara M. Hepatitis C Virus: Viral Quasispecies and Genotypes. *Int J Mol Sci*. 2017;19(1):23. Published 2017 Dec 22. doi:10.3390/ijms19010023

Uysal KT, Wiesbrock SM, Marino MW, Hotamisligil GS. Protection from obesity-induced insulin resistance in mice lacking TNF-alpha function. *Nature*. 1997;389(6651):610-614. doi:10.1038/39335

van Meer G, Voelker DR, Feigenson GW. Membrane lipids: where they are and how they behave. *Nat Rev Mol Cell Biol*. 2008;9(2):112-124. doi:10.1038/nrm2330

Verna EC, Morelli G, Terrault NA, et al. DAA therapy and long-term hepatic function in advanced/decompensated cirrhosis: Real-world experience from HCV-TARGET cohort. *J Hepatol*. 2020;73(3):540-548. doi:10.1016/j.jhep.2020.03.031

Vescovo T, Romagnoli A, Perdomo AB, et al. Autophagy protects cells from HCV-induced defects in lipid metabolism. *Gastroenterology*. 2012;142(3):644-653.e3. doi:10.1053/j.gastro.2011.11.033

Vignuzzi, M., López, C.B. Defective viral genomes are key drivers of the virus–host interaction. *Nat Microbiol* **4**, 1075–1087 (2019). https://doi.org/10.1038/s41564-019-0465-y

Vogt DA, Camus G, Herker E, et al. Lipid droplet-binding protein TIP47 regulates hepatitis C Virus RNA replication through interaction with the viral NS5A protein. *PLoS Pathog*. 2013;9(4):e1003302. doi:10.1371/journal.ppat.1003302

Wakita T, Pietschmann T, Kato T, et al. Production of infectious hepatitis C virus in tissue culture from a cloned viral genome [published correction appears in Nat Med. 2005 Aug;11(8):905]. *Nat Med*. 2005;11(7):791-796. doi:10.1038/nm1268

Wakita T, Pietschmann T, Kato T, et al. Production of infectious hepatitis C virus in tissue culture from a cloned viral genome [published correction appears in Nat Med. 2005 Aug;11(8):905]. *Nat Med*. 2005;11(7):791-796. doi:10.1038/nm1268

Wang H, Jia X, Zhang M, et al. Isoliquiritigenin inhibits virus replication and virus-mediated inflammation via NRF2 signaling. *Phytomedicine*. 2023;114:154786. doi:10.1016/j.phymed.2023.154786

Wang H, Tai AW. Continuous de novo generation of spatially segregated hepatitis C virus replication organelles revealed by pulse-chase imaging. *J Hepatol*. 2017;66(1):55-66. doi:10.1016/j.jhep.2016.08.018

Wang H, Tai AW. Mechanisms of Cellular Membrane Reorganization to Support Hepatitis C Virus Replication. *Viruses*. 2016;8(5):142. Published 2016 May 20. doi:10.3390/v8050142

Wang M, Qiu L, Ru X, Song Y, Zhang Y. Distinct isoforms of Nrf1 diversely regulate different subsets of its cognate target genes. *Sci Rep*. 2019;9(1):2960. Published 2019 Feb 27. doi:10.1038/s41598-019-39536-0

Wang W, Kwok AM, Chan JY. The p65 isoform of Nrf1 is a dominant negative inhibitor of ARE-mediated transcription. *J Biol Chem*. 2007;282(34):24670-24678. doi:10.1074/jbc.M700159200

Wang Y. Scotomas in molecular virology and epidemiology of hepatitis C virus. *World J Gastroenterol*. 2013;19(44):7910-7921. doi:10.3748/wjg.v19.i44.7910

Welbourn S, Pause A. The hepatitis C virus NS2/3 protease. *Curr Issues Mol Biol*. 2007;9(1):63-6

Westerhoff M, Ahn J. Chronic Hepatitis C and Direct Acting Antivirals. *Surg Pathol Clin*. 2018;11(2):287-296. doi:10.1016/j.path.2018.02.002

Widenmaier SB, Snyder NA, Nguyen TB, et al. NRF1 Is an ER Membrane Sensor that Is Central to Cholesterol Homeostasis. *Cell*. 2017;171(5):1094-1109.e15. doi:10.1016/j.cell.2017.10.003

Wiley TE, McCarthy M, Breidi L, McCarthy M, Layden TJ. Impact of alcohol on the histological and clinical progression of hepatitis C infection. *Hepatology*. 1998;28(3):805-809. doi:10.1002/hep.510280330

Williamson CD, Colberg-Poley AM. Access of viral proteins to mitochondria via mitochondria-associated membranes. *Rev Med Virol*. 2009;19(3):147-164. doi:10.1002/rmv.611

Wong-Staal F, Syder AJ, McKelvy JF. Targeting HCV entry for development of therapeutics. *Viruses*. 2010;2(8):1718-1733. doi:10.3390/v2081718

Xiang Y, Wang M, Hu S, et al. Mechanisms controlling the multistage post-translational processing of endogenous Nrf1α/TCF11 proteins to yield distinct isoforms within the coupled positive and negative feedback circuits. *Toxicol Appl Pharmacol*. 2018;360:212-235. doi:10.1016/j.taap.2018.09.036

Xie ZC, Riezu-Boj JI, Lasarte JJ, et al. Transmission of hepatitis C virus infection to tree shrews. *Virology*. 1998;244(2):513-520. doi:10.1006/viro.1998.9127

Xu Z, Chen L, Leung L, Yen TS, Lee C, Chan JY. Liver-specific inactivation of the Nrf1 gene in adult mouse leads to nonalcoholic steatohepatitis and hepatic neoplasia. *Proc Natl Acad Sci U S A*. 2005;102(11):4120-4125. doi:10.1073/pnas.0500660102

Yang JD, Hainaut P, Gores GJ, Amadou A, Plymoth A, Roberts LR. A global view of hepatocellular carcinoma: trends, risk, prevention and management. *Nat Rev Gastroenterol Hepatol*. 2019;16(10):589-604. doi:10.1038/s41575-019-0186-y

Yoshimura T, Oppenheim JJ. Chemerin reveals its chimeric nature. *J Exp Med*. 2008;205(10):2187-2190. doi:10.1084/jem.20081736

Zayas M, Long G, Madan V, Bartenschlager R. Coordination of Hepatitis C Virus Assembly by Distinct Regulatory Regions in Nonstructural Protein 5A. *PLoS Pathog*. 2016;12(1):e1005376. Published 2016 Jan 4. doi:10.1371/journal.ppat.1005376

Zephyr J, Kurt Yilmaz N, Schiffer CA. Viral proteases: Structure, mechanism and inhibition. *Enzymes*. 2021;50:301-333. doi:10.1016/bs.enz.2021.09.004

Zevini A, Ferrari M, Olagnier D, Hiscott J. Dengue virus infection and Nrf2 regulation of oxidative stress. *Curr Opin Virol*. 2020;43:35-40. doi:10.1016/j.coviro.2020.07.015

Zhang L, Wang J, Wang Z, Li Y, Wang H, Liu H. Upregulation of nuclear factor E2-related factor 2 (Nrf2) represses the replication of herpes simplex virus type 1. *Virol J*. 2022;19(1):23. Published 2022 Jan 31. doi:10.1186/s12985-021-01733-7

Zhang Y, Ren Y, Li S, Hayes JD. Transcription factor Nrf1 is topologically repartitioned across membranes to enable target gene transactivation through its acidic glucose-responsive domains. *PLoS One*. 2014;9(4):e93458. Published 2014 Apr 2. doi:10.1371/journal.pone.0093458

Zhang Y, Xiang Y. Molecular and cellular basis for the unique functioning of Nrf1, an indispensable transcription factor for maintaining cell homoeostasis and organ integrity. *Biochem J*. 2016;473(8):961-1000. doi:10.1042/BJ20151182

Zhang Z, He G, Filipowicz NA, et al. Host Lipids in Positive-Strand RNA Virus Genome Replication. *Front Microbiol*. 2019;10:286. Published 2019 Feb 26. doi:10.3389/fmicb.2019.00286

Zhao S, Feng H, Jiang D, et al. ER Ca^{2+} overload activates the IRE1α signaling and promotes cell survival. *Cell Biosci*. 2023;13(1):123. Published 2023 Jul 3. doi:10.1186/s13578-023-01062-y

Zhong J, Gastaminza P, Cheng G, et al. Robust hepatitis C virus infection in vitro. *Proc Natl Acad Sci U S A*. 2005;102(26):9294-9299. doi:10.1073/pnas.0503596102

Zhou J, Zheng Q, Chen Z. The Nrf2 Pathway in Liver Diseases. *Front Cell Dev Biol*. 2022;10:826204. Published 2022 Feb 10. doi:10.3389/fcell.2022.826204

Zhou M, Learned RM, Rossi SJ, Tian H, DePaoli AM, Ling L. Therapeutic FGF19 promotes HDL biogenesis and transhepatic cholesterol efflux to prevent atherosclerosis. *J Lipid Res*. 2019;60(3):550-565. doi:10.1194/jlr.M089961

Zhu H, Briggs JM. Mechanistic role of NS4A and substrate in the activation of HCV NS3 protease. Proteins. 2011;79(8):2428-2443. doi:10.1002/prot.23064

Zhu J, Lian J, Wang X, et al. Role of endogenous and exogenous antioxidants in risk of six cancers: evidence from the Mendelian randomization study. Front Pharmacol. 2023;14:1185850. Published 2023 Jun 27. doi:10.3389/fphar.2023.1185850

10 Acknowledgments

I would like to take this opportunity to thank all the people who have contributed to the success of my doctoral thesis.

My greatest thanks go to **Prof. Dr. Eberhard Hildt** for his trust in my academic and scientific work and his exemplary supervision, for his patience and support when problems arose and for giving me this amazing chance of development when I was still a bachelor student searching for a place to perform my internship.

I would also like to thank **Prof. Dr. Beatrix Süß** for supervising and reviewing my doctoral thesis.

A huge tribute also goes to TAs **Gert Carra** and **Robin Murra**, for their incredible support during experiments and the maintenance of the labs.

Thanks also to **Dr. Fabian Elgner,** my very first supervisor, for his patience, as well as, **Dr. Hussein Ibrahim** for his support. Many thanks also to **Dr. Mirco Glitscher**, **Dr. Daniela Bender** and **Dr. Catarina Sabino** for their professional expertise and support, as well as the motivation and encouragement during my work.

I would also like to thank **Dr. Marie-Luise Ise Theuerkauf, Dr. QingYan Wu** and **Dr. Vanessa Haberger** for their helpfulness and support in the lab.

Special thanks to **Patricia Maria Renelt**, **Olga Szostek** and **Anja Schollmeier** for the ups and downs, many laughs and lunches/coffee breaks.

Thank all former and current "Hildt-Guys" for a great working atmosphere and the wonderful, unforgettable time.